



DEVELOPMENT OF CHITOSAN-BASED ADSORBENTS FOR
REMOVAL OF REACTIVE AZO DYES FROM
AQUEOUS SOLUTION

ASSOC.PROF.DR.BASSIM H HAMEED

UNIVERSITI SAINS MALAYSIA
KAMPUS KEJURUTERAAN
2008

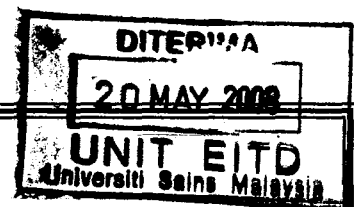


Laporan Akhir Projek Penyelidikan Jangka Pendek

Development of Chitosan-Based Adsorbents for Removal of Reactive Azo Dyes from Aqueous Solution

by
Assoc. Prof. Dr. Bassim H. Hameed
Prof. Dr. Abdul Latif Ahmad

2008



Final Report

**Development of chitosan-based adsorbents for removal of reactive azo
dyes from aqueous solution**

Short-term USM grant

Prepared by:

Assoc. Prof. Dr. Bassim H. Hameed

School of Chemical Engineering,

Engineering Campus,

Universiti Sains Malaysia,

14300 Nibong Tebal, Penang, Malaysia

April 2008

LAPORAN AKHIR PROJEK PENYELIDIKAN JANGKA PENDEK
FINAL REPORT OF SHORT TERM RESEARCH PROJECT

Sila kemukakan laporan akhir ini melalui Jawatankuasa Penyelidikan di Pusat Pengajian dan Dekan/Pengarah/Ketua Jabatan kepada Pejabat Pelantar Penyelidikan

1. Nama Ketua Penyelidik: Assoc. Prof. Dr. Bassim H. Hameed <i>Name of Research Leader</i> <input checked="" type="checkbox"/> Profesor Madya/ <i>Assoc. Prof.</i> <input type="checkbox"/> Dr./ <i>Dr.</i> <input type="checkbox"/> Encik/Puan/Cik <i>Mr/Mrs/Ms</i>					
2. Pusat Tanggungjawab (PTJ): School of Chemical Engineering <i>School/Department</i>					
3. Nama Penyelidik Bersama: Prof. Dr. Abdul Latif Ahmad <i>Name of Co-Researcher</i>					
4. Tajuk Projek: <i>Title of Project</i> Development of Chitosan based adsorbents for removal of reactive azo dyes from aqueous solution					
5. Ringkasan Penilaian/ <i>Summary of Assessment:</i>	Tidak Mencukupi <i>Inadequate</i>		Boleh Diterima <i>Acceptable</i>	Sangat Baik <i>Very Good</i>	
	1	2	3	4	5
i) Pencapaian objektif projek: <i>Achievement of project objectives</i>	<input type="checkbox"/>	<input type="checkbox"/>	<input type="checkbox"/>	<input type="checkbox"/>	<input checked="" type="checkbox"/>
ii) Kualiti output: <i>Quality of outputs</i>	<input type="checkbox"/>	<input type="checkbox"/>	<input type="checkbox"/>	<input checked="" type="checkbox"/>	<input type="checkbox"/>
iii) Kualiti impak: <i>Quality of impacts</i>	<input type="checkbox"/>	<input type="checkbox"/>	<input type="checkbox"/>	<input checked="" type="checkbox"/>	<input type="checkbox"/>
iv) Pemindahan teknologi/potensi pengkomersialan: <i>Technology transfer/commercialization potential</i>	<input type="checkbox"/>	<input type="checkbox"/>	<input checked="" type="checkbox"/>	<input type="checkbox"/>	<input type="checkbox"/>
v) Kualiti dan usahasama : <i>Quality and intensity of collaboration</i>	<input type="checkbox"/>	<input type="checkbox"/>	<input checked="" type="checkbox"/>	<input type="checkbox"/>	<input type="checkbox"/>
vi) Penilaian kepentingan secara keseluruhan: <i>Overall assessment of benefits</i>	<input type="checkbox"/>	<input type="checkbox"/>	<input type="checkbox"/>	<input checked="" type="checkbox"/>	<input type="checkbox"/>

7. Sila sediakan laporan teknikal lengkap yang menerangkan keseluruhan projek ini.
[Sila gunakan kertas berasingan]
*Applicant are required to prepare a Comprehensive Technical Report explaining the project.
(This report must be appended separately)*

The comprehensive technical report is given in Appendix A.

Senaraikan kata kunci yang mencerminkan penyelidikan anda:
List the key words that reflects your research.

Bahasa Malaysia

Silang-sambungan kitosan/abu kelapa sawit
Isotem Penjerapan
Kinetik
Termodinamik
Lengkung-lengkung Bulus

Bahasa Inggeris

Cross-linked chitosan/oil palm ash
Adsorption isotherm
Kinetic
Thermodynamic
Breakthrough Curve

8. **Output dan Faedah Projek**
Output and Benefits of Project

(a) * **Penerbitan Jurnal**

Publication of Journals

(Sila nyatakan jenis, tajuk, pengarang/editor, tahun terbitan dan di mana telah diterbit/diserahkan)
(State type, title, author/editor, publication year and where it has been published/submitted)

(1) M. Hasan, A.L. Ahmad, B.H. Hameed, Adsorption of reactive dye onto cross-linked chitosan/oil palm ash composite beads, Chemical Engineering Journal 136 (2008) 164–172. (Impact factor of this journal 2006: 1.594)

(2) Masitah Hasan, Bassim H. Hameed and A. Latiff Ahmad, Adsorption of reactive orange dye using cross-linked-chitosan/oil palm ash composite adsorbent, Proceeding International Conference on Science & Technology: Application in Industry & Education (2006).

(3) Masitah Hasan, Bassim H. Hameed and A. Latiff Ahmad, Adsorption of reactive azo dye using Chitosan/oil palm ash composite adsorbent, Proceeding 1st Penang International Conference for Young Chemists, Universiti Sains Malaysia, 24-27 May 2006.

A copy of each paper is given in Appendix B

(b) **Faedah-faedah lain seperti perkembangan produk, pengkomersialan produk/pendaftaran paten atau impak kepada dasar dan masyarakat.**
State other benefits such as product development, product commercialisation/patent registration or impact on source and society.

- The developed adsorbent can be used to remove other type of dye pollutants from wastewater.
- The developed adsorbent can be further tested to study its feasibility on removal of gases pollutants from polluted air stream.

* Sila berikan salinan/*Kindly provide copies*

(c) **Latihan Sumber Manusia**
Training in Human Resources

- 1) **Pelajar Sarjana:**
Graduates Students
(Perincikan nama, ijazah dan status)
(Provide names, degrees and status)

Masitah Binti Hassan, Adsorption of reactive azo dyes on Chitosan/oil-Palm ash composite adsorbent: Batch and continous Studies, MSc Thesis, School of Chemical Engineering, Universiti Sains Malaysia, 2008. (Completed)
A copy of Thesis abstract is given in
Appendix C

10) **Lain-lain:**
Others

Research Assiatant:
(1) *Billy Loo Toon Li*
(2) *Looi Phaik Yee*

No equipment purchased under vot 35.

Tandatangan Penyelidik
Signature of Researcher

Tarikh
Date

(b) Faedah-faedah lain seperti perkembangan produk, pengkomersialan produk/pendaftaran paten atau impak kepada dasar dan masyarakat.
State other benefits such as product development, product commercialisation/patent registration or impact on source and society.

- The developed adsorbent can be used to remove other type of dye pollutants from wastewater.
- The developed adsorbent can be further tested to study its feasibility on removal of gases pollutants from polluted air stream.

* Sila berikan salinan/*Kindly provide copies*

(c) Latihan Sumber Manusia
Training in Human Resources

- i) Pelajar Sarjana:
Graduates Students
(Perincikan nama, ijazah dan status)
(Provide names, degrees and status)

Masitah Binti Hassan, Adsorption of reactive azo dyes on Chitosan/oil-Palm ash composite adsorbent: Batch and continuous Studies, MSc Thesis, School of Chemical Engineering, Universiti Sains Malaysia, 2008. (Completed)

- ii) Lain-lain:
Others
Research Assiatant:
(1) Billy Loo Toon Li
(2) Looi Phaik Yee

9. Peralatan yang Telah Dibeli:

Equipment that has been purchased

No equipment purchased under vot 35.



Tandatangan Penyelidik
Signature of Researcher

29/4/08

Tarikh
Date

Komen Jawatankuasa Penyelidikan Pusat Pengajian/Pusat
Comments by the Research Committees of Schools/Centres

Penyelidikan telah tamat dan
dan dikehendaki geran penyelidikan
telah pun tercapai.

Latif 12/5

PROFESOR ABDUL LATIF AHMAD, CEng FICHEM E
Dekan
Pusat Pengajian Kejuruteraan Kimia
Kampus Kejuruteraan
Universiti Sains Malaysia, Seri Ampangan
14300 Nibong Tebal, Seberang Perai Selatan
Pulau Pinang.

TANDATANGAN PENERUSI
JAWATANKUASA PENYELIDIKAN
PUSAT PENGAJIAN/PUSAT

Signature of Chairman
[Research Committee of School/Centre]

Tarikh
Date

APPENDIX A: Technical Report

Technical Report

**Development of chitosan-based adsorbents for removal of reactive azo
dyes from aqueous solution**

Prepared by:

Assoc. Prof. Dr. Bassim H. Hameed

School of Chemical Engineering,
Engineering Campus,
Universiti Sains Malaysia,
14300 Nibong Tebal, Penang, Malaysia

April 2008

APPENDIX A: Technical Report

Development of Chitosan-based adsorbents for removal of reactive azo dyes from aqueous solution

Assoc. Prof. Dr. Bassim H. Hameed

School of Chemical Engineering, Engineering Campus,

Universiti Sains Malaysia, 14300 Nibong Tebal, Penang, Malaysia

Abstract

In this research project, a cross-linked chitosan/oil palm ash composite beads adsorbent was prepared and characterized for removal of reactive blue 19(RB-19), reactive orange 16 (RO-16) and reactive black 5 (RB-5) from aqueous solutions in a batch process and continuous column. In batch process, the system was studied at different initial dye concentration (50-500 mg/L), contact time, pH of solution (2-13) and temperature (30-50 °C). The data were analyzed using the Langmuir, Freundlich, Temkin and Dubinin-Raduskevich models. Adsorption kinetic and thermodynamic was also studied. The performance of adsorption column is described through the concept of the breakthrough curves for the adsorption of dyes on the adsorbent under different operating conditions including initial dye concentration (100, 200, 300 mg/L), flow rate (5–25 mL/min) and height of adsorbent bed (60, 80, 100 mm). It was found that the amount of adsorbate adsorbed (mg/g) increased with increasing initial dye concentration and height of adsorbent bed; and decreased with increasing flow rate. Boharts and Adam, Thomas and Yoon and Nelson models were applied to the experimental data to simulate the breakthrough curves. It was found that the Thomas model was best fitted to describe the adsorption of the dyes on cross-linked chitosan/oil palm ash composite beads, which analysis on average percentage error, $\epsilon\%$ give less than 3.1%.

Keywords: Cross-linked chitosan/oil palm ash; Adsorption isotherm; Kinetic; Thermodynamic; Breakthrough; Modeling

1. Introduction:

One of the major problems concerning environmental pollutants is wastewater problem. Wastewater comes from domestic and industry. In industry, most of wastewater comes from textiles industries, leather industries, paper, plastic and other dyeing industries. Water contamination contains organics, bleaches, and salts. Therefore, Department of Environment, Ministry of Natural Resources and Environment, Malaysia has established interim national water quality standards for Malaysia. For example the maximum contaminant level for colour is 15 colour units [1].

The main problem found in the decontamination of wastewater is the removal of colour. Decolourisation is one of the major problems in wastewaters pollutants. Various kinds of synthetic dyestuffs appear in the effluents of wastewater in some industries such as dyestuffs, textiles, leather, paper-making, plastics, food, rubber, and cosmetic [2]. It has been estimated that about 9 % (or 40,000 tons) of the total amount (450,000 tons) of dyestuffs produced in the world are discharged in textiles wastewaters [3]. Removing color from wastes is important because the presence of small amounts of dyes (below 1ppm) is clearly visible and influences the water environment considerably [4]. These colored compounds are not only aesthetically displeasing, but also impede light penetration in the treatment plants, thus upsetting the biological treatment processes within the treatment plant. Most dyes are non-biodegradable in nature, which are stable to light and oxidation. Therefore, the degradation of dyes in wastewater either traditional chemical or biological process has not been very effective [5].

Dyes are released into wastewaters from various industrial units, mainly from the dye manufacturing and textiles and other fabric finishing. About a half of global production of synthetic textile dyes (700,000 tons per year) are classified into azo compounds that have the chromophore of $-N=N-$ unit in their molecular structure and over 15 % of the textile dyes are lost in wastewater stream during dyeing operation [4]. The dyes are, generally mutagenic and carcinogenic and can cause severe damage to human beings, such as dysfunction of the kidneys, reproductive system, liver, and brain and central nervous system.

Reactive dyes are most problematic compounds among other dyes in textile wastewater. Reactive dyes are the largest single group of dyes used in the textile industry. It is highly water-soluble and estimated that 10-20% of reactive dyes remain in the wastewater during the production process of these dyes [6] and nearly 50 % of reactive dyes may be lost to the effluent during dyeing processes of cellulose fibers [7]. Wastewater containing reactive dyes has limited biodegradability in an aerobic environment and many azo dyes under anaerobic conditions decompose into potentially carcinogenic aromatic amines [8].

Adsorption process has been found becoming a prominent method of treating aqueous effluent in industrial processes for a variety of separation and purification purposes. This technique is also found to be highly efficient for the removal of colour in terms of initial cost, simplicity of design, ease of operation and insensitivity to toxic substances [9]. Therefore, adsorption using activated carbon is currently of great interest for the removal of dyes and pigments.

Activated carbon has been the most popular and widely used adsorbent in wastewater treatment applications throughout the world. This is due to its high adsorption

capacity, high surface area, microporous structure, and high degree of surface reactivity [10]. In spite of its prolific use, activated carbon remains an expensive material since higher the quality of activated carbon, the greater in cost. Therefore, this situation makes it no longer attractive to be widely used in small-scale industries because of cost inefficiency. Due to the problems mentioned previously, research interest into the production of alternative adsorbent to replace the costly activated carbon has intensified in recent years. Recently, our research group has focused on developing low-cost adsorbents as alternative adsorbent materials. Such alternatives include palm ash [11,12], pomelo (*Citrus grandis*) peel [13], pumpkin seed hull [14], broad bean peels [15], oil palm trunk fibre [16] and durian (*Durio zibethinus Murray*) peel [17].

Recently, chitosan that is used as an adsorbent has drawn attentions due to its high contents of amino and hydroxy functional groups showing high potentials of the adsorption of dyes [18], metal ions [19] and proteins [20]. Chitosan is the deacetylated form of chitin, which is linear polymer of acetylamino-D-glucose. Other useful features of chitosan include its abundance, non-toxicity, hydro-philicity, biocompatibility, biodegradability and anti-bacterial property [21]. Moreover, the adsorption of reactive dyes (Reactive Red 189, Reactive Red 222, Reactive Yellow 2 and Reactive Black 5), basic dyes (methylene blue), and acidic dyes (Acid Orange 51, Acid Green 25) in natural solutions using chitosan shows large adsorption capacities [22]. Although chitosan shows better adsorption ability in the bead form than in the flake form due to its higher specific surface area [23], the weak mechanical property (highly swollen in water) and low specific gravity of the beads make them inconvenient for practical use in column mode adsorption.

Therefore, the objective of this research was to synthesize a chitosan-oil palm ash composite with good adsorption properties. The oil palm ash was chosen because of it is highly abundant in Malaysia. The high oxide contents in palm ash give its structure the creditability as a good adsorbent [11,12]. The effect of initial concentration, contact time, temperature and pH solution were studied experimentally. Characterization of this adsorbent were carried out to obtain its properties. Dynamic study will also be conducted to obtain the breakthrough curves for the pollutants and the adsorption capacity of the adsorbent.

2. Objectives:

The objectives of the research are to:

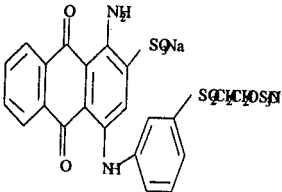
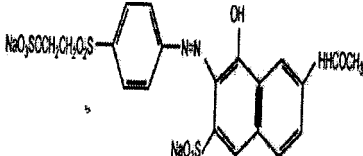
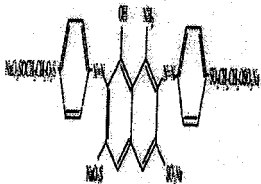
- (1) Synthesize and characterize the composite of chitosan and oil palm ash adsorbents.
- (2) Study the adsorption of reactive azo dyes (RB-19, RO-16 and RB-5) on chitosan/oil palm ash composite in batch process under varying operating conditions such as: effect of adsorption time, effect of initial concentration, effect of pH of solution and effect of temperature.
- (3) Study the kinetic and thermodynamic properties of reactive azo dyes on chitosan/oil palm ash composite.
- (4) Determine the breakthrough characteristic of reactive azo dyes on chitosan/oil palm ash under varying operating parameters namely, initial concentration of adsorbent, flowrate and height of column bed and to correlate the experimental results using suitable adsorption dynamic model.

3. Materials and methods

3.1 Adsorbates

The three reactive azo dyes, Reactive Blue 19 (RB-19), Reactive Orange 16 (RO-16) and Reactive Black 5 (RB-5) used in this work were obtained from Sigma-Aldrich, Malaysia and used without further purification. The properties of the three dyes are summarized in Table 1.

Table 1: Properties of reactive dyes

Chemical Index (C.I.) Name	Reactive blue 19	Reactive orange 16	Reactive black 5
Chemical Index (C.I.) No	61200	17757	20505
Class	Anthraquinone	Azo	Disazo
Ionization	Acid	Acid	Acid
λ_{max}	592	494	597
Colour	Blue	Orange	Black
Mwt.	626.56	617.54	991.82
Molecular formula	$C_{22}H_{16}N_2Na_2O_{11}S_3$	$C_{20}H_{17}N_3Na_2O_{11}S_3$	$C_{26}H_{21}N_5Na_4O_{19}S_6$
Molecular structure			

3.2 Chitosan and oil palm ash

The chitosan derived from deacetylated lobster shell wastes was supplied by Hunza Pharmaceutical Sdn Bhd., Nibong Tebal, Malaysia. The chitosan was washed three times with deionized water and dried in an oven at 50 °C before use. Some properties of chitosan are given in Table 2.

Table 2:

Properties of chitosan flake*

Deacetylation degree	> 90.0%
Solubility in 1% acetic acid	> 99.0%
Moisture	< 10.0%
Ash content	< 1.0%
Appearance	Off-white

* Hunza Pharmaceutical Sdn.Bhd.

The oil palm ash (OPA) was obtained from United Oil Palm Mill, Penang. It was sieved through a stack of U.S. standard sieves and the fine particle size of 63 μm was used. Then, OPA was washed with deionized water and oven dried overnight at 110 °C. OPA (50 g) was activated by refluxing with 250 mL of 1 mol/L H_2SO_4 at 80 °C in a round-bottom flask for 4 hours. The slurry was air-cooled and filtered with a glass fiber. The filter cake was repeatedly washed with deionized water until the filtrate was neutral. It was then dried in an oven at 110 °C before use.

3.3 Preparation of chitosan/oil palm ash composite beads

Chitosan (1g) was dissolved in 1 mol/L acetic acid (100 mL) and mixed with activated oil palm ash (1g) and agitated for 1 hour. Then the viscous solution was sprayed dropwise through a syringe, at a constant rate, into neutralization solution containing 15 % NaOH and 95 % ethanol in a volume ratio of 4:1. They were left in the solution for one day [24]. The formed composite beads were washed with deionized water until solution become neutral and then stored in distilled water.

3.4 Preparation of cross-linked chitosan/oil palm ash composite beads

Epichlorohydrin (ECH) purchased from Sigma-Aldrich was used as cross-linking agent in this study. The procedure for cross-linking was same as reported previously [25]. Basically, wet non-cross-linked chitosan/oil palm ash composite beads (0.1 g dry basis of chitosan) and 50 cm³ of 1N sodium hydroxide solution were poured together in a 500 cm³ flask. ECH was added into the above solution, and shaken for 6 hours at 50 °C with water bath. The molar ratio of cross-linking reagent/chitosan was 0.5. The cross-linking chitosan/oil palm ash composite beads (CC/OPA) were filtered out, washed with deionized water and stored in distilled water. Then, the beads (2-3 mm) were dried in a freeze dryer for 6 h before used as adsorbent.

3.5 Effect of initial concentration and contact time

The adsorption studies of cross-linked chitosan/oil palm ash composite beads using the three dyes were investigated at different initial dye concentration ranging 50-

500 mg/L. A 0.2g adsorbent was added to each 100 mL of adsorbate. The operating temperature was set at $30 \pm 0.1^\circ\text{C}$ and the solutions were shaken at 110 rpm for 48 hrs. At predetermined time intervals or contact time, the sample was withdrawn to analyze the residual dye concentration.

The amount of adsorption at equilibrium time t , q_e (mg/g), is calculated by:

$$q_e = \frac{(C_0 - C_t)V}{W} \quad (1)$$

where C_0 and C_t (mg/L) are the liquid-phase concentrations of dye at initial and any time t , respectively. V is the volume of the solution (L), and W is the mass of dry adsorbent used (g).

3.6 Effect of pH solution

The different of initial pH ranging from 2-13 were prepared by adding 0.1M NaOH or 0.1M HCL. The pH measurement was conducted using pH meter (model Mettler Toledo 320, Switzerland). A 0.2 g adsorbent was added to each 100 ml of dye. The agitation rate was set at 110 rpm and temperature was at $30 \pm 0.1^\circ\text{C}$. At predetermined time intervals, the samples were withdrawn to analyze the residual dye concentration.

3.7 Effect of temperature

The experiment were conducted at 30, 40, 50 °C in order to investigate the effect of temperature on the adsorption process. A 0.2 g adsorbent was added to each 100 mL of

each dye. The solutions were shaken at 110 rpm for 48 hrs. At predetermined time intervals, the samples were withdrawn to analyze the residual dye concentration.

3.8 Batch kinetic studies

The procedures of kinetic experiments are basically identical to those of equilibrium tests. The aqueous samples were taken at present time intervals, and the concentrations of dye were similarly measured. The amount of adsorption at time t , q_t (mg/g), is calculated by:

$$q_t = \frac{(C_0 - C_t)V}{W} \quad (2)$$

where C_t (mg/L) is the liquid-phase concentrations of dye at time t .

3.9 Continuous adsorption system

Fig. 1 shows a schematic diagram of the experimental set up of continuous adsorption system. The feed stock of dye solution was supplied from an amber glass container to the system through a variable-speed peristaltic pump (Masterflex, Cole-Parmer Instrument Co.). The pump was regulated at specified number and the solution flowrate was measured periodically to maintain the desire flowrate of solution along the experiment. The adsorption column was packed with a known amount of adsorbent. The solution was passed through the adsorption column. The time at which the adsorbate load enters the column was recorded. Th input and output concentrations of solution were analyzed periodically using UV/Vis-spectrophotometer. The desired breakthrough

concentration was determined at 10% of inlet initial concentration and the flow through the tested column was continued until the adsorbate concentration of effluent approached $1.0 C_t/C_0$, which indicated the exhaustion point.

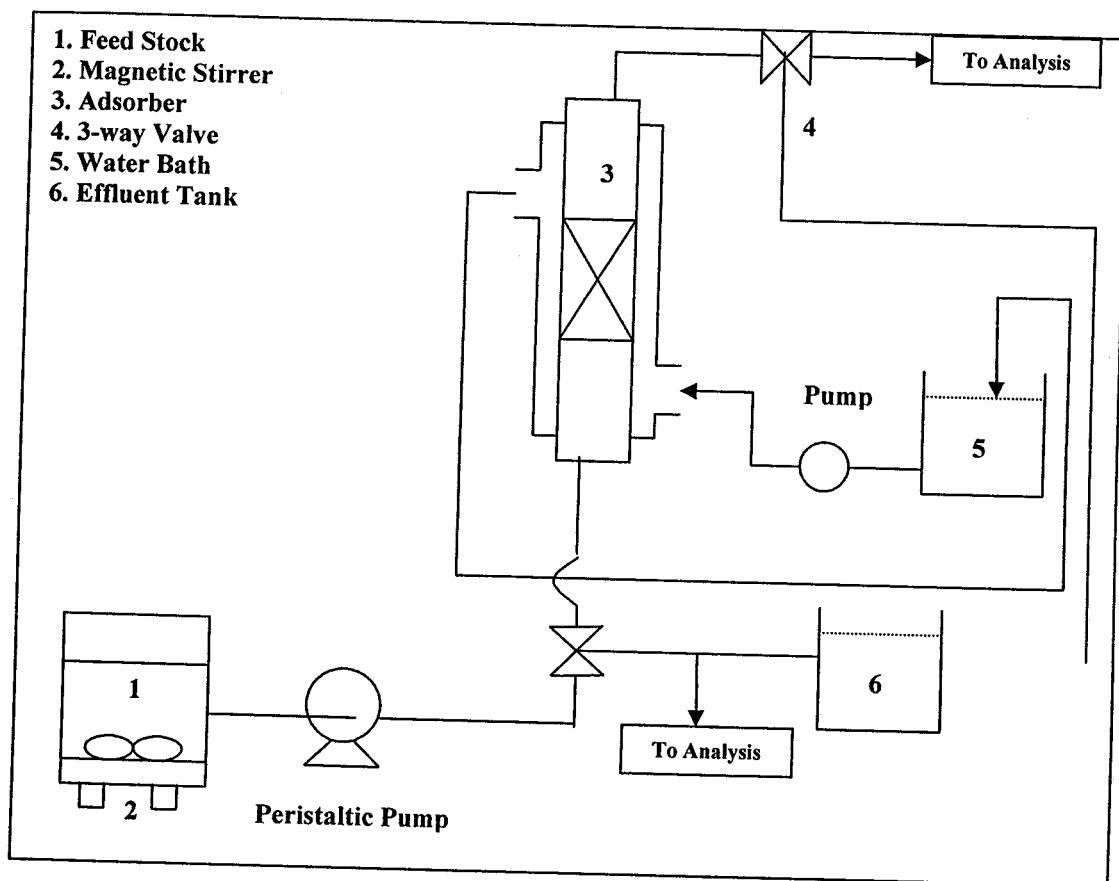


Fig. 1: Schematic diagram of the experimental set up of continuous adsorption system.

3.9.1 Effect of initial concentration of the solute solution

The effect of initial concentration was studied at temperature of $30 \pm 0.1^\circ\text{C}$ by varying the adsorbate concentration 100, 200 and 300 mg/L, respectively. The amount of adsorbent was fixed at 1.4 g while the flowrate was maintained at 15 mL/min.

3.9.2 Effect of height of adsorbent

The experiments were carried out for various amount of adsorbent: 1.2, 1.4 and 1.6 g adsorbent of 1mm particle size which corresponding to 60, 80 and 100 mm of adsorbent height. The influent flowrate and initial adsorbate concentration were preset at 15 mL/min and 200 mg/L, respectively. The experiments were conducted at temperature of $30 \pm 0.1^\circ\text{C}$.

3.9.3 Effect of flowrate

The experiments were conducted at different flowrate of 5, 15 and 25 mL/min at temperature of $30 \pm 0.1^\circ\text{C}$. The bed was packed with 1.4 g of adsorbent and the initial concentration of dyes solution was fixed at 200 mg/L.

4. Results and discussion

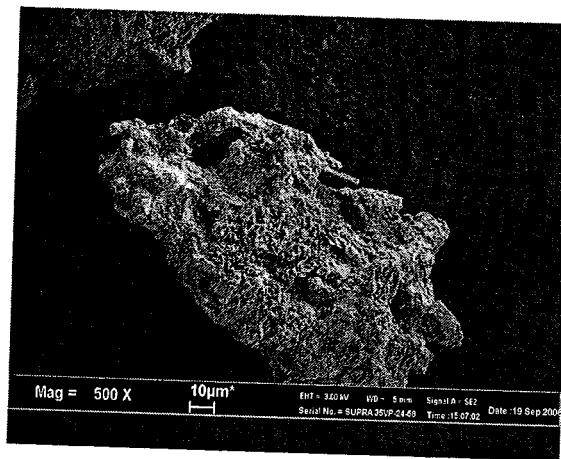
4.1 Characterization of adsorbents

4.1.1 Scanning Electron Microscopy (SEM)

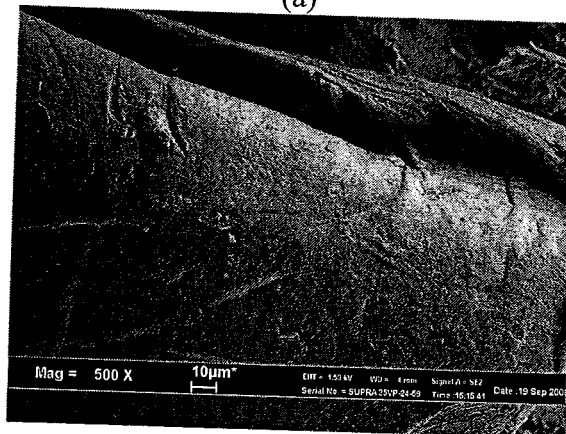
Fig. 2 shows the SEM photographs of fresh oil palm ash, chitosan flake and cross-linked chitosan/oil palm ash composite beads, respectively.

4.1.2 Fourier Transform Infrared (FT-IR) Spectroscopy

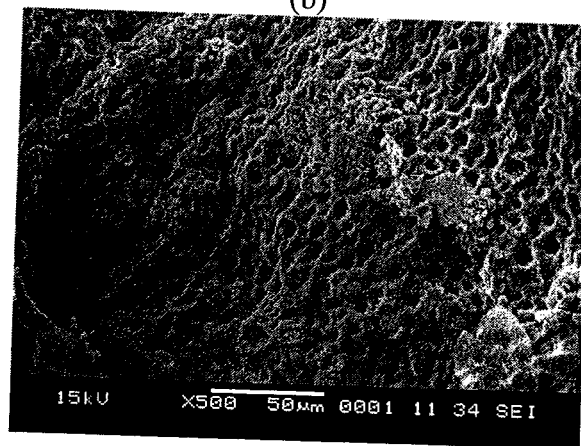
The FTIR spectrum was carried out as a qualitative analysis to determine the main functional groups present in the adsorbent that were involved in the adsorption process.



(a)



(b)



(c)

Fig. 2: SEM images (a) Fresh oil palm ash (X 500 magnification) (b) Chitosan flake (X 500 magnification) (c) Cross-linked chitosan/oil palm ash composite beads (X 500 magnification)

The peaks of 3400.94 cm^{-1} (-OH) alcohols, 2346.28 cm^{-1} (P-H phosphines), 1650.76 cm^{-1} stretching (-N=O), 1459.70 cm^{-1} (-CH₃ antisymmetric deformation), 1407.83 cm^{-1} (CO-NH₂) primary amides, 1048.21 cm^{-1} (-S=O) alkyl sulfoxides, 1010.22 cm^{-1} (ring vibration) are the original peaks of fresh oil palm ash (Figure 4.1 (a)). However, Fig. 3 (b) (activated oil palm ash) shows the peak at 3400.94 cm^{-1} (-OH) alcohol shifted to be 3411.54 cm^{-1} , peak at 1650.76 cm^{-1} (-N=O) shifted to 1624.31 cm^{-1} , the peak 1048.21 cm^{-1} (alkyl sulfoxides) shifted to 1054.64 cm^{-1} , respectively. Furthermore, the new peaks appeared at 1459.70 cm^{-1} (-CH₂), whereas 2 peaks was disappeared 2346.28 cm^{-1} (P-H) and 1010.22 cm^{-1} (ring vibration).

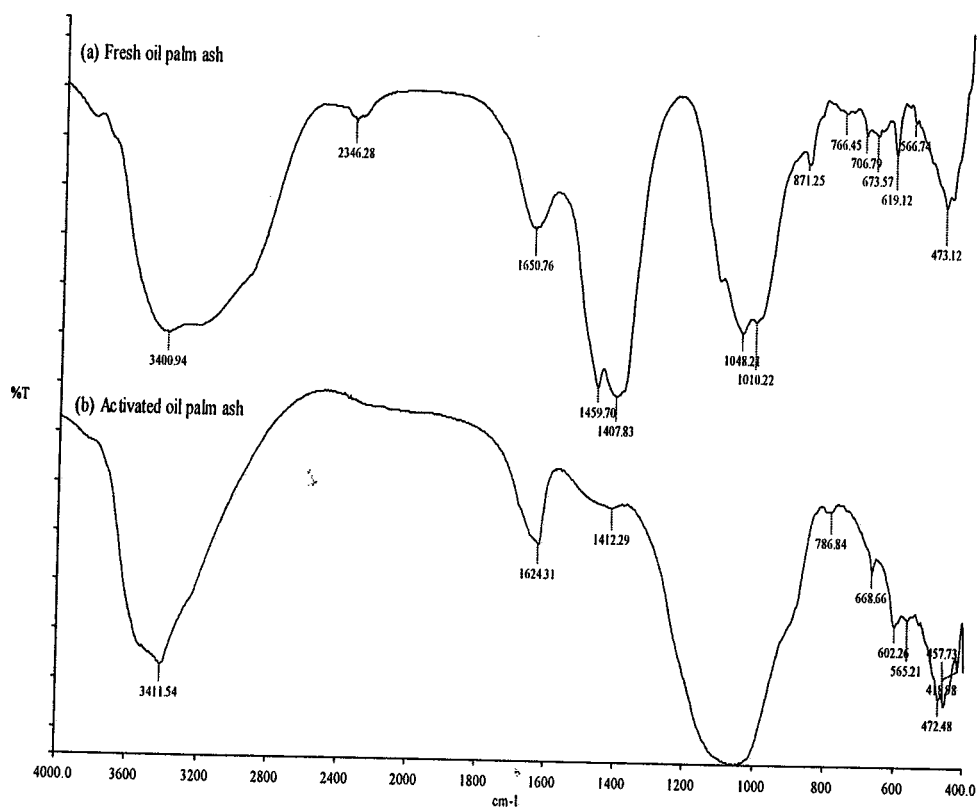


Fig. 3: FT-IR spectra of (a) Fresh oil palm ash and (b) activated oil palm ash

Fig. 4 shows FTIR spectra of chitosan flake. The peaks are 3446.41 cm^{-1} ($-\text{NH}_2$), 2906.01 cm^{-1} ($-\text{CH}_2$), 2362.38 cm^{-1} ($-\text{NH}_3$), 2344.96 cm^{-1} (P-H), 2272.59 cm^{-1} (diazonium salts), 1648.04 cm^{-1} ($\text{C}=\text{N}$ -), 1423.64 cm^{-1} (NH deformation), 1375.72 cm^{-1} (CH_3 deformation), 1340.58 cm^{-1} ($-\text{SO}_2\text{NH}_2$), 1323.99 cm^{-1} ($-\text{NO}_2$) aromatic nitro compound, 1250.03 cm^{-1} (t-butyl), 1150.92 cm^{-1} ($-\text{C}=\text{S}$), 1083.97 cm^{-1} (Si-O-Si and Si-O-C) silicones and silanes group, 1036.40 cm^{-1} ($-\text{C}-\text{O}-\text{C}$) and 895.17 cm^{-1} (CH), respectively.

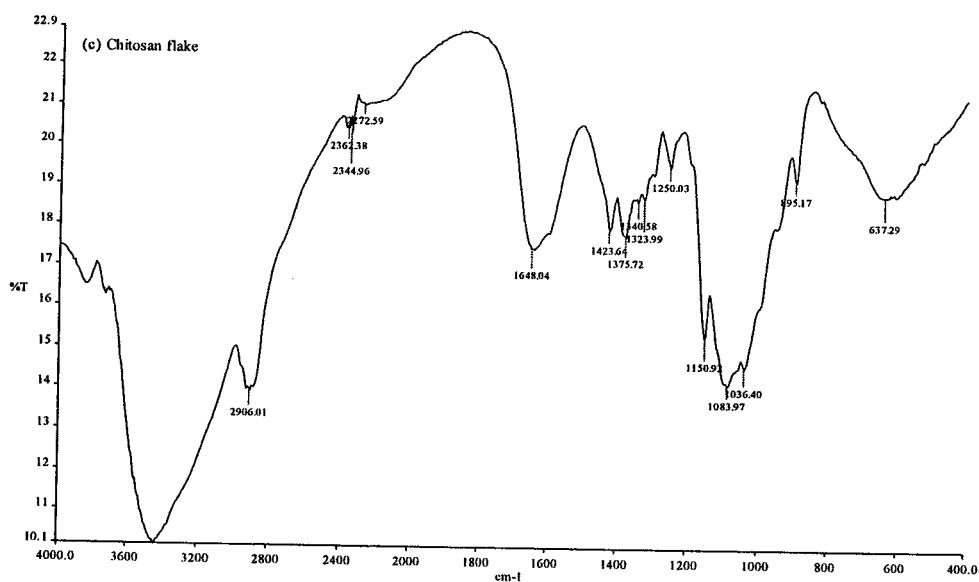


Fig. 4: FT-IR spectra of chitosan flake

Fig. 5 (d, e) represents FTIR spectra of cross-linked chitosan/oil palm ash composite beads and chitosan/oil palm ash composite beads. The spectrum for chitosan/oil palm ash composite beads displayed the following bands:

- 3436.38 cm^{-1} : ($-\text{NH}_2$) aromatic and primary amines
- 2978.00 cm^{-1} : two bands for $-\text{CH}_2$ group
- 2929.05 cm^{-1} : two band for $-\text{CH}_2$ group

- 2363.88 cm^{-1} : sharp peak of phosphines (P-H)
- 2116.51 cm^{-1} : silanes, azides
- 1638.66 cm^{-1} : two band of primary amides
- 1423.75 cm^{-1} : NH deformation
- 1376.04 cm^{-1} : (C-CH₃), CH₃ deformation,
- 1080.14 cm^{-1} : sulfonic acids (-SO₂H),

The spectrum for cross-linked chitosan/oil palm ash composite beads displayed the following bands:

- 3446.12 cm^{-1} : (-NH₂) aromatic and primary amines
- 2978.00 cm^{-1} : two bands for -CH₂ group
- 2126.36 cm^{-1} : silanes, azides
- 1638.81 cm^{-1} : -NH₃⁺
- 1424.97 cm^{-1} : NH₄⁺ ion, NH deformation
- 1340.41 cm^{-1} : (-SO₂NH₂), sulfonamides
- 1320.41 cm^{-1} : -NO₂, aromatic nitro compounds
- 1152.48 cm^{-1} : sulfonamide (-SO₂NH₂).
- 1064.04 cm^{-1} : cyclic alcohols (-CH-O-H)
- 1035.54 cm^{-1} : (P-O-C), aliphatic compounds

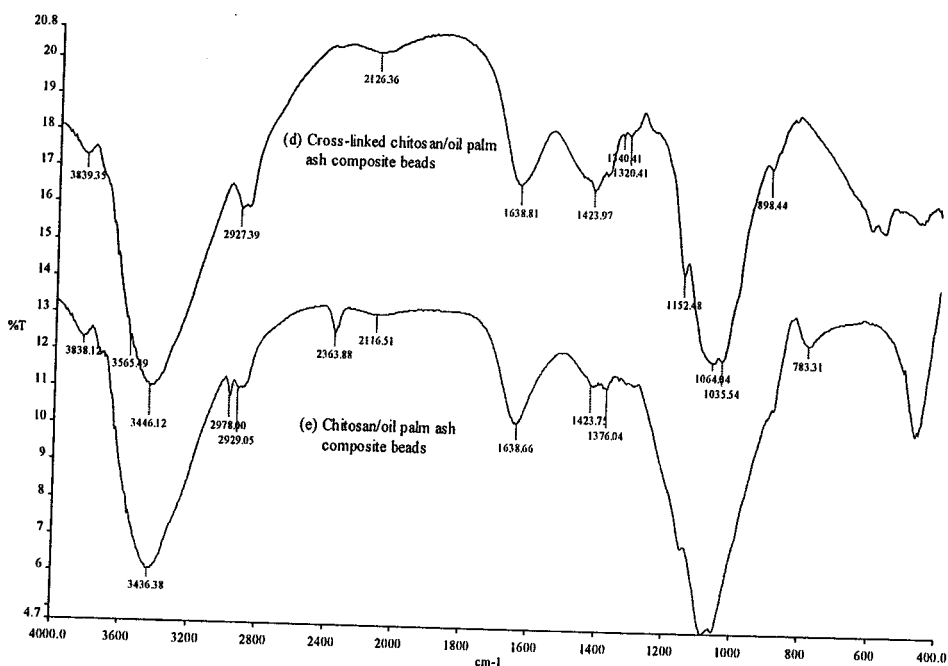


Fig. 5: FT-IR spectra of (d) cross-linked chitosan/oil palm ash composite bead (e) chitosan/oil palm ash composite beads

4.2 Effect of initial concentration of dyes and contact time

The effect of initial concentration on dyes adsorption by cross-linked chitosan/oil palm ash composite beads was studied at different initial RB19, RO16 and RB5 concentrations as shown in Fig. 6 a, b and c. This parameter was studied at temperature 30 °C and without any pH adjustment (pH=6.2).

The adsorption capacity at equilibrium increases from 43.4 mg/g to 423.5 mg/g, with increase in the initial dye concentration from 50 to 500 mg/L for RB19 dye. This similar trend was observed for RO16 and RB5 dye when an increase in initial dye concentration leads to increase in the adsorption capacity of dye on cross-linked chitosan/oil palm ash composite beads for temperature 30°C. Similar trend was observed for the amount of adsorbed dyes of RB 19, RO16 and RB5 at 40°C and 50°C, respectively (Figs. not shown). This indicates that initial dye concentrations played an important role

on the adsorption of RB19, RO16 and RB5 on the cross-linked chitosan/oil palm ash composite beads.

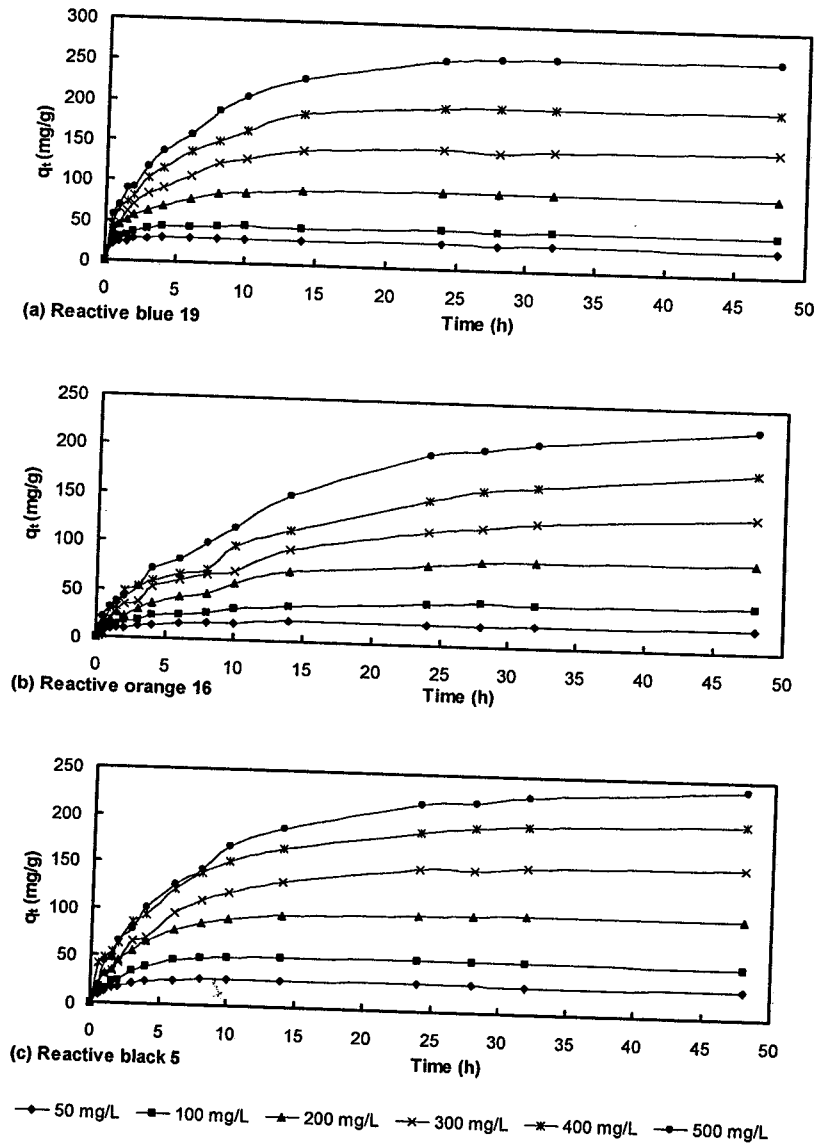


Fig. 6 Effect of initial concentration and contact time on the uptake of (a) reactive blue 19 (b) reactive orange 16 and (c) reactive black 5 on cross-linked chitosan/oil palm ash composite adsorbent (W=0.2g, pH= 6.2, Temperature= 30⁰C)

4.3 Effect of solution pH

The effect of pH for adsorption of RB19, RO16 and RB5 on cross-linked chitosan/oil palm ash composite beads was studied over a pH range of 2-13 at 30 °C. The studies were carried out for 24 h at constant initial dye concentration, 200 mg/L and agitation speed, 110 rpm. Fig. 7 shows the effect of pH on the adsorption of RB19, RO16 and RB5 dyes on cross-linked chitosan/oil palm ash composite beads.

As can be seen from Fig. 7, at pH 2-5 the uptake of RB19 dye by adsorption on cross-linked chitosan/oil palm ash composite beads slowly increased from 82.8 mg/g to 99.5 mg/g (89 - 93% percent removal). However, higher uptake was observed in the pH range 6-8 (108.2 mg/g), which is evident that maximum adsorption was achieved for RB19. Furthermore, the uptake of RB19 was sharp decreased to 35.2 mg/g by increasing the pH of solution from 10 to 13.

It can be seen that the uptake for adsorption RB5 dye on cross-linked chitosan/oil palm ash composite beads exhibited a maximum uptake of 105.8 mg/g at pH 2. On the other hand, a gradually decrease uptake trend was observed with increasing solution pH from 3 to 8. In contrast, a sharp decrease was observed at pH 9, reducing the adsorption capacity to 8.42 mg/g. The trend was similar to the adsorption of RO16 on cross-linked chitosan/oil palm ash composite beads. The uptake of RO16 dye was a maximum at pH 2 at 100.7 mg/g. However, the uptake within acidic solution with pH 3 to 9 was about 88.8 to 80.3 mg/g. However, increase in pH from 10 -13 greatly decreased the uptake of RO16 to 10.9 mg/g.

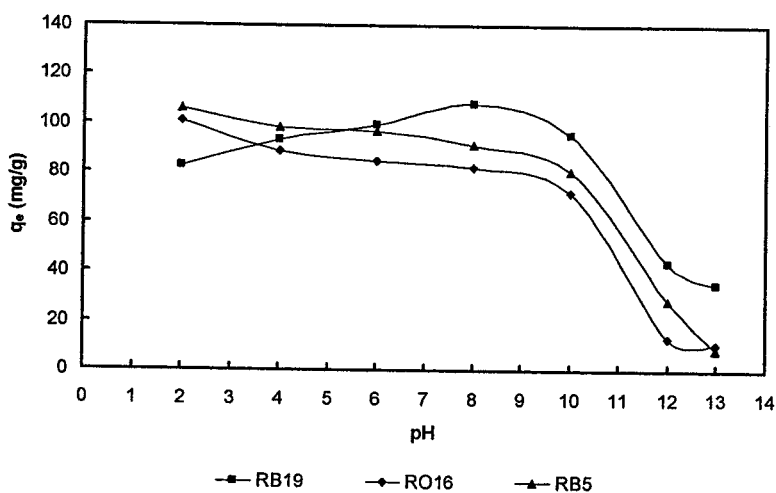


Fig. 7: Effect of pH on adsorption of RB19, RO16 and RB5 on cross-linked chitosan/oil palm ash composite beads.

4.4 Effect of temperature

The effect of temperature on the adsorption of the three adsorbate namely, RB19, RO16 and RB5 dyes onto cross-linked chitosan/oil palm ash composite beads was studied at 30, 40 and 50 °C. Fig. 8 (a), (b) and (c) shows that the dyes uptake increased as the temperature increased for all dyes, except for RB5. The adsorbed RB19 and RO16 dyes amounts increased with increasing the temperature from 30 to 50 °C. However, at 50 °C, both dyes were strongly adsorbed by the cross-linked chitosan/oil palm ash composite beads and it slightly decreased at 30 °C. For RB19 and RO16 dyes, there is a slight increase between 40 and 50 °C.

It was different for RB5 dye trends. It can be seen from Fig. 8 (c), the adsorbed amount of RB5 dye decreased with increased in the temperature studied. Amount of RB5 dye adsorbed higher at 30 °C while lower uptake of dye at 40 °C. This trend could be explained due to RB5 dye structure contains two azo chromophore. This chromophores makes the RB5 dye difficult to degrade even the temperature of the system was

increased. Therefore, the process is exothermic for adsorption of RB5 dye onto cross-linked chitosan/oil palm ash composite beads.

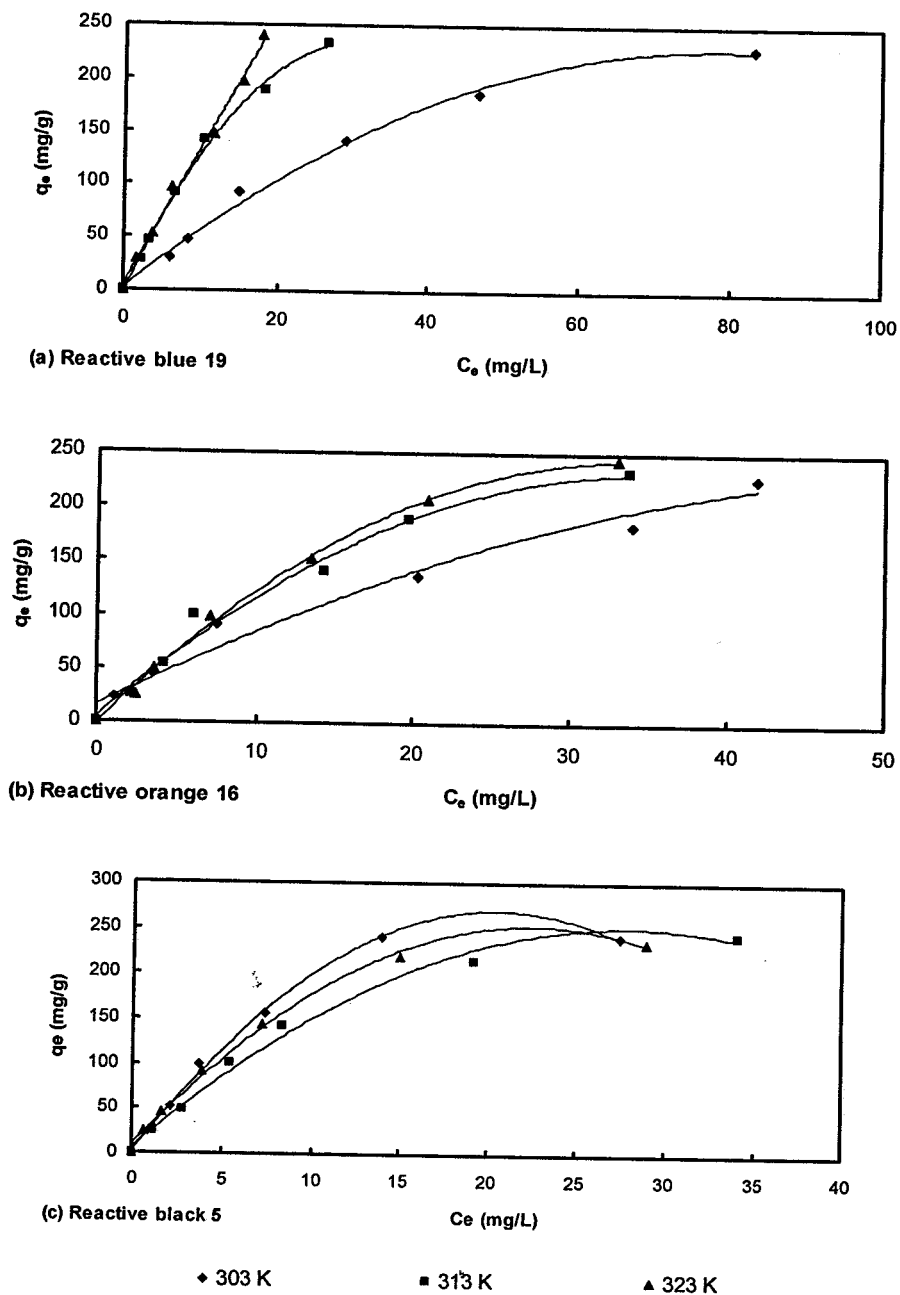


Fig. 8: Plots of equilibrium adsorption of (a) reactive blue 19 (b) reactive orange 16 and (c) reactive black 5 on cross-linked chitosan/oil palm ash composite beads adsorbent

Further, it is clear that the process are endothermic in nature onto adsorption of cross-linked chitosan/oil palm ash composite beads for RB19 and RO16 dyes studied, where increasing the temperature increases the value of adsorption capacity. Results indicate that the adsorption capacity of cross-linked chitosan/oil palm ash composite beads for adsorption of dyes increase with increasing temperature which is typical for the adsorption of most organics from their solutions. The effect of temperature is fairly common and increasing the temperature increases the mobility of the dye molecule.

4.5 Adsorption isotherm

The experimental data of the three dyes at different temperatures were fitted to the Langmuir, Freundlich, Temkin and Dubinin-Raduskevich models and the results are listed in Tables 3-5.

4.6 Kinetic study

The experimental data were fitted to the pseudo-first-order and pseudo-second-order kinetic models and intraparticle diffusion model and the results are listed in Table 6-8. In order to quantitatively compare the applicability of each solid-phase kinetic model, pseudo-first-order, pseudo-second-order and intraparticle diffusion, a normalized standard deviation Δq (%) is calculated:

$$\Delta q(\%) = 100 \times \sqrt{\frac{\sum [(q_{\text{exp}} - q_{\text{cal}}) / q_{\text{exp}}]^2}{(n-1)}} \quad (3)$$

where n is the number of data points.

Table 3: Adsorption constants of RB19 on cross-linked chitosan/palm ash composite adsorbent using Langmuir, Freundlich, Temkin and Dubinin-Radushkevich isotherm model

Adsorbate	Isotherm	Temperature (°C)	Constants				
			Q ₀ (mg/g)	b (L/mg)	R ²	R _L	
RB19	Langmuir	30	416.7	0.02	0.93	0.172	
		40	666.7	0.02	0.72	0.133	
		50	909.1	0.02	0.60	0.154	
	Freundlich	Temperature (°C)	K _F (mg/g)(L/mg) ^{1/n}	n	R ²		
			30	9.62	1.32	0.96	
			40	15.43	1.15	0.97	
		50	18.30	1.14	0.99		
		Temkin	Temperature (°C)	K _t (L/mg)	B ₁	R ²	
				30	0.23	76.62	1.00
40	0.52			85.10	0.99		
50	0.63	85.37	0.91				
Dubinin-Radushkevich	Temperature (°C)	q _m (mg/g)	E (J/mol)	R ²			
		30	168.90	223.61	0.91		
		40	174.15	500.00	0.92		
		50	155.30	707.11	0.76		

Table 4: Adsorption constants of RO16 on cross-linked chitosan/palm ash composite adsorbent using Langmuir, Freundlich, Temkin and Dubinin-Radushkevich isotherm model

Adsorbate	Isotherm	Temperature (°C)	Constants					
			Q_0 (mg/g)	b (L/mg)	R^2	R_L		
RO16	Langmuir	30	303.0	0.05	0.94	0.058		
		40	434.8	0.04	0.87	0.086		
		50	588.2	0.02	0.73	0.123		
	Freundlich	Temperature (°C)	K_F (mg/g)(L/mg) ^{1/n}	n	R^2			
			30	21.67	1.60	0.99		
			40	17.71	1.28	0.95		
		50	15.12	1.17	0.96			
		Temkin	Temperature (°C)	K_t (L/mg)	B_1	R^2		
				30	0.88	54.85	0.93	
40	0.57			75.43	0.98			
Dubinin-Radushkevich	Temperature (°C)	q_m (mg/g)	E (J/mol)	R^2				
					30	132.20	790.57	0.72
					40	161.90	500.00	0.86
					50	183.60	408.25	0.93

Table 5: Adsorption constants of RB5 on cross-linked chitosan/palm ash composite adsorbent using Langmuir, Freundlich, Temkin and Dubinin-Radushkevich isotherm model

Adsorbate	Isotherm	Temperature ($^{\circ}\text{C}$)	Constants							
			Q_0 (mg/g)	b (L/mg)	R^2	R_L				
RB5	Langmuir	30	357.1	0.08	0.97	0.023				
		40	344.8	0.07	0.98	0.028				
		50	303.0	0.12	1.00	0.016				
	Freundlich	Temperature ($^{\circ}\text{C}$)	K_F (mg/g)(L/mg) $^{1/n}$	n	R^2					
						30	30.57	1.44	0.96	
						40	26.13	1.46	0.95	
		50	35.42	1.62	0.97					
		Temkin	Temperature ($^{\circ}\text{C}$)	K_t (L/mg)	B_1	R^2				
							30	1.10	70.75	0.85
							40	0.97	66.42	0.98
		50	1.66	58.66	0.97					
		Dubinin-Radushkevich	Temperature ($^{\circ}\text{C}$)	q_m (mg/g)	E (J/mol)	R^2				
	30						167.00	790.57	0.85	
	40						152.10	790.57	0.80	
	50						146.30	1290.99	0.77	

Table 6: Comparison between Pseudo-first-order, Pseudo-second-order models for RB19 dye adsorption on cross-linked chitosan/palm ash composite beads at different concentration and 30⁰C

Pseudo-first-order model					
Initial dye concentration (mg/L)	q_{e,exp} (mg/g)	q_{e,cal} (mg/g)	k_f (1/h)	R²	Δq (%)
50	30.81	12.49	0.460	0.76	0.21
100	47.40	30.54	0.419	0.91	2.13
200	91.53	69.57	0.292	0.95	2.67
300	140.71	117.54	0.217	0.96	2.39
400	185.73	159.85	0.205	0.97	2.31
500	229.28	197.83	0.181	0.96	2.99
Pseudo-second-order model					
Initial dye concentration (mg/L)	q_{e,exp} (mg/g)	q_{e,cal} (mg/g)	k_s (g/mg h)	R²	Δq (%)
50	30.81	30.12	0.193	1.00	1.19
100	47.40	46.51	0.049	0.99	1.02
200	91.53	82.64	0.018	0.97	0.82
300	140.71	116.28	0.009	0.95	0.68
400	185.73	149.25	0.006	0.93	0.65
500	229.28	175.44	0.005	0.92	0.62

Table 7: Comparison between Pseudo-first-order, Pseudo-second-order models for RO16 dye adsorption on cross-linked chitosan/palm ash composite beads at different concentration and 30⁰C

Pseudo-first-order model					
Initial dye concentration (mg/L)	q_{e,exp} (mg/g)	q_{e,cal} (mg/g)	k_f (1/h)	R²	Δq (%)
50	23.02	18.61	0.147	0.95	0.19
100	45.33	37.61	0.099	0.96	7.20
200	90.43	82.24	0.098	0.97	5.95
300	136.93	126.36	0.075	0.96	2.21
400	183.78	167.73	0.062	0.95	4.11
500	227.82	216.32	0.069	0.99	2.93
Pseudo-second-order model					
Initial dye concentration (mg/L)	q_{e,exp} (mg/g)	q_{e,cal} (mg/g)	k_s (g/mg h)	R²	Δq (%)
50	23.02	23.58	0.016	0.88	0.60
100	45.33	38.17	0.012	0.95	0.65
200	90.43	76.34	0.004	0.87	0.59
300	136.93	147.06	0.001	0.34	0.63
400	183.78	128.21	0.002	0.86	0.65
500	227.82	172.41	0.001	0.82	0.65

Table 8: Comparison between Pseudo-first-order, Pseudo-second-order models for RB5 dye adsorption on cross-linked chitosan/palm ash composite beads at different concentration and 30⁰C

Pseudo-first-order model					
Initial dye concentration (mg/L)	q_{e,exp} (mg/g)	q_{e,cal} (mg/g)	k_f (1/h)	R²	Δq (%)
50	28.42	22.87	0.376	0.98	1.37
100	52.37	54.20	0.369	1.00	1.53
200	100.22	91.66	0.235	1.00	1.94
300	156.10	150.56	0.148	0.99	1.75
400	202.99	182.47	0.133	0.98	3.81
500	239.79	226.73	0.112	0.98	1.07
Pseudo-second-order model					
Initial dye concentration (mg/L)	q_{e,exp} (mg/g)	q_{e,cal} (mg/g)	k_s (g/mg h)	R²	Δq (%)
50	28.42	29.94	0.034	0.98	0.88
100	52.37	61.35	0.007	0.89	0.71
200	100.22	101.01	0.005	0.91	0.65
300	156.10	142.86	0.002	0.77	0.59
400	202.99	156.25	0.003	0.88	0.59
500	239.79	188.68	0.002	0.79	0.60

4.7 Intraparticle diffusion model

The experimental results were further fitted to the intraparticle diffusion model and the results are listed in Table 9.

Table 9: Intraparticle diffusion models for RB19, RO16 and RB5 dyes

Reactive Blue 19

Initial dye concentration (mg/L)	$q_{e,exp}$ (mg/g)	$q_{e,cal}$ (mg/g)	k_i (g/mg h ^{0.5})	R^2	Δq (%)
50	30.81	78.75	16.08	0.13	5.50
100	47.40	108.62	22.17	0.29	2.32
200	91.53	135.52	36.22	0.77	9.34
300	140.71	173.77	46.44	0.96	11.34
400	185.73	216.99	57.99	0.98	13.00
500	229.28	252.05	67.36	0.97	14.44

Reactive Orange 16

Initial dye concentration (mg/L)	$q_{e,exp}$ (mg/g)	$q_{e,cal}$ (mg/g)	k_i (g/mg h ^{0.5})	R^2	Δq (%)
50	23.02	42.36	6.11	0.85	4.85
100	45.33	70.44	10.17	0.95	3.46
200	90.43	142.48	20.56	0.95	9.00
300	136.93	164.60	23.75	0.95	11.80
400	183.78	201.43	29.07	0.96	11.85
500	227.82	248.25	35.82	0.96	14.02

Reactive Black 5

Initial dye concentration (mg/L)	$q_{e,exp}$ (mg/g)	$q_{e,cal}$ (mg/g)	k_i (g/mg h ^{0.5})	R^2	Δq (%)
50	28.42	59.19	11.19	0.84	5.39
100	52.37	96.56	18.25	0.97	4.42
200	100.22	152.89	31.21	0.99	10.08
300	156.10	250.57	36.16	0.95	12.23
400	202.99	336.20	48.51	0.99	13.22
500	239.79	334.76	48.31	0.96	14.98

4.8 Thermodynamic studies

The thermodynamic parameters for adsorption of RB19, RO16 and RB5 dyes are listed in Tables 10.

Table 10: Thermodynamic parameters for adsorption of r RB19, RO16 and RB5 dyes

Adsorbate	Temperature (°C)	ΔG° (kJ/mol)	ΔH° (kJ/mol)	ΔS° J/(mol K)
Reactive Blue 19	30	-3.86	46.21	166.20
	40	-6.43		
	50	-7.15		
Reactive Orange 16	30	-5.59	6.78	41.07
	40	-6.22		
	50	-6.57		
Reactive Black 5	30	-7.27	-3.48	11.60
	40	-6.92		
	50	-5.15		

4.9 Activation energy

The values of activation energy, E_a can be evaluated using a pseudo-second-order rate constant, k_2 dependence on reciprocal temperature. By assuming that the correlation of the rate constant k_2 for pseudo-second-order reaction follows the Arrhenius equation,

$$\ln k_2 = \ln A - \frac{E_a}{RT} \quad (4)$$

where E_a is the Arrhenius activation energy (kJ/mol), A is Arrhenius factor, R is gas constant (8.314 J/mol K), and T is the solution temperature (K). The values of E_a were

obtained from the slope of plot between $\ln k_2$ versus $1/T$. Table 11 listed the results for the three dyes.

Table 11: Activation values for adsorption of reactive dyes

Adsorbent	Adsorbate	Activation energy, E (kJ/mol)
Cross-linked chitosan/oil palm ash composite beads	Reactive Blue 19	12.92
	Reactive Orange 16	2.24
	Reactive Black 5	16.29

4.10 Column adsorption studies

The performance of column adsorption studies of reactive blue 19 (RB19), reactive orange 16 (RO16) and reactive black 5 (RB5) were conducted on cross-linked chitosan/oil palm ash composite beads. The experimental tests were carried out at room temperature (30°C) without any adjustment of pH solution. Several experimental parameters for column/continuous adsorption studies were: (a) Effect of initial dye concentration (b) Effect of flowrate and (c) Effect of adsorbent height.

These parameters are discussed and evaluated using column performance analysis. The total amount of dye adsorbed in the column can be calculated using the following equation:

$$q_{total} = \frac{QA_b}{1000} = \frac{Q}{1000} \int_{t=0}^{t=total} C_{ads} dt \quad (5)$$

where Q is volumetric flowrate (mL/min), t_{total} is total flow time (min) and A_b is the area under the breakthrough curve which can be obtained by integrating the adsorbed dye concentration (C_{ads} (mg/L) = inlet dye concentration (C_0) – effluent dye concentration

(C_t) versus time, t (min). Moreover, the equilibrium dye uptake (q_{eq}) (or column capacity) in the column is defined as the total amount of dye adsorbed (q_{total}) per gram of sorbent (X) as shown in Equation (4.5), and the volume of effluent at specific time was calculated based on equation (4.6), respectively.

$$q_{eq} = \frac{q_{total}}{X} \quad (6)$$

$$V_{eff} = Qt_{total}$$

4.10.1 Effect of initial dye concentration

Fig. 9 (a), (b) and (c) show the effect of initial dye concentration on the shape of breakthrough curves at of $30 \pm 0.1^\circ\text{C}$ varying the adsorbate concentration 100, 200 and 300 mg/L, respectively. This concentration was chosen because the textile industry effluents discharge higher intensity of colour (dye). The amount of adsorbent was fixed at 1.4 g while the flowrate was maintained at 15 mL/min.

As shown in Fig. 9 (a), in the interval of 10 min, the value of C_t/C_0 reached 0.48, 0.54 and 0.84 when influent concentration was 100, 200 and 300 mg/L, respectively. Results showed that higher the influent reactive blue 19 (RB19) dye concentration, the lower will be the breakthrough time. At lower influent RB19 dye concentrations, breakthrough curves were dispersed and slower. Similar trend occurred for all adsorption systems both on reactive orange 16 (RO16) and reactive black 5 (RB5). As influent concentration increased, sharper breakthrough curves were obtained.

The result in Table 12 showed higher amount of dyes were adsorbed (q_{total}) when the initial dye concentration is 300 mg/L. Similarly, an increase in initial dye concentration would increase the capacity of column (q_e). The larger the influent dye

concentration, the steeper is the slope of breakthrough curve and smaller is the breakthrough time. This indicated that the change of concentration gradient affects the saturation rate and breakthrough time, or in other words, the diffusion process is concentration dependent.

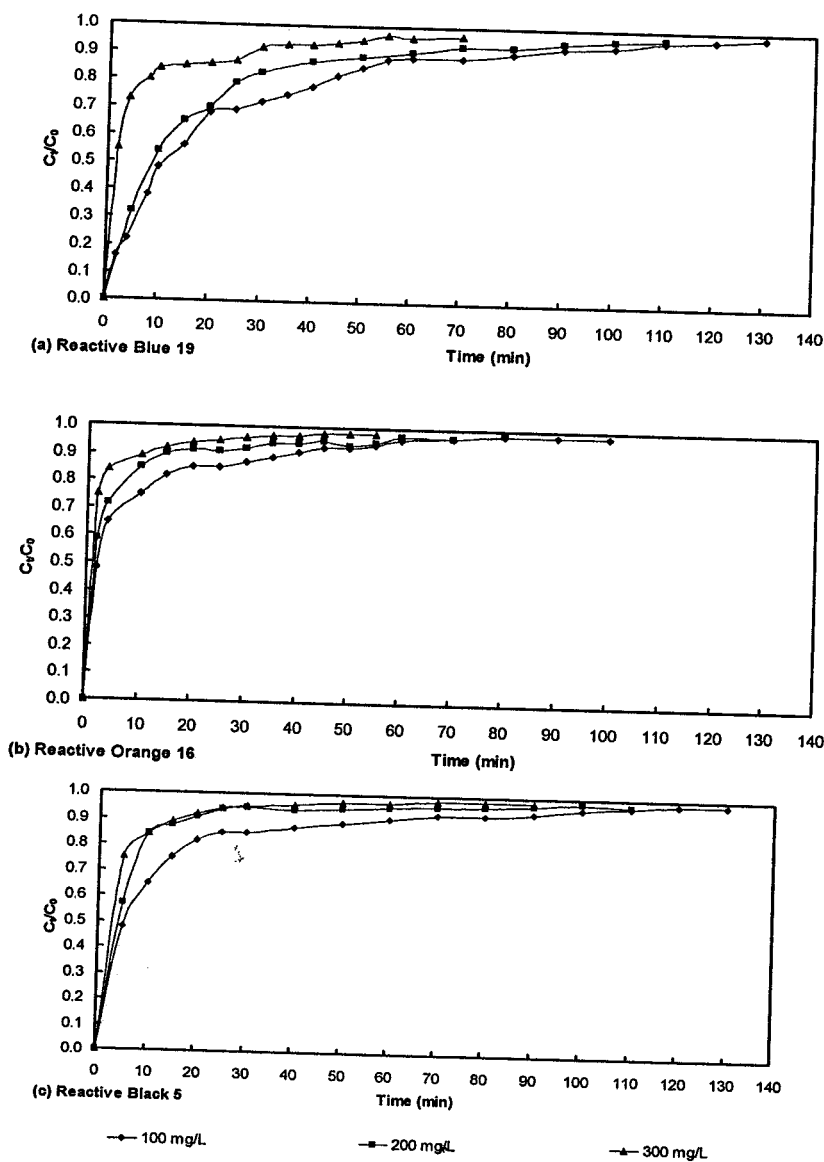


Fig. 9: Breakthrough curves of (a) reactive blue 19, (b) reactive orange 16 and (c) reactive black 5 on cross-linked chitosan/oil palm ash composite beads at different initial concentrations. (80 mm bed height; 15 mL/min flowrate ; 30 °C temperature)

Table 12: The performance of column for adsorption of reactive dyes at different initial concentration, 80mm height of adsorbent and 15 mL/min flowrate.

Adsorbate	Initial conc. (mg/L)	q _{total} (mg)	t _{total} (min)	q _{eq} (mg/g)
Reactive blue 19	100	139.09	130	99.35
	200	343.46	110	245.32
	300	354.06	80	252.90
Reactive orange 16	100	136.08	100	97.20
	200	240.63	80	171.88
	300	262.44	55	187.46
Reactive black 5	100	173.45	130	123.89
	200	308.53	110	220.38
	300	407.56	90	291.11

4.10.2 Effect of flow rate

Fig. 10 (a), (b) and (c) shows the breakthrough curves for different flow rate of RB19, RO16 and RB5 dyes, respectively. The experiments were conducted at different flowrate of 5, 15 and 25 mL/min at $30 \pm 0.1^\circ\text{C}$. The bed was packed with 1.4 g of adsorbent (80 mm) and the initial concentration of dyes solution was fixed at 200 mg/L. It was shown that the breakthrough occurred faster at higher flow rate. The breakthrough time reach a saturation period faster with a decreased in the flow rate. At low flow rate, RB19 dye had more time to contact with cross-linked chitosan/oil palm ash composite beads, thus inducing in higher removal of RB19 dye in column. Similar trend was also observed for RO16 and RB5 dyes.

As seen in Table 13, the greatest amount of adsorbate adsorbed (q_{total}) and the highest adsorption column capacity (q_{eq}) was observed at the lowest flowrate of 5 mL/min. The variation in the trend of the breakthrough curve and adsorption column capacity may be explained on the basis of mass transfer fundamentals. This behaviour may be due to insufficient time for the adsorbate inside the column and the diffusion limitations of the adsorbate into the pores of the adsorbent at higher flowrates.

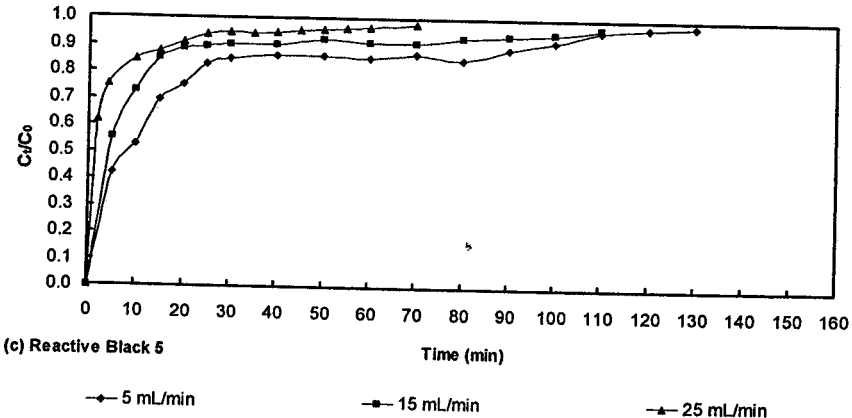
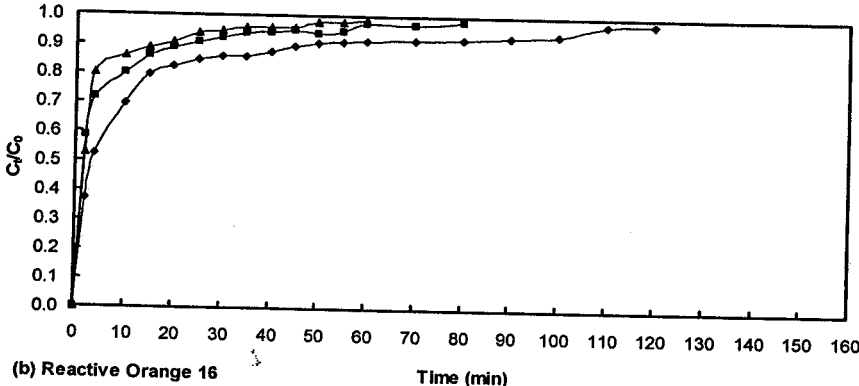
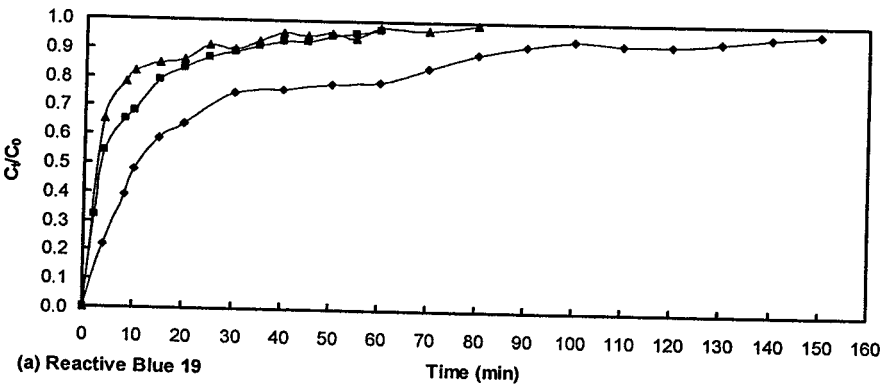


Fig. 10: Breakthrough curve of (a) reactive blue 19, (b) reactive orange 16 and (c) reactive black 5 on cross-linked chitosan/oil palm ash composite beads at different flowrates. (80 mm bed height; 200 mg/L initial concentration; 30 °C temperature)

Table 13 The performance of column for adsorption of reactive dyes at different flowrate, 80mm height of adsorbent and 200mg/L initial concentration.

Adsorbate	Flowrate (mL/min)	q _{total} (mg)	t _{total} (min)	q _{eq} (mg/g)
Reactive blue 19	5	417.00	150	297.86
	15	343.46	110	245.33
	25	239.49	80	171.06
Reactive orange 16	5	367.40	120	262.43
	15	240.63	80	171.88
	25	183.33	60	130.95
Reactive black 5	5	376.25	130	268.75
	15	308.53	110	220.38
	25	204.55	80	146.11

4.10.3 Effect of adsorbent height

Fig. 11 (a), (b) and (c) showed the breakthrough curve of various amount of adsorbent (1.2, 1.4 and 1.6 g adsorbent) which correspond to 60, 80 and 100 mm of adsorbent height. The influent flow rate and initial adsorbate concentration were 15 mL/min and 200 mg/L, respectively. From Fig. 11, as the bed height increases, dyes had more time to contact with cross-linked chitosan/oil palm ash composite bead that resulted in higher removal efficiency of RB19 dye in column.

As presented in Table 14, the total amount of adsorbate adsorbed (q_{total}) was found to increase with the increase of bed height from 60 to 100 mm. High dye uptake

Further, from Table 14, the values of t_{total} were found to be increased by increasing the bed height. So the higher bed height resulted in a decrease in the solute concentration in the effluent at the same time. The slope of breakthrough curve decreased with increasing bed height, which resulted more contact between adsorbent and adsorbate. Hence, increase the broadened of mass transfer zone. Therefore, the bed of higher amount of adsorbent was saturated slower than the one with small amount of adsorbent because of its greater number of active sites available in the system.

Table 14: The performance of column for adsorption of reactive dyes on at different height, 15 mL/min flowrate and 200mg/L initial concentration.

Adsorbate	Height of adsorbent (mm)	q_{total} (mg)	t_{total} (min)	q_{eq} (mg/g)
Reactive blue 19	60	268.65	90	223.88
	80	343.46	110	245.32
	100	365.00	140	228.13
Reactive orange 16	60	131.96	45	109.97
	80	240.63	80	171.88
	100	343.65	110	214.78
Reactive black 5	60	207.14	70	172.62
	80	308.53	110	220.38
	100	431.51	140	263.44

4.10.4 Breakthrough curve models

The experimental data for the adsorption of reactive blue 19 (RB19), reactive orange 16 (RO16) and reactive black 5 (RB5) on cross-linked chitosa/oil palm ash

composite beads were fitted to three models, namely Yoon and Nelson model, Thomas model and Bohart and Adams model at 30°C, 200 mg/L of initial dye concentration, 80 mm adsorbent height and flow rate of 15 mL/min. The fitted of experimental and calculated data were compared based on the average percentage errors, ε % according to Eqn. 4.7.

$$\varepsilon = \frac{\sum_{i=1}^N \frac{(C/C_0)_{\text{exp}} - (C/C_0)_{\text{cal}}}{(C/C_0)}}{N} \times 100 \quad (7)$$

where 'exp' and 'cal' refer to experimental and calculated values respectively, and N is the number of measurement. The lowest value of ε % indicates the best model to represent the experimental data.

4.10.5 Boharts and Adam Model

The derivation of plotting $\ln [C/(C_0-C)]$ versus t is based on the definition that 50% breakthrough occurs at $t = \tau$. Thus, the bed would be completely saturated at $t = 2\tau$. Due to the symmetrical nature of the breakthrough curve, the amount of dye adsorbed by cross-linked chitosan/oil palm ash composite beads is equal to the half of the total dye entering the column within the 2τ period.

From Table 15, it can be seen that the values of τ are similar for almost all systems studied. This showed that at similar bed height, the values of τ are identical for both initial dye concentration and flow rate. However, the k value follows a decreasing trends of a RO16 < RB19 < RB5. Furthermore, the values of τ follow the same trend as a k value. At the same time, the values of bed capacity q_0 is poorly predicted by the model as compared with the experimental values $q_{0,\text{exp}}$ for each adsorption system. On the other hand, for the values of correlation coefficient $R^2 > 0.7$, it does not describe well with

Boharts and Adam model. This is again confirm by the analysis on average percentage error, $\epsilon\%$ in which the values lies in a range of $19.5 < \epsilon\% < 38.9$. Fig. 12 shows a plot of experimental and calculated breakthrough curves for continuous adsorption system of RB19, RO16 and RB5 on cross-linked chitosan/oil palm ash composite beads.

Table 15: Parameters predicted from the Boharts and Adam model and model deviation for adsorption of RB19, RO16 and RB5 dyes

Adsorbate	k (1/min)	τ (min)	$q_{0,cal}$ (mg/g)	$q_{0,exp}$ (mg/g)	R^2	$\epsilon\%$
Reactive blue 19	23.77	3.0	56.6	343.5	0.867	38.9
Reactive orange 16	19.99	2.7	51.1	240.6	0.848	26.8
Reactive black 5	26.79	3.3	60.9	308.5	0.714	19.5

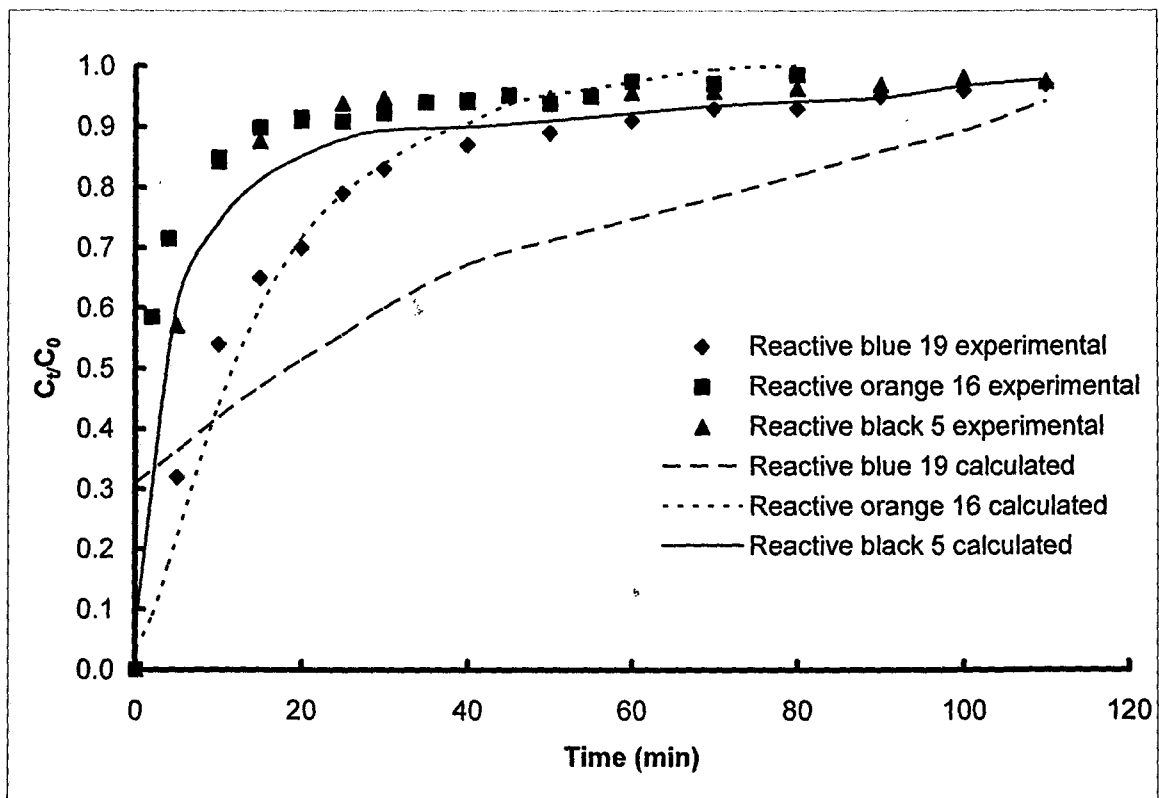


Fig. 12: Comparison of experimental and calculated breakthrough curves for continuous adsorption system of RB19, RO16 and RB5 dyes on cross-linked chitosan/oil palm ash composite beads according to the Boharts and Adam model

4.10.6 Thomas model

The application of the Thomas model to the data in the concentration, C_t range of $0.01 \text{ mg/L} < C_t < 0.9C_0$ with respect to initial dye concentration, flow rate and height of adsorbent helped in the determination of the Thomas' kinetic coefficients for this system. The coefficients were determined from the slope and intercepts obtained from the plot of $[(C_0/C_t)-1]$ versus sampling time, t for the adsorption of RB19, RO16 and RB5 on cross-linked chitosan/oil palm ash composite beads. As shown in Table 16, analysis of the regression coefficients indicated that the regressed lines fitted well to the experimental data with $R^2 > 0.8$ for each adsorption system.

Moreover, the values in Table 16 also presents the values of k_{Th} and $q_{0,cal}$. The values of predicted bed capacity q_0 is better by this model as compared with the experimental values, q_0 . Furthermore, the average percentage error, $\epsilon\%$ shows lower values for all the three dyes. This showed that Thomas model is the best model described the adsorption behavior of RB19, RO16 and RB5 dyes on cross-linked chitosan/oil palm ash composite beads. Fig. 13 shows plot of experimental and calculated breakthrough curves for continuous adsorption system of RB19, RO16 and RB5 on cross-linked chitosan/oil palm ash composite beads.

Table 16: Parameters predicted from the Thomas model and model deviation for adsorption of RB19, RO16 and RB5 dyes on cross-linked chitosan/oil palm ash composite beads

Adsorbate	k_{TH} ($\text{mL mg}^{-1} \text{ min}^{-1}$)	$q_{0,cal}$ (mg/g)	$q_{0,exp}$ (mg/g)	R^2	$\epsilon\%$
Reactive blue 19	0.491	188.8	343.5	0.877	1.4

Reactive orange 16	0.478	103.4	240.7	0.816	3.1
Reactive black 5	0.431	168.2	308.5	0.828	1.6

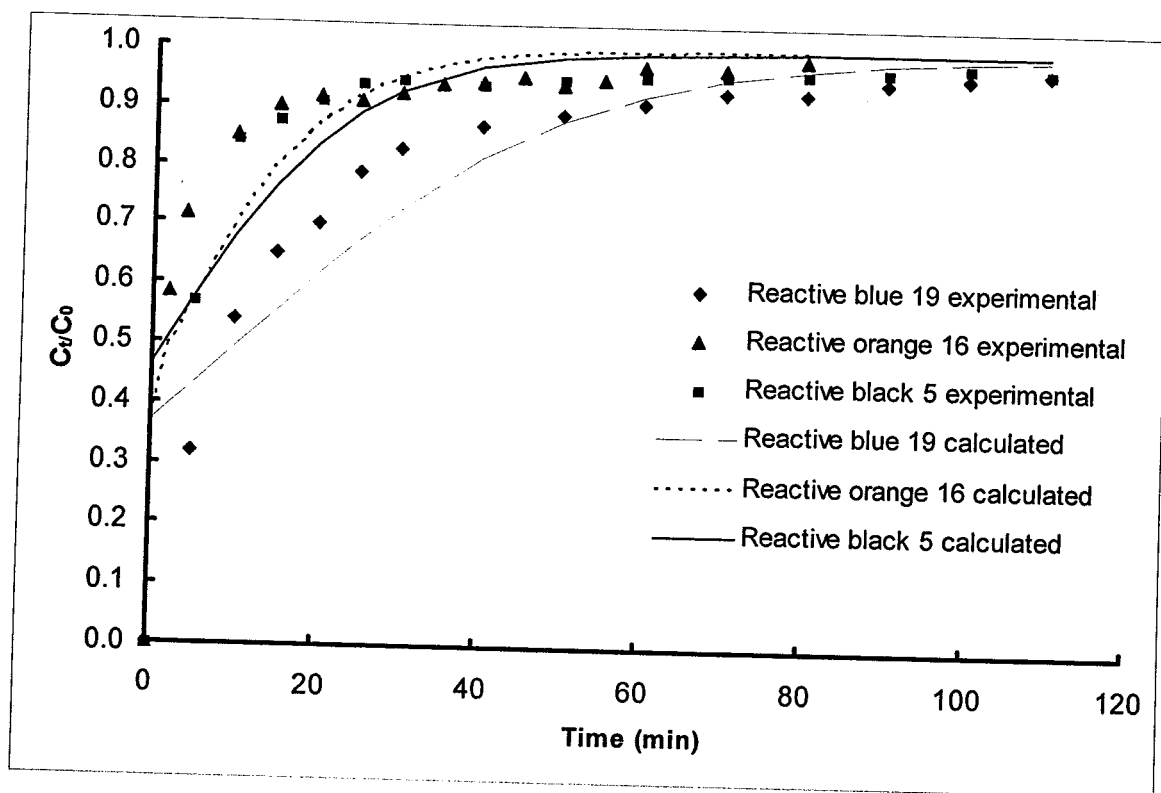


Fig. 13: Comparison of experimental and calculated breakthrough curves for continuous adsorption system of RB19, RO16 and RB5 dyes on cross-linked chitosan/oil palm ash composite beads according to the Thomas model

4.10.7 Yoon and Nelson model

The simple Yoon and Nelson model was applied to investigate the breakthrough behaviour of these three dyes onto cross-linked chitosan/oil palm ash composite beads. This model introduces the parameter τ , which shows the treatment time taken for C_t (effluent exit concentration) to be half the initial concentration ($C_0/2$). The values of the model parameters k_{YN} (rate constant) and τ were determined from the slope and

intercept of the linear plot of $\ln [C_t/(C_0-C_t)]$ versus sampling time, t (min) for adsorption of RB19, RO16 and RB5, respectively.

Table 17 presented the values of τ and K_{YN} . The experimental data for RB19 exhibited good fits to the model with linear regression coefficients 0.916, while for RO16 and RB5 exhibited poorly fits to the model with $R^2 < 0.9$. The experimental and calculated τ -values are very close to each other only for RB19 indicating that the Yoon and Nelson models fitted well to the experimental data, while for RO16 and RB5 dyes show inversely. The trend of τ_{theo} follows the order of $RO16 < RB5 < RB19$ for adsorption onto cross-linked chitosan/oil palm ash composite beads. However, K_{YN} values show the trend $RB19 < RO16 < RB5$. These values indicated that a smaller values of K_{YN} , showed slower adsorption behavior of dyes onto adsorbent.

However, the analysis on average percentage error, $\varepsilon\%$ confirms that adsorption of RB19, RO16 and RB5 gives higher percentage values. This mean that the experimental data do not described well with by Yoon and Nelson model. Comparison of breakthrough curves obtained experimentally with those calculated using the Yoon and Nelson model are shown in Fig. 14.

Table 17: Parameters predicted from the Yoon and Nelson model and model deviation for adsorption of RB19, RO16 and RB5 dyes

Adsorbate	k_{YN} ($Lmin^{-1}$)	τ_{theo} min	τ_{exp} min	R^2	$\varepsilon\%$
Reactive blue 19	0.031	9	10	0.916	78.1
Reactive orange 16	0.043	2	22	0.848	62.3
Reactive black 5	0.048	5	21	0.665	69.8

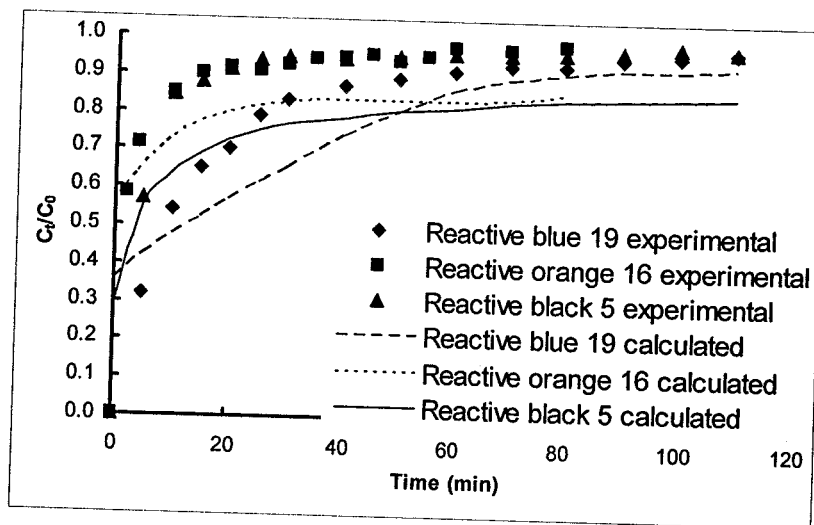


Fig. 14: Comparison of experimental and calculated breakthrough curves for continuous adsorption system of RB19, RO16 and RB5 on cross-linked chitosan/oil palm ash composite beads according to the Yoon and Nelson model

Table 18 summarized the values of average percentage error, $\epsilon\%$ for all adsorption system studied. These studies show that the fixed bed adsorption of a RB19, RO16 and RB5 using cross-linked chitosan/oil palm ash composite beads was experimentally and theoretically best presented by Thomas model with values of $\epsilon\% < 3.1$.

Table 18 Summarization of values of average percentage error, $\epsilon\%$ for all adsorption systems studied.

Adsorbate	$\epsilon\%$		
	Boharts and Adam	Thomas	Yoon and Nelson
Reactive blue 19	38.9	1.4	78.1
Reactive orange 16	26.8	3.1	62.3
Reactive black 5	19.5	1.6	69.8

5. Conclusions:

This study confirmed that cross-linked chitosan/oil palm ash composite beads were an excellent adsorbent for removal of RB-19, RO-16 and RB-5 from aqueous solution in a batch process. Langmuir, Freundlich, Redlich-Peterson, and Temkin isotherm equation were used to describe the adsorption of the three dyes. It was found that the pseudo-second-order equation was better in describing the adsorption kinetics of dyes. The data obtained from adsorption isotherms at different temperatures were used to calculate thermodynamic quantities such as ΔG^0 , ΔH^0 and ΔS^0 of adsorption. The adsorption of dyes on chitosan/palm ash adsorbent was studied in a continuous system in order to determine the breakthrough characteristic of reactive azo dyes on chitosan/oil palm ash under varying operating parameters namely, initial concentration of adsorbent, flowrate and height of column bed and to correlate the experimental results using suitable adsorption dynamic model. These studies show the adsorption process was experimentally and theoretically best presented by Thomas model with values of $\epsilon\% < 3.1$.

Acknowledgments

The authors acknowledge the research grant provided by Universiti Sains Malaysia, under short-term grant that has resulted in this article.

References:

- [1] Interim National Water Quality Standards for Malaysia (2004) [Online], [Accessed 12 April 2008]. Available from World Wide Web: http://www.jas.sains.my/jas/river/interim_2-3.htm
- [2] A. Z. Aroguz, J. Gulen, R.H. Evers, , Adsorption of methylene blue from aqueous solution on pyrolyzed petrified sediment, *Bioresource Technology* 99 (2008) 1503–1508.
- [3] C. O'neil, F.R. Hawkes, D.L. Hawkes, N.D. Lourenco, H.M. Pinheiro, W. Delee. Colour in textiles effluents-sources, measurement, discharge consents and simulations: a review. *J. Chem Technol. Biotechnol.* 74 (1999) 1009-1018.
- [4] M.H. Habibi, A. Hassanzadeh, S. Mahdavi., The effect of operational parameters on the photocatalytic degradation of three textiles azo dyes in aqueous TiO₂ suspensions, *J. Photochem Photobiology A: Chem.* 172(2005) 89-96.
- [5] H. M. Pignon, C.F. Brasquet, P. L. Cloirec, Adsorption of dyes onto activated carbon cloths: approach of adsorption mechanisms and coupling of ACC with ultrafiltration to treat coloured wastewaters. *Sep. Purif. Technol.* 31 (2003)3-11.
- [6] N. Kopvanac, A.L. Bozic, S. Papic, Cleaner Production processes in the synthesis of blue anthraquinone reactive dyes, *Dyes Pigments* 44(2000)33.
- [7] S. Netpradit, P. Thiravetyan, S. Towprayoon, Evaluation of metal hydroxide sludge for reactive dye adsorption in a fixed-bed column system, *Water Res.* 38 (2004) 71-78.
- [8] S. Netpradita, P. Thiravetyan, S. Towprayoon, Application of 'waste' metal hydroxide sludge for adsorption of azo reactive dyes, *Water Res.* 37 (2003)763-772.

- [9] V. K. Garg, M. Anita, R. Kumar, R. Gupta, Basic dye (methylene blue) removal from simulated wastewater by adsorption using Indian Rosewood sawdust: a timber industry waste, *Dyes Pigments* 63 (2004)243-250.
- [10] A. S.Ozcan, A.Ozcan, Adsorption of acid dyes from aqueous solutions onto acid-activated bentonite, *J. Coll. Interf. Sci.* 276 (2004) 39-46.
- [11] A.A. Ahmad, B.H. Hameed, N. Aziz, Adsorption of direct dye on palm ash: Kinetic and equilibrium modeling, *J. Hazard. Mater.* 141 (2007)70–76.
- [12] B.H. Hameed, A.A. Ahmad, N. Aziz, Isotherms, kinetics and thermodynamics of acid dye adsorption on activated palm ash, *Chem. Eng. J.* 133 (2007) 195-203.
- [13] B.H. Hameed, D. K. Mahmoud, A. L. Ahmad, Sorption of basic dye from aqueous solution by Pomelo (*Citrus grandis*) peel in a batch system, *Colloids Surf., A: Physicochem. Eng. Aspects* 316 (2008) 78-84.
- [14] B.H. Hameed and M.I. El-Khaiary, Removal of basic dye from aqueous medium using a novel agricultural waste material: pumpkin seed hull, *J. Hazard. Mater.* doi:10.1016/j.jhazmat.2007.11.102
- [15] B.H. Hameed and M.I. El-Khaiary, Sorption kinetics and isotherm studies of a cationic dye using agricultural waste: Broad bean peels, *J. Hazard.* 154 (2008) 639-648.
- [16] B.H. Hameed and M.I. El-Khaiary, Batch removal of malachite green from aqueous solutions by adsorption on oil palm trunk fibre: Equilibrium isotherms and kinetic studies, *J. Hazard. Mater.* 154 (2008) 237-244.
- [17] B. H. Hameed and H. Hakimi, Utilization of durian (*Durio zibethinus* Murray) peel as low cost sorbent for the removal of acid dye from aqueous solutions, *Biochem. Eng. J.* 39 (2008) 338-343.

- [18] I. Uzun, F. Guzel. Kinetics and thermodynamics of the adsorption of some dyestuffs and *p*-nitrophenol by chitosan and MCM-chitosan from aqueous solution. *J.colloid Interface Sci* 274 (2004) 398-412.
- [19] F. C. Wu, R.L.Tseng, R.S. Juang, Comparative adsorption of metal and dye on flake-and bead- types of chitosans prepared from fishery waste, *J. Hazard. Mater.* B73 (2000) 63-75.
- [20] X. F.Zeng, E. Ruckenstein, Trypsin purification by *p*-aminobenzamide immobilized on macroporous chitosan membrane, *Ind. Eng. Chem. Res.* 37(1998) 159-165.
- [21] M.N.VR, Kumar. A review of chitin and chitosan applications. *React Funct Polym* 46 (2000) 1-27.
- [22] I. Uzun, F. Guzel. Kinetics and thermodynamics of the adsorption of some dyestuffs and *p*-nitrophenol by chitosan and MCM-chitosan from aqueous solution. *J.colloid Interface Sci* 274 (2004) 398-412.
- [23] F. C.Wu, R.L.Tseng, R.S.Juang, Comparative adsorption of metal and dye on flake-and bead- types of chitosans prepared from fishery waste, *J. Hazard. Mater.* B73 (2000) 63-75.
- [24] M.Y. Chang, R.S. Juang, Adsorption of tannic acid, humic acid, and dyes from water using the composite of chitosan and activated clay. *J Colloid Interface Sci* 278 (2004) 18-25.
- [25] M.S. Chiou, H.Y. Li, Adsorption behavior of reactive dye in aqueous solution on chemical cross-linked chitosan beads. *Chemosphere* 50 (2003) 1095-1105.

APPENDIX B: PUBLICATIONS

Adsorption of reactive dye onto cross-linked chitosan/oil palm ash composite beads

M. Hasan, A.L. Ahmad, B.H. Hameed*

*School of Chemical Engineering, Engineering Campus, University Science Malaysia,
14300 Nibong Tebal, Penang, Malaysia*

Received 13 December 2006; received in revised form 14 February 2007; accepted 21 March 2007

Abstract

Adsorption of reactive dye from aqueous solution onto cross-linked chitosan/oil palm ash composite beads (CC/OPA) was investigated in a batch system. Kinetic and isotherm studies were carried out by considering the effects of various parameters, such as initial concentration (50–500 mg/L), contact time, pH (2–13), and temperature (30, 40, 50 °C). It was found that the dye uptakes were much higher in acidic solutions than those in neutral and alkaline conditions. Langmuir, Freundlich, Redlich–Peterson, and Temkin isotherms were used to analyze the equilibrium data at different temperatures. The Redlich–Peterson isotherm fits the experimental data significantly better than the other isotherms. Adsorption kinetics data were tested using pseudo-first-order and pseudo-second-order models. Kinetic studies showed that the adsorption followed a pseudo-second-order model. The pseudo-first-order and pseudo-second-order rate constants for different initial concentrations were evaluated and discussed. Thermodynamic parameters such as standard Gibbs free energy (ΔG°), standard enthalpy (ΔH°), and standard entropy (ΔS°) were evaluated by applying the Van't Hoff equation. The thermodynamics of reactive dye adsorption onto cross-linked chitosan/oil palm ash composite beads indicates its spontaneous and endothermic nature.

© 2007 Elsevier B.V. All rights reserved.

Keywords: Adsorption; Cross-linked chitosan/oil palm ash composite beads; Reactive blue 19; Isotherms; Kinetics

1. Introduction

The major problems concerning environmental pollutants is removing colour from water and wastewater industrial activities. Dyes are released into wastewaters from various industrial units, mainly from the dye manufacturing and textiles and other fabric finishing [1]. Most dyes are non-biodegradable in nature, which are stable to light and oxidation. Therefore, the degradation of dyes in wastewater either traditional chemical or biological process has not been very effective [2–4].

Reactive dyes are most problematic compounds among other dyes in textile wastewater. Reactive dyes are highly water-soluble and estimated that 10–20% of reactive dyes remain in the wastewater during the production process of these dyes [5] and nearly 50% of reactive dyes may be lost to the effluent during dyeing processes of cellulose fibers [6]. Reactive dye wastewater has limited biodegradability in an aerobic environment and many azo dyes under anaerobic conditions decompose into potentially carcinogenic aromatic amines [7,8].

Adsorption process has been found becoming a prominent method of treating aqueous effluent in industrial processes for a variety of separation and purification purpose [9]. This technique also found to be highly efficient for the removal of colour in terms of initial cost, simplicity of design, ease of operation and insensitivity to toxic substances [10]. Therefore, adsorption using activated carbon is currently of great interest for removal of dyes and pigments. In spite of its prolific use, activated carbon remains an expensive material since higher the quality of activated carbon, the greater in cost. This has led to the search for cheaper substitutes. Today, attention has been focused on the low-cost adsorbents as alternative adsorbent materials such as oil palm ash [11]. This ash is produced after combustion of oil palm fiber and shell as boiler fuel to produce steam for palm-oil mill consumption. This solid waste is highly abundant in Malaysia, which is one of the largest palm-oil exporters in the world. Malaysia thus generates huge loads of palm ash each year. The oil palm ash showed very high adsorption capacity to remove direct dye [11].

Recently, chitosan that is used as an adsorbent has drawn attentions due to its high contents of amino and hydroxy functional groups showing high potentials of the adsorption

* Corresponding author. Tel.: +60 4 599 6422; fax: +60 4 594 1013.

E-mail address: chbassim@eng.usm.my (B.H. Hameed).

Nomenclature

a_R	constant of Redlich–Peterson (L/mg)
A	Arrhenius factor
b	Langmuir constant (L/mg)
B_1	Temkin isotherm constant
C_e	equilibrium liquid-phase solute concentration (mg/L)
C_0	initial liquid-phase solute concentration (mg/L)
E	mean energy of adsorption (kJ/mol)
E_a	Arrhenius activation energy of sorption (kJ/mol)
ΔG°	Gibbs free energy of adsorption (kJ/mol)
ΔH°	enthalpy of adsorption (kJ/mol)
k_a	adsorption rate constant
k_d	desorption rate constant
k_1	pseudo-first-order rate constant (1/h)
k_2	pseudo-second-order rate constant (g/mg h)
K_C	equilibrium constant
K_F	Freundlich constant ((mg/g) (L/mg) ^{1/n})
K_R	Redlich–Peterson isotherm constant (L/g)
K_t	equilibrium binding constant (L/mg)
n	Freundlich isotherm constant related to adsorption intensity
q_e	amount of adsorption at equilibrium (mg/g)
$q_{e\text{ cal}}$	calculated value of adsorbate concentration at equilibrium (mg/g)
$q_{e\text{ exp}}$	experimental value of adsorbate concentration at equilibrium (mg/g)
q_m	maximum adsorption capacity of adsorbent per unit mass (mg/g)
q_t	amount of adsorbate adsorbed by adsorbent at time t (mg/g)
Q_0	Langmuir constant (mg/g)
R	universal gas constant (8.314 J/mol K)
R_L	dimensionless constant separation factor
R^2	correlation coefficient
ΔS°	entropy of adsorption
t	time (h)
T	absolute temperature (K)
V	volume of the solution (L)
W	mass of dry adsorbent (g)

Greek letter

β	constant of Redlich–Peterson isotherm
---------	---------------------------------------

cationized and they adsorb the dye anions strongly by electrostatic attraction [15]. However, chitosan formed gels below pH 5.5 and could not be evaluated. This problem limits the use of chitosan as adsorbent for dye removal, as this compound is highly soluble in such environments. This has led to prepare cross-linked chitosan adsorbent which is necessary to stabilize the prepared adsorbent in acid medium as well as to grant the material the mechanical strength necessary for the adsorption studies in dynamic systems. Yoshida et al. [17] used Denacol EX841 as a cross-linking reagent and obtained a high adsorption capacity (1200–1700 g/kg) of orange II (AO7) on the cross-linked chitosan fibers in acid solutions of pH 3.0 and 4.0. Chiou and Li [18] prepared cross-linked chitosan by epichlorohydrin (ECH) and exhibited a high adsorption capacity (1802–1840 g/kg) of reactive dye (RR189) on the cross-linked chitosan beads in acid aqueous solutions at 30 °C and pH 3.0.

The aim of this study was to investigate the adsorption of reactive blue 19 (RB19) dye onto cross-linked chitosan/oil palm ash composite beads, which is a low-cost adsorbent for the removal of dye.

2. Materials and methods

2.1. Adsorbate: reactive blue 19

The reactive blue 19 (RB19) used in this work was obtained from Sigma–Aldrich, Malaysia and used without further purification. The dye was chosen as adsorbate because it is very important in dyeing of cellulosic fibers and is regarded as dye contaminant in the discharged effluent. The properties of RB19 are summarized in Table 1. The aqueous solution was prepared by dissolving solute in deionized water to the required concentrations without any pH adjustment. The wavelength of maximum absorbance (λ_{max}) for RB19 was 598 nm.

2.2. Chitosan and oil palm ash

The chitosan derived from deacetylated lobster shell wastes was supplied by Hunza Pharmaceutical Sdn Bhd., Nibong Tebal, Malaysia. The chitosan was washed three times with deionized water and dried in an oven at 50 °C before use. Some properties of chitosan are given in Table 2.

The oil palm ash (OPA) was provided by United Oil Palm Mill, Penang, Malaysia. It was sieved through a stack of U.S. standard sieves and the fine particle size of 63 μm was used. Then, OPA was washed with deionized water and oven dried overnight at 110 °C. OPA (50 g) was activated by refluxing with 250 mL of 1 mol/L H_2SO_4 at 80 °C in a round-bottom flask for 4 h. The slurry was air-cooled and filtered with a glass fiber. The filter cake was repeatedly washed with deionized water until the filtrate was neutral. It was then dried in an oven at 110 °C before use.

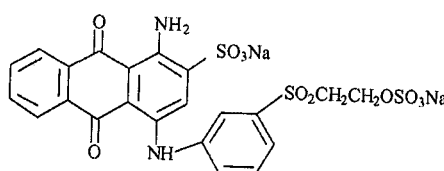
2.3. Preparation of chitosan/oil palm ash composite beads

Chitosan (1 g) was dissolved in 1 mol/L acetic acid (100 mL) and mixed with activated oil palm ash (1 g) and agitated for

of dyes [12], metal ions [13] and proteins [14]. Chitosan is the deacetylated form of chitin, which is linear polymer of acetylamino-D-glucose. Other useful features of chitosan include its abundance, non-toxicity, hydro-philicity, biocompatibility, biodegradability and anti-bacterial property [15]. Moreover, the adsorption of reactive dyes, basic dyes and acidic dyes in natural solutions using chitosan shows large adsorption capacities [12,16].

Many textile wastewaters are highly acid. In acid aqueous solutions, the amino groups of chitosan are much easier to be

Table 1
Properties of reactive blue 19

Chemical index (CI)	No. 61200
Class	Anthraquinone
Ionisation	Acid
Maximum wavelength, λ_{\max} (nm)	598
Colour	Blue
Relative molecular weight	626.56
Chemical structure	

1 h. Then, the viscous solution was sprayed dropwise through a syringe, at a constant rate, into neutralization solution containing 15% NaOH and 95% ethanol in a volume ratio of 4:1. They were left in the solution for 1 day [19]. The formed composite beads were washed with deionized water until solution become neutral and then stored in distilled water.

2.4. Preparation of cross-linked chitosan/oil palm ash composite beads

Epichlorohydrin (ECH) purchased from Sigma–Aldrich was used as cross-linking agent in this study. The procedure for cross-linking was same as reported previously [18]. Basically, wet non-cross-linked chitosan/oil palm ash composite beads (0.1 g dry basis of chitosan) and 50 cm³ of 1N sodium hydroxide solution were poured together in a 500 cm³ flask. ECH was added into the above solution, and shaken for 6 h at 50 °C with water bath. The molar ratio of cross-linking reagent/chitosan was 0.5. The cross-linking chitosan/oil palm ash composite beads (CC/OPA) were filtered out, washed with deionized water and stored in distilled water. Then, the beads (2–3 mm) were dried in a freeze dryer for 6 h before used as adsorbent.

2.5. Batch equilibrium studies

Adsorption isotherms were performed in a set of 43 Erlenmeyer flasks (250 mL), where solutions of dye (100 mL) with different initial concentrations (50–500 mg/L) were placed in these flasks. The original pH (6) of the solutions was used. Equal masses of 0.2 g of particle size (2–3 mm) CC/OPA (adsorbent) were added to dye solutions, and the mixtures were then kept in an isothermal shaker (30 ± 0.1 °C) for 48 h to reach equilibrium. A similar procedure was followed for another set of

Erlenmeyer flask containing the same dye concentration without adsorbent to be used as a blank. The flasks were then removed from the shaker, and the final concentration of dye in the solution was measured at 598 nm, using UV–vis spectrophotometer (Shimadzu UV/Vis1601 spectrophotometer, Japan). The amount of adsorption at equilibrium time t , q_e (mg/g), is calculated by

$$q_e = \frac{(C_0 - C_t)V}{W} \quad (1)$$

where C_0 and C_t (mg/L) are the liquid-phase concentrations of dye at initial and any time t , respectively; V the volume of the solution (L); W is the mass of dry adsorbent used (g).

To study the effect of initial pH on the RB19 removal by CC/OPA, the pH was adjusted by adding a few drops of dilute 1.0 M NaOH or 1.0 M HCl before each experiment. Experimental conditions consisted of 0.2 g adsorbent, 100 mL of 200 mg/L RB19 solution, temperature equal to 30 °C and contact time 48 h. The effect of temperature (at 30, 40 and 50 °C) on the adsorption of RB19 by CC/OPA was studied at pH 6.0, 0.2 g adsorbent and initial RB19 concentration of 50–500 mg/L for 48 h.

2.6. Batch kinetic studies

The procedures of kinetic experiments are basically identical to those of equilibrium tests. The aqueous samples were taken at present time intervals, and the concentrations of dye were similarly measured.

The amount of adsorption at time t , q_t (mg/g), is calculated by

$$q_t = \frac{(C_0 - C_t)V}{W} \quad (2)$$

where C_0 and C_t (mg/L) are the liquid-phase concentrations of dye at initial and any time t , respectively; V the volume of the solution (L); W is the mass of dry adsorbent used (g).

3. Results and discussion

3.1. Effect of solution pH

Fig. 1 shows the effect of pH on adsorption of RB19 onto CC/OPA at 30 °C and initial dye concentration 200 mg/L, particle size 2–3 mm. The adsorption of RB19 was studied over

Table 2
Properties of chitosan flake^a

Deacetylation degree	>90.0%
Solubility in 1% acetic acid	>99.0%
Moisture	<10.0%
Ash content	<1.0%
Appearance	Off-white

^a Hunza Pharmaceutical Sdn. Bhd.

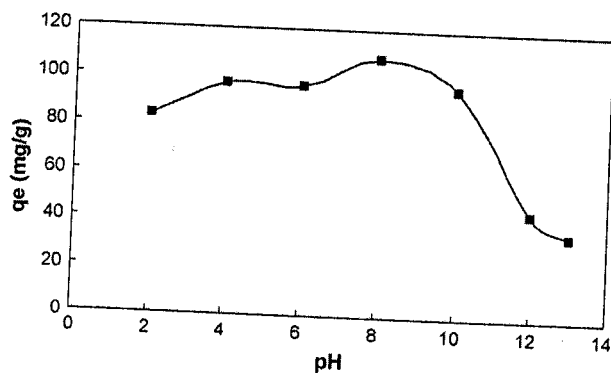


Fig. 1. Effect of pH on the RB19 adsorption ($C_0 = 200$ mg/L, $T = 30$ °C).

a pH range 2–13 and the studies were carried out for 48 h. Fig. 1 indicates that the pH is significantly affected the adsorption of the reactive blue 19 onto CC/OPA. It was clear that the dye uptakes were much higher in acidic solutions than those in neutral and alkaline conditions. Yoshida et al. [16] and Kumar [15] reported that at lower pH more protons will be available to protonate amino groups of chitosan molecules to form groups $-NH_3^+$, thereby increasing the electrostatic attractions between negatively charged dye anions and positively charged adsorption sites and causing an increase in dye adsorption. This explanation agrees well with our result on pH effect. Similar result was also reported for the adsorption of RR 189 (reactive dye) on cross-linked chitosan beads [18]. From pH 10.0 to 13.0, the adsorption was lower than at acidic solution. This might be explained by the fact that chemical cross-linking reduces either the total number and/or the diameter of the pores in chitosan beads, making the dye molecule more difficult to transfer [18].

3.2. Effect of initial dye concentration

The adsorption of dye by CC/OPA was studied at different initial RB19 concentrations ranging from 50 to 500 mg/L. Fig. 2 shows the result for effect of initial dye concentration on adsorption of RB19 onto CC/OPA at pH 6. As can be seen from Fig. 2, the amount of the adsorbed dye at low initial concentration (50–200 mg/L) achieve adsorption equilibrium in about 4 h, at some point in time, reaches a constant value beyond which

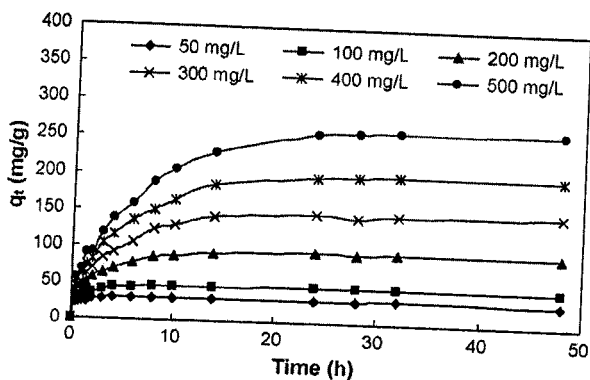


Fig. 2. Effect of initial concentration on the adsorption of RB19 on CC/OPA at pH 6, 30 °C.

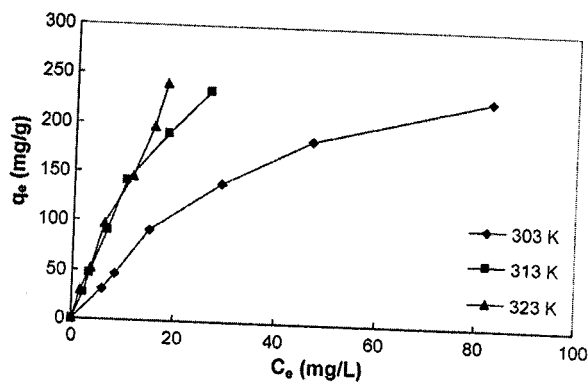


Fig. 3. Effect of temperature on the adsorption of RB19 on CC/OPA.

no more is removed from solution. While at high initial dye concentration (300–500 mg/L), the time necessary to reach equilibrium was about 24 h. However, the experimental data were measured at 48 h to make sure that full equilibrium was attained. The adsorption capacity at equilibrium increases from 43.4 to 423.5 mg/g, with increase in the initial dye concentration from 50 to 500 mg/L. An increase in initial dye concentration leads to increase in the adsorption capacity of dye on CC/OPA. This indicates that initial dye concentrations played an important role in the adsorption of RB19 on the CC/OPA. A similar phenomenon was observed for the adsorption of reactive blue 15 dye from an aqueous solution on cross-linked chitosan beads [20] and drim yellow-K4G on the shale oil ash [21].

3.3. Effect of temperature

A study of the temperature dependence of adsorption process gives valuable information about the enthalpy during adsorption. The effect of temperature on the adsorption isotherm was studied by carrying out a series of isotherms at 30, 40 and 50 °C as shown in Fig. 3. At temperature 50 °C, more dye strongly adsorbed by the CC/OPA and thus induced a higher Q_0 value (Table 3). This process was endothermic, where increasing the temperature increases the value of Q_0 .

3.4. Adsorption isotherm

The adsorption isotherm is the most important information which indicates how the adsorbate molecules distribute between the liquid phase and the solid phase when the adsorption process reaches an equilibrium state. To optimize the design of an adsorption system for the adsorption of adsorbates, it is important to establish the most appropriate correlation for the equilibrium curves. Various isotherm equations like those Langmuir, Freundlich, Redlich–Peterson, Tempkin and Dubinin–Raduskevich were used to describe the equilibrium characteristics of adsorption.

The linear form of Langmuir isotherm is expressed as

$$\frac{C_e}{q_e} = \frac{1}{Q_0 b} + \frac{C_e}{Q_0} \quad (3)$$

Table 3
Langmuir, Freundlich, Redlich–Peterson and Temkin isotherm model constants and correlation coefficients for adsorption of RB19 onto CC/OPA

Temperature (°C)	b (L/mg)	Q_0 (mg/g)	R_L	R^2
Langmuir isotherm				
30	0.016	416.7	0.111	0.93
40	0.022	666.7	0.133	0.72
50	0.018	909.1	0.154	0.60
Temperature (°C)	K_F	n	R^2	
Freundlich isotherm				
30	9.619	1.318	0.96	
40	15.427	1.147	0.97	
50	18.302	1.144	0.99	
Temperature (°C)	K_R	a_R	β	R^2
Redlich–Peterson isotherm				
30	7.626	0.021	0.9991	1.00
40	17.360	0.040	0.9649	0.99
50	22.310	0.414	0.1879	0.99
Temperature (°C)	K_T (L/mg)	B_1	R^2	
Temkin isotherm				
30	0.232	76.617	1.00	
40	0.519	85.098	0.98	
50	0.630	85.370	0.91	

where q_e is the amount of dye adsorbed per unit weight of adsorbent (mg/g) and C_e is the equilibrium concentration of dye in solution (mg/L). The constant Q_0 signifies the adsorption capacity (mg/g) and b is related with the energy of the adsorption (L/mg). A plot of C_e/q_e versus C_e (Fig. 4) yields a straight line with slope $1/Q_0$ and intercept $1/Q_0b$. Table 3 lists that the computed maximum adsorption capacity Q_0 of RB19 onto the CC/OPA at different temperatures.

The essential characteristics of the Langmuir isotherm can be expressed in terms of dimensionless constant separation factor R_L given by [22]:

$$R_L = \frac{1}{1 + bC_0} \quad (4)$$

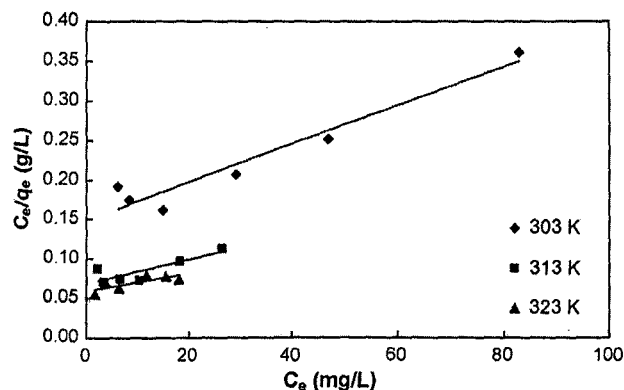


Fig. 4. Linearized Langmuir isotherms at different temperatures.

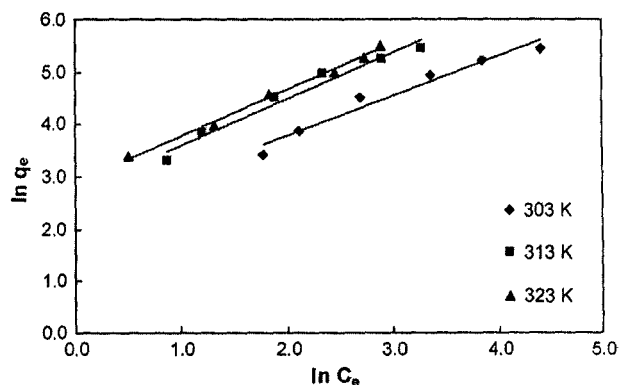


Fig. 5. Linearized Freundlich isotherms at different temperatures.

where b is the Langmuir constant and C_0 is the highest initial dye concentration (mg/L). According to the value of R_L the isotherm shape may be interpreted as follows:

Value of R_L	Type of adsorption
$R_L > 1.0$	Unfavourable
$R_L = 1.0$	Linear
$0 < R_L < 1.0$	Favourable
$R_L = 0$	Irreversible

Values of R_L calculated at 30, 40 and 50 °C were in range between 0 and 1 which indicate that the adsorption is favourable at operation conditions studied.

The Freundlich isotherm [23] is an empirical equation based on a heterogeneous surface. A linear form of the Freundlich expression will yield the constants K_F and n . Hence

$$\ln q_e = \ln K_F + \frac{1}{n} \ln C_e \quad (5)$$

therefore, a plot of $\ln q_e$ versus $\ln C_e$ (Fig. 5) enables the constant K_F and exponent n to be determined. K_F can be defined as adsorption of distribution coefficient and represents the quantity of dye adsorbed onto adsorbent for an equilibrium concentration. The slope $1/n$, ranging between 0 and 1, is a measure of adsorption intensity or surface heterogeneity, becoming more heterogeneous as its value gets closer to zero. These values together with the correlation coefficient are presented in Table 3.

Based on the correlation coefficient (R^2) shown in Table 3, the adsorption isotherm with CC/OPA can be described by Freundlich equation. Also, the Freundlich equation yields a better fit of the experimental data than Langmuir equation (Fig. 5). In principle, the Freundlich equation is an empirical approach for adsorbent with very uneven adsorbing surface, and is applicable to the adsorption of single solutes within a fixed range of concentration.

Another equation used in the analysis of isotherms was proposed by Temkin and Pyzhev [24]. Temkin isotherm contains a factor that explicitly takes into account adsorbing species–adsorbate interactions. This isotherm assumes that: (i) the heat of adsorption of all the molecules in the layer decreases linearly with coverage due to adsorbate–adsorbate interactions,

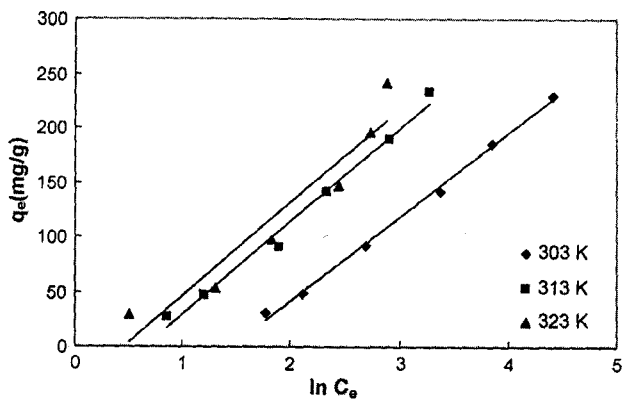


Fig. 6. Temkin isotherms at different temperatures.

and (ii) adsorption is characterized by a uniform distribution of binding energies, up to some maximum binding energy [24,25]. Temkin isotherm is represented by the following equation:

$$q_e = \frac{RT}{b} \ln(K_f C_e) \tag{6}$$

Eq. (6) can be expressed in its linear form as

$$q_e = B_1 \ln K_f + B_1 \ln C_e \tag{7}$$

where

$$B_1 = \frac{RT}{b} \tag{8}$$

the adsorption data can be analyzed according to Eq. (7). A plot of q_e versus $\ln C_e$ enables the determination of the isotherm constants K_f and B_1 . K_f is the equilibrium binding constant (L/mg) corresponding to the maximum binding energy and constant B_1 is related to the heat of adsorption. This isotherm is plotted in Fig. 6 and values of the parameters are given in Table 3.

Redlich and Peterson [26] incorporate three parameters into an empirical isotherm. The Redlich–Peterson isotherm has a linear dependence on concentration in the numerator and an exponential function in the denominator. It approaches the Freundlich model at high concentration and is in accordance with the low concentration limit of the Langmuir equation. Furthermore, the R–P equation incorporates three parameters into an empirical isotherm, and therefore, can be applied either in homogeneous or heterogeneous systems due to the high versatility of the equation. It can be described as follows:

$$q_e = \frac{K_R C_e}{1 + a_R C_e^\beta} \tag{9}$$

where K_R is the R–P isotherm constant (L/g); a_R the R–P isotherm constant (L/mg); β is the exponent which lies between 1 and 0, where $\beta = 1$:

$$q_e = \frac{K_R C_e}{1 + a_R C_e} \tag{10}$$

It becomes a Langmuir equation. Where $\beta = 0$:

$$q_e = \frac{K_R C_e}{1 + a_R} \tag{11}$$

i.e. the Henry’s law equation.

Eq. (9) can be converted to a linear form by taking logarithms:

$$\ln \left(K_R \frac{C_e}{q_e} - 1 \right) = \ln a_R + \beta \ln C_e \tag{12}$$

The constants were determined by non-linear regression using MATLAB. The R–P isotherm constants a_R , K_R and β and the correlation coefficients, R^2 , for the R–P isotherm are shown in Table 3. The correlation coefficients are significantly higher than the Langmuir isotherm R^2 values. Based on the values of correlation coefficients listed in Table 3, we can conclude that the Redlich–Peterson isotherm fits the experimental data for RB19 adsorption significantly better than the other isotherms.

3.5. Adsorption kinetics

In order to investigate the mechanism of adsorption, the pseudo-first-order and pseudo-second-order equations were used to test the experimental data of initial concentration. The Lagergren [27] rate equation, which is the first rate equation developed for sorption in liquid/solid systems, is based on solid capacity. The pseudo-first-order equation is represented as

$$\log(q_e - q_t) = \log q_e - \frac{k_1}{2.303} t \tag{13}$$

where q_e and q_t are the amounts of dye adsorbed on adsorbent at equilibrium and at time t , respectively (mg/g). The slope and intercept of plot of $\log(q_e - q_t)$ versus t were used to determine the pseudo-first-order rate constant k_1 (h^{-1}) (Fig. 7).

The pseudo-second-order kinetic model [28,29] expressed as

$$\frac{t}{q_t} = \frac{1}{k_2 q_e^2} + \frac{t}{q_e} \tag{14}$$

where k_2 (g/mg h) is the rate constant of pseudo-second-order adsorption. If pseudo-second-order kinetics is applicable, the plot t/q_t versus t shows a linear relationship. There is no need to know any parameter beforehand and q_e and k_2 can be determined from the slope and intercept of the plot (Fig. 8). Also, it is more likely to predict the behavior over the whole the range

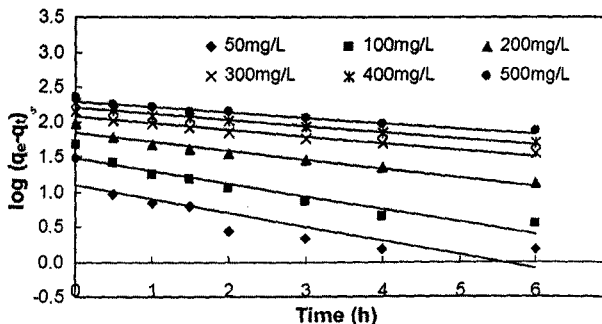


Fig. 7. Pseudo-first-order kinetics of RB19 adsorption onto CC/OPA at various initial concentrations (pH 6.0 at 30 °C).

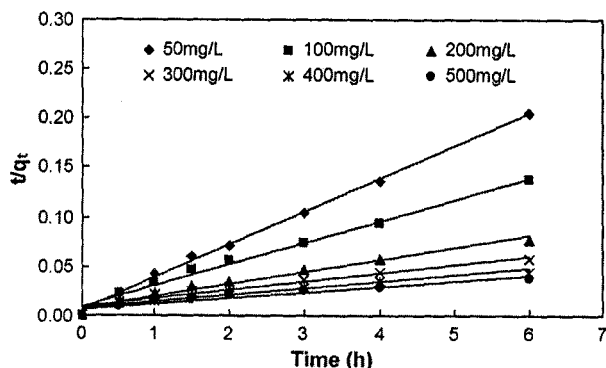


Fig. 8. Pseudo-second-order kinetics of RB19 adsorption onto CC/OPA at various initial concentrations (pH 6.0 at 30 °C).

of adsorption and is in agreement with chemical sorption being the rate-controlling step [30] which may involve valency forces through sharing or exchange of electrons between dye anions and adsorbent.

The correlation coefficients of the pseudo-second-kinetic model for the linear plots are more than 0.92. The values of the parameters k_1 , k_2 were also calculated and summarized in Table 4. Based on the results of correlation coefficients, at initial concentrations 50–200 mg/L, the adsorption kinetics obeys a pseudo-second-order model, while at higher concentrations (300–500 mg/L) it obeys a pseudo-first-order model. This result means that sometimes the correlation coefficient is not a sufficient criteria for selection of an adsorption kinetic model [31]. Aziaian [32] derived theoretically that the pseudo-first-order rate coefficient (k_1) is not the intrinsic adsorption rate constant but is a combination of adsorption (k_a) and desorption (k_d) rate constants [32] as

$$k_1 = k_a C_0 + k_d \quad (15)$$

According to Eq. (15), if the adsorption kinetic follows pseudo-first-order, then its rate coefficient is a linear form. Table 4 shows that the relation between k_1 versus C_0 is not linear and also decrease with increasing C_0 (figure not shown). Therefore, it is concluded that in the initial concentration between 300 and 500 mg/L the adsorption of RB19 on CC/OA does not obey the pseudo-first-order model.

Azizian [32] also reported that the rate coefficient of pseudo-second-order rate model (k_2) is a complex function of the initial concentration of solute (C_0). Inspection the results shown in Table 4, when the rate coefficient of the pseudo-second-order

Table 5
Thermodynamic parameters for the adsorption of RB19 on CC/OPA

E_a (kJ/mol)	12.9
ΔH° (kJ/mol)	46.2
ΔS° (J/mol K)	166.2
ΔG° (kJ/mol)	
303 K	-3.86
313 K	-6.43
323 K	-7.15

rates model (k_2) was plotted versus initial concentration of RB19 (figure not shown), the relation between k_2 and C_0 is not a simple function. Therefore, the adsorption of RB19 onto CC/OPA followed a pseudo-second-order model. This result agreed with that of adsorption of 18-crown-6 from aqueous solution on a granular activated carbon [31].

3.6. Adsorption thermodynamic

In order to evaluate the thermodynamic parameters for adsorption of RB19 on CC/OPA, the adsorption studies were carried out at different temperatures 30, 40 and 50 °C. The adsorption standard free energy changes (ΔG°) can be calculated according to:

$$\Delta G^\circ = -RT \ln K_C \quad (16)$$

$$K_C = \frac{q_e}{C_e} \quad (17)$$

where R is the universal gas constant (8.314 J/mol K); q_e the amount of dye (mg) adsorbed on the adsorbent per liter of the solution at equilibrium; C_e the equilibrium concentration (mg/L) of the dye in the solution; T is the temperature in K. The average standard enthalpy change (ΔH°) is obtained from Van't Hoff equation:

$$\ln K_C = \frac{\Delta S^\circ}{R} + \frac{\Delta H^\circ}{RT} \quad (18)$$

where K_C is the equilibrium constant; T the solution temperature (K); R is the gas constant. ΔH° and ΔS° were calculated from the slope and intercept of plot of $\ln K_C$ versus $1/T$. The results are given in Table 5.

The results show that the enthalpy of adsorption ΔH° for RB19 was 46.2 kJ/mol. A positive standard enthalpy change (ΔH°) suggests that the interaction of RB19 adsorbed by

Table 4
Kinetic parameters of RB19 adsorbed onto CC/OPA at different initial concentrations

C_0 (mg/L)	q_{exp} (mg/g)	Pseudo-first-order kinetic model			Pseudo-second-order kinetic model		
		q_{ecal} (mg/g)	k_1 (h^{-1})	R^2	q_{ecal} (mg/g)	k_2 (g/mg h)	R^2
50	30.81	12.49	0.46	0.76	30.12	0.19	1.00
100	47.40	30.54	0.42	0.91	46.51	0.05	0.99
200	91.53	69.57	0.29	0.95	82.64	0.02	0.97
300	140.71	117.54	0.22	0.96	116.28	0.01	0.95
400	185.73	159.85	0.20	0.97	149.25	0.01	0.93
500	229.28	197.83	0.18	0.96	175.44	0.01	0.92

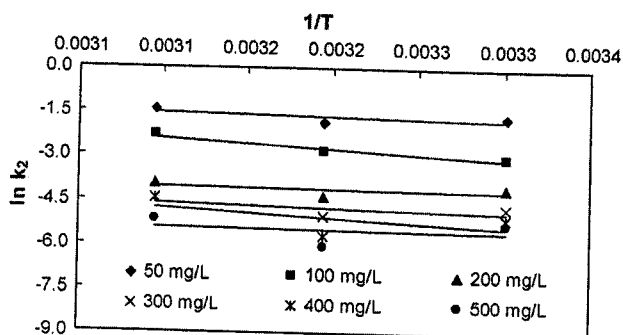


Fig. 9. Plots of $\ln(k_2)$ against reciprocal temperature for RB19 adsorption onto CC/OPA.

CC/OPA is endothermic, which is supported by the increasing adsorption of RB19 with the increase in temperature while a negative adsorption standard free energy change (ΔG°) and a positive standard entropy change (ΔS°) indicate that the adsorption reaction is a spontaneous process [33] and more favorable at high temperature. Generally, the absolute magnitude of the change in free energy for physical adsorption is smaller than that of chemisorption. The former ranges from -20 to 0 kJ/mol, and the latter ranges from -80 to -400 kJ/mol [34]. When the temperature increased from 30 to 50 °C, ΔG° was increased from -3.86 to -7.15 kJ/mol. This could be considered as physical adsorption and more favorable at high temperature.

The pseudo-second-order rate constant of dye adsorption is expressed as a function of temperature by the Arrhenius type relationship:

$$\ln k_2 = \ln A - \frac{E_a}{RT} \quad (19)$$

where E_a is the Arrhenius activation energy of sorption, representing the minimum energy that reactants must have for the reaction to proceed; A the Arrhenius factor; R the gas constant; T is the solution temperature. When $\ln k_2$ is plotted versus $1/T$ (Fig. 9), a straight line with slope $-E_a/R$ is obtained. The chemisorption or physisorption mechanisms are often an important indicator to describe the type of interaction between dye molecule and adsorbent. The physisorption processes usually have energies in the range of 4 – 40 kJ/mol, while higher activation energies (40 – 400 kJ/mol) suggest chemisorption [35]. The value of E_a was 12.9 kJ/mol and indicates that process was physisorption mechanism.

4. Conclusions

This study confirmed that cross-linked chitosan/oil palm ash composite beads were an excellent adsorbent for removal of reactive blue 19 dye from aqueous solution. The maximum adsorption observed at pH 6 for cross-linked chitosan/oil palm ash composite beads. A decrease in the pH of solutions leads to a significant increase in the adsorption capacity of dye RB199 on the adsorbent. Langmuir, Freundlich, Redlich–Peterson, and Temkin isotherm equation were used to describe the adsorp-

tion of RB19 onto CC/OPA. Redlich–Peterson showed better correlation coefficient than the other models at all temperatures studied. The prepared adsorbent exhibits a high adsorption capacity to remove RB19, whose adsorption maximum monolayer adsorption capacity is greater than 400 mg/g at pH 6 and 30 °C. It was found that the pseudo-second-order equation was better in describing the adsorption kinetics of reactive blue 19 on CC/OPA. The data obtained from adsorption isotherms at different temperatures were used to calculate thermodynamic quantities such as ΔG° , ΔH° and ΔS° of adsorption. The results indicate that RB19 adsorption onto CC/OPA is spontaneous and physical in nature.

Acknowledgement

The authors acknowledge the research grant provided by University Science Malaysia, under short-term grant that has resulted in this article.

References

- [1] P. Janos, H. Buchtova, M. Ryznarova, Sorption of dyes from aqueous solutions onto fly ash, *Water Res.* 37 (2003) 4938–4944.
- [2] H. Metivier-Pignon, C. Faur-Brasquet, P. Le Cloirec, Adsorption of dyes onto activated carbon cloths: approach of adsorption mechanisms and coupling of ACC with ultrafiltration to treat coloured wastewaters, *Sep. Purif. Technol.* 31 (2003) 3–11.
- [3] J. Orthman, H.Y. Zhu, G.Q. Lu, Use of anion clay hydrotalcite to remove coloured organics from aqueous solutions, *Sep. Purif. Technol.* 31 (2003) 53–59.
- [4] P. Waranasantigul, P. Pokethitayook, M. Kruatrachue, E.S. Upatham, Kinetics of basic dye (methylene blue) biosorption by giant duckweed (*Spirodela polyrrhiza*), *Environ. Pollut.* 125 (2003) 385–392.
- [5] N. Koprivanac, A. Loncaric Bozic, S. Papic, Cleaner production processes in the synthesis of blue anthraquinone reactive dyes, *Dyes Pigments* 44 (2000) 33–40.
- [6] S. Netpradit, P. Thiravetyan, S. Towprayoon, Adsorption of three azo reactive by metal hydroxide sludge: effect of temperature, pH and electrolytes, *J. Colloid Interface Sci.* 270 (2004) 255–261.
- [7] S. Netpradit, P. Thiravetyan, S. Towprayoon, Application of 'waste' metal hydroxide sludge for adsorption of azo reactive dyes, *Water Res.* 37 (2003) 763–772.
- [8] T. Panswad, W. Luangdilok, Decolorization of reactive dyes with different molecular structures under different environmental conditions, *Water Res.* 34 (2000) 4177–4184.
- [9] Y.E. Benkli, M.F. Can, M. Turan, M.S. Celik, Modification of organo-zeolite surface for the removal of reactive azo dyes in fixed-bed reactors, *Water Res.* 39 (2005) 487–493.
- [10] V.K. Garg, M. Anita, R. Kumar, R. Gupta, Basic dye (methylene blue) removal from simulated wastewater by adsorption using Indian rosewood sawdust: a timber industry waste, *Dyes Pigments* 63 (2004) 243–250.
- [11] A.A. Ahmad, B.H. Hameed, N. Aziz, Adsorption of direct dye on palm ash: kinetic and equilibrium modeling, *J. Hazard. Mater.* 141 (2007) 70–76.
- [12] I. Uzun, F. Guzel, Kinetics and thermodynamics of the adsorption of some dyestuffs and *p*-nitrophenol by chitosan and MCM-chitosan from aqueous solution, *J. Colloid Interf. Sci.* 274 (2004) 398–412.
- [13] F.C. Wu, R.L. Tseng, R.S. Juang, Comparative adsorption of metal and dye on flake- and bead-types of chitosans prepared from fishery waste, *J. Hazard. Mater.* 73 (2000) 63–75.
- [14] X. Zeng, E. Ruckenstein, Cross-linked macroporous chitosan anion-exchange membranes for protein separations, *J. Membr. Sci.* 148 (1998) 195–205.

- [15] M.N.V. Ravi Kumar, A review of chitin and chitosan applications, *React. Funct. Polym.* 46 (2000) 1–27.
- [16] H. Yoshida, S. Fukuda, A. Okamoto, T. Kataoka, Recovery of direct dye and acid dye by adsorption on chitosan fiber-equilibria, *Water Sci. Technol.* 23 (1991) 1667–1676.
- [17] H. Yoshida, A. Okamoto, T. Kataoka, Adsorption of acid dye on cross-linked chitosan fibers: equilibria, *Chem. Eng. Sci.* 48 (1993) 2267–2272.
- [18] M.S. Chiou, H.Y. Li, Adsorption behavior of reactive dye in aqueous solution on chemical cross-linked chitosan beads, *Chemosphere* 50 (2003) 1095–1105.
- [19] M.Y. Chang, R.S. Juang, Adsorption of tannic acid, humic acid, and dyes from water using the composite of chitosan and activated clay, *J. Colloid Interf. Sci.* 278 (2004) 18–25.
- [20] M.S. Chiou, G.S. Chuang, Competitive adsorption of dye metanil yellow and RB15 in acid solutions on chemically cross-linked chitosan beads, *Chemosphere* 62 (2006) 731–740.
- [21] Z. Al-Qoda, Adsorption of dyes using shale oil ash, *Water Res.* 34 (2000) 4295–4303.
- [22] K.R. Hall, L.C. Eagleton, A. Acrivos, T. Vermeulen, Pore and solid diffusion kinetics in fixed-bed adsorption under constant pattern conditions, *Ind. Eng. Chem. Fundam.* 5 (1996) 212–223.
- [23] H.M.F. Freundlich, Über die adsorption in lösungen, *Z. Phys. Chem.* 57 (1906) 385–470.
- [24] M.I. Temkin, V. Pyzhev, Kinetics of ammonia synthesis on promoted iron catalyst, *Acta Physiochim., URSS* 12 (1940) 327–356.
- [25] Y. Kim, C. Kim, I. Choi, S. Rengraj, J. Yi, Arsenic removal using mesoporous alumina prepared via a templating method, *Environ. Sci. Technol.* 38 (2004) 924–931.
- [26] O. Redlich, D.L. Peterson, A useful adsorption isotherm, *J. Phys. Chem.* 63 (1959) 1024.
- [27] S. Lagergren, Zur theorie der sogenannten adsorption gelöster stoffe, *K. Sven. Vetenskapsakad Handl.* 24 (1898) 1–39.
- [28] Y.S. Ho, Adsorption of heavy metals from waste streams by peat, PhD Thesis, University of Birmingham, Birmingham, UK, 1995.
- [29] G. McKay, Y.S. Ho, Pseudo-second order model for sorption processes, *Process Biochem.* 34 (1999) 451–465.
- [30] G. McKay, Y.S. Ho, The sorption of lead (II) on peat, *Water Res.* 33 (1999) 578–584.
- [31] S. Azizian, B. Yahyaei, Adsorption of 18-crown-6 from aqueous solution on granular activated carbon: a kinetic modeling study, *J. Colloid Interf. Sci.* 299 (2006) 112–115.
- [32] S. Azizian, Kinetic models of sorption: a theoretical analysis, *J. Colloid Interf. Sci.* 276 (2004) 47–52.
- [33] R. Niwas, U. Gupta, A.A. Khan, K.G. Varshney, The adsorption of phosphamidon on the surface of styrene supported zirconium tungstophosphate: a thermodynamic study, *Colloid Surf. A: Physicochem. Eng. Asp.* 164 (2000) 115–119.
- [34] M.J. Jaycock, G.D. Parfitt, *Chemistry of Interfaces*, Ellis Horwood, Onichester, 1981, pp. 12–13.
- [35] H. Nolle, M. Roels, P. Lutgen, P. Van der Meeren, W. Verstraete, Removal of PCBs from wastewater using fly ash, *Chemosphere* 53 (2003) 655–665.

ADSORPTION OF REACTIVE ORANGE DYE USING CROSS-LINKED CHITOSAN/OIL PALM ASH COMPOSITE ADSORBENT

Masitah Hasan, Bassim H.Hameed and A.Latiff Ahmad

School of Chemical Engineering, Engineering Campus, Universiti Sains Malaysia, 14300 Nibong Tebal, Penang, Malaysia

Abstract

This paper presents adsorption of reactive dye (Reactive Orange 16) from aqueous solutions on cross-linked chitosan/palm ash composite beads. The adsorption studies were carried out at different initial dye concentration (50 – 500 mg/L) and at temperature 30 °C. The Langmuir and Freundlich isotherm were applied to describe the experimental data. It was found that the experimental data of adsorbent correlated well with the Freundlich isotherm equation. The maximum adsorption capacity of adsorbent obtained from Langmuir isotherm was 303.03 mg/g. The adsorption kinetic at different initial dye concentrations were evaluated by the pseudo first-order and second-order models. The experimental data obtained showed a good correlation with the pseudo first-order kinetic model.

Introduction

Various kinds of synthetic dyestuffs appear in the effluents of wastewater in some industries such as dyestuffs, textiles, leather, paper-making, plastics, food, rubber, and cosmetics (O'Neil *et al.*, 1999). Among these industries, effluents from the dyeing and finishing processes in the textile industry are highly colored, with a large amount of suspended organic solids, which are important sources of water pollution (Kannan and Sundram., 2001). It has been estimated that about 9 % (or 40,000 tons) of the total amount (450, 000 tons) of dyestuffs produced in the world are discharged in textiles wastewaters (O'Neil *et al.*, 1999).

Dyes can be classified as follows (Mishra and Tripathy, 1993): anionic (direct, acid and reactive dyes). Cationic (basic dyes) and non-ionic (disperse dyes). Different types of reactive dyes commercially react with textiles fibers to achieve a covalent dye-fiber bond (Karcher *et al.*, 2001). Reactive dyes are typically azo-based chromophores combined with different types of reactive groups. They differ from all other classes of dyes in that they bind to the textile fibers such cotton to form covalent bonds (Aksu and Tezer, 2000). Many of dyes used in industry are stable to light and oxidation, as well as resistant to aerobic digestion (Gupta *et al.*, 2003). Most dyes are considered to be non-oxidizable substances by conventional biological and physical treatment because of their complex structure and large molecular size (Weber and Morris, 1962). The dyes can generally cause severe problems, as dyes can poison aquatic life and damage the aesthetic nature of the environment.

In order to improve the efficiency of the adsorption processes, it is necessary to develop cheap and easily available adsorbents with high adsorption capacities. The successful removal using low cost adsorbents have been carried out by several researchers (Mall *et al.*, 1996 and Bailey *et al.*, 1999). Fytianos *et al.*, (2002) investigated the removal of dyes on three low-cost adsorbents, fly ash, bentonite, bleaching earth and also on activated carbon. Armagan *et al.*, (2004) have studied the adsorption of reactive azo dyes on zeolite and modified of zeolite. Besides that, waste materials from seafood processing industry such as chitosan (Sakkayawong *et al.*, 2005), cross-linked chitosan (Chiou and Li, 2002) used to adsorb anionic dyes. Natural materials such as rice husk, sawdust and plum kernels also occupy a position in the production of inexpensive adsorbents (Davila-Jimenez *et al.*, 2005).

Recently, chitosan that is used as an adsorbent has drawn attentions due to its high contents of amino and hydroxy functional groups showing high potentials of the adsorption of dyes (Uzun and Guzel., 2004), metal ions (Wu *et al.*, 2000) and proteins (Zeng and Ruckenstein, 1998). Chitosan is the deacetylated form of chitin, which is

linear polymer of acetylamino-D-glucose. Other useful features of chitosan include its abundance, non-toxicity, hydro-philicity, biocompatibility, biodegradability and anti-bacterial property (Kumar, 2000). However, the effect of pH may be important factor on the dye-binding capacity of chitosan because at low pH, the amino groups of chitosan are much easier to be cationed and they adsorb the dye anions strongly by electrostatic attraction (Kumar, 2000). To overcome such a problem, some cross-linking reagents have been used to stabilize chitosan in acid solutions (Zeng and Ruckenstein, 1996). Moreover, the adsorption of reactive dyes (Reactive Red 189, Reactive Red 222, Reactive Yellow 2 and Reactive Black 5), basic dyes (methylene blue), and acidic dyes (Acid Orange 51, Acid Green 25) in natural solutions using chitosan shows large adsorption capacities (Uzun and Guzel 2004 and Yoshida *et al.*, 1991). Although chitosan shows better adsorption ability in the bead form than in the flake form due to its higher specific surface area (Wu *et al.*, 2000), the weak mechanical property (highly swollen in water) and low specific gravity of the beads make them inconvenient for practical use in column mode adsorption.

The oil palm ash is chosen because of it is highly abundant in Malaysia. The high oxide contents in palm ash give its structure the creditability as a good adsorbent (Zainuddin *et al.*, 2005). Hence, the addition of activated palm ash not only enhances the capability of chitosan to agglomerate and round gel beads, but also improves the hardness of the beads. This can facilitate the separation of the adsorbents from the solution, which is especially important for practical applications. The objective of this work was to evaluate the potential of cross-linked chitosan / oil palm ash composite for the adsorption of reactive orange 16 dye.

Materials and Methods

Chitosan and activated palm ash

The dried oil palm ash (OPA) was sieved through a stack of U.S. standard sieves, and the fine particle size of 63 μm are used. Then, OPA were washed with deionized water until neutral. Fifty grams of OPA were activated by refluxing with 250 ml of 1 mol L⁻¹ H₂SO₄ at 80 °C in a round-bottom flask for 4 hours. The slurry was air-cooled and filtered with a glass fiber. The filter cake was repeatedly washed with deionized water until the filtrate is neutral. It is then dried in an oven at 110 °C before use.

The Reactive Orange 16 (RO16) dye used in this work was obtained from Sigma-Aldrich, Malaysia and used without further purification. The aqueous solution was prepared by dissolving solutes in deionized water to the required concentrations without any pH adjustment. The wavelength of maximum absorbance (λ_{max}) for RB19 was 494 nm.

Cross-linked chitosan / oil palm ash composite beads

Chitosan flake (1g) was dissolved in 1 mol L⁻¹ acetic acid (100 ml) and mixed with activated oil palm ash (1g) and were agitated for 1 hour. Then the viscous solution is sprayed dropwise through a syringe, at a constant rate, into neutralization solution containing 15 % NaOH and 95 % ethanol in a volume ratio of 4:1. They are left in the solution for one day. The formed composite beads were washed with deionized water until solution become neutral and then stored in distilled water. Epichlorohydrin (ECH) purchased from Sigma-Aldrich was used as cross-linking agent in this study and used without further purification. The procedure for cross-linking was same as reported previously (Chiou and Chuang, 2006). Basically, the cross-linking bath agent contained 50 cm³ of 1N sodium hydroxide solution and chemical cross-linking reagent ECH were mixed and shaken for 6h at 50 °C with water bath. The molar ratio of cross-linking reagent/chitosan was 0.5. The cross-linking composite beads were filtered out, washed with deionized water and stored in distilled water. Then, the beads were dried in a freeze dryer for 6 h before used as an adsorbent

Experimental Procedures

Adsorption isotherm was performed in a set of 43 Erlenmeyer flasks (250 mL), where solutions of dye (100 mL) with different initial concentrations (50-500 mg/L) are placed. An equal masses of 0.2 g of particle size (2-3 mm) composite bead (adsorbent) are added to dye solution, and the mixture are then kept in an isothermal shaker (30 °C \pm 0.1) for 48 hours to reach equilibrium. A similar procedure is followed for another set of Erlenmeyer flask containing the same dye concentration without adsorbent to be used as a blank. The flasks are then removed from the shaker, and the final concentrations of dyes in the solution was measured at 494nm, using UV-Visible spectrophotometer (Shimadzu UV/Vis1601 Spectrophotometer, Japan). The amount of adsorption at equilibrium time t , q_e (mg/g), is calculated by:

$$q_e = \frac{(C_0 - C_t)V}{W} \quad (1)$$

where C_0 and C_t (mg/L) are the liquid-phase concentrations of dye at initial and any time t , respectively. V is the volume of the solution (L), and W is the mass of dry adsorbent used (g).

The procedures of kinetic experiments are basically identical to those of equilibrium tests. The aqueous samples are taken at present time intervals, and the concentrations of dye are similarly measured.

The amount of adsorption at time t , q_t (mg/g), is calculated by:

$$q_t = \frac{(C_0 - C_t)V}{W} \quad (2)$$

where C_0 and C_t (mg/L) are the liquid-phase concentrations of dye at initial and any time t , respectively. V is the volume of the solution (L), and W is the mass of dry adsorbent used (g).

Results and discussions

Effect of initial dye concentration

Figure 1 shows the effect of initial RO 16 concentration studies ranging from 50 to 500 mg/L on the adsorption kinetics of cross-linked chitosan/palm ash composite beads at pH 6.0, 30 °C. As can be seen from figure, the amount of the adsorbed dye at low initial concentration (50-200 mg/L) achieve adsorption equilibrium in about 4 h, at some point in time, reaches a constant value beyond which no more is removed from solution. While at high initial dye concentration (300-500 mg/L), the time necessary to reaches equilibrium was about 24h. However, the experimental data were measured at 48 h to make sure that full equilibrium was attained. An increase in initial dye concentration leads to increase in the adsorption capacity of dye on cross-linked chitosan/palm ash composite beads. This indicates that initial dye concentrations played an important role in the adsorption of RO16 on the cross-linked chitosan/palm ash composite beads. This is due to increase in the driving force of the concentration gradient, as an increase in the initial dye concentration.

Adsorption isotherms

To optimize the design of an adsorption system for the adsorption of adsorbates, it is important to establish the most appropriate correlation for the equilibrium curves. Various isotherm equations have been used to describe the equilibrium nature of adsorption. The Langmuir and Freundlich equations are in common use for describing adsorption isotherms at a constant temperature for water and wastewater treatment applications (Ozacar *et al.*, 2002). Figure 2 shows the equilibrium adsorption of RO 16 at pH 6.0, 30 °C, on the cross-linked chitosan/palm ash composite beads.

Langmuir isotherm

It is the most commonly used adsorption model described by the following equation

$$q = \frac{QbC_e}{1 + bC_e} \quad (3)$$

where q is the amount of solute adsorbed in mg/g and C_e is the concentration (mg/L) of solute in the solution at equilibrium and the Langmuir constants Q and b represents adsorption equilibrium constants and saturated monolayer adsorption capacity, respectively. Rearranging the Eq. (3) results in the following equation:

$$\frac{1}{q_e} = \frac{1}{Q} + \frac{1}{bQ} \frac{1}{C_e} \quad (4)$$

where q_e is amount of dye adsorbed per unit weight of adsorbent (mg/g), C_e is the equilibrium concentration of dye in solution (mg/L). The constant Q signifies the adsorption capacity (mg/g) and b is related with the energy of the adsorption (l/mg). A plot of $1/q_e$ versus $1/C_e$ yields a straight line slope $1/bQ$ and intercept $1/Q$. Table 1 indicates that the computed maximum adsorption capacity Q (303.03 mg/g) of RB 19 on the cross-linked chitosan/palm ash composite beads.

Freundlich isotherm

The empirical Freundlich equation based on sorption onto a heterogeneous surface is given as

$$q_e = k_F C_e^{1/n} \quad (5)$$

where k_F and n are the Freundlich constants for the system, which are indicators of adsorption capacity and intensity, respectively (Aksu and Donmez, 2003).

The values of the Freundlich and Langmuir parameters were obtained, respectively, from the linear correlation between the values of C_e/q_e and C_e and $\ln q_e$ and $\ln C_e$ (graph not given). The adsorption isotherm parameters along with the correlation coefficients are presented in Table 1. The linear relationships were evidenced by the R^2 value (for Langmuir model 0.94; for Freundlich model 0.99, respectively). These indicate the applicability of the two adsorption isotherms and the monolayer coverage on the adsorbent surface. The maximum amount of RO16 on cross-linked chitosan/palm ash composite beads is 303.03 mg/g.

The essential characteristics of the langmuir isotherm can be expressed by the dimensionless constant called equilibrium parameter, R_L (Al-Degs *et al.*, 2000 and Namasivayam *et al.*, 2001), which is defined by

$$R_L = \frac{1}{1 + bC_0} \quad (6)$$

where b is the Langmuir constant (L/mg) and C_0 the highest initial dye concentration (mg/L). The value R_L indicates the type of the isotherm to be either unfavorable ($R_L > 1$), linear ($R_L = 1$), favorable ($0 < R_L < 1$) or irreversible ($R_L = 0$). The values of R_L were found to be in range of 0 -1, indicating that the adsorption process is favorable for this adsorbent. In addition, the Freundlich adsorption constant, n should be among 1-10 for beneficial adsorption. Table 1 shows that n value are in the range of 1-10. Based on the correlation coefficient R^2 shown in Table 1, cross-linked chitosan/palm ash composite beads can be better described by the Freundlich model. The Freundlich equation also yield a better fit of the experimental data than the Langmuir equation for cross-linked chitosan/palm ash composite adsorbent onto RO16 dye. The similar phenomenon was observed in the adsorption of Reactive Black 5 onto powdered activated carbon and Afsin-Elbistan fly ash (Eren and Acar, 2006).

Adsorption kinetics

Two simplified kinetic models including pseudo first-order and pseudo second-order equation are analyzed [25,26]. The pseudo first-order model is given by: (Ho and McKay 1999)

$$dq_t / dt = k_1 (q_e - q_t) \quad (7)$$

Where k_1 is the pseudo-first-order rate constant (h^{-1}) and q_e is the pseudo-equilibrium adsorption corresponding to the initial liquid concentration C_0 . After integrating Eq.(7) with the conditions $qt=0, t = 0$ and $qt = qt, t = t$, we have

$$\ln(q_e - q_t) = \ln q_e - k_1 t \quad (8)$$

On the other hand, the pseudo-second-order model is express as

$$dq_t / dt = k_2 (q_e - q_t)^2 \quad (9)$$

where k_2 is the pseudo-second-order rate constant (g mg/h). Similarly, the following equation can be obtained after integration:

$$\frac{t}{q} = \frac{1}{k_2 q_e^2} + \frac{t}{q_e} \quad (10)$$

The aforementioned two models basically include all steps of adsorption such as external film diffusion, adsorption, and internal particle diffusion, so they are pseudo-models. The parameter in these two models are determined from the linear plots of $\ln(q_e - q_t)$ vs t and (t/qt) vs t (figure not given), respectively. The results are shown in Figs. 5 and 6. The validity of each model is determined by correlation coefficient (R^2) values (Table 2). It is found that adsorption on cross-linked chitosan/palm ash follows pseudo-first order model. The values of correlation coefficient (R^2) for the first-kinetic model ($R^2 \geq 0.95$) were greater than second-kinetic model. The calculated q_e values agree very well with experimental data in the case of pseudo-first order kinetics. These results suggest that the dye sorption is first-order model, based on the assumption that the rate limiting step may be chemisorption. Similar results were reported in the adsorption of dye RR222 on composite beads using chitosan and activated clay (Chang and Juang., 2004). Besides that, similar phenomenon are also observed in adsorption of dye RY2 and RB5 on chitosan (Chiou and Li, 2002).

Conclusions

To improve removal efficiencies and adsorption capacities, chemical modification of low-cost adsorbents such as chitosan and palm ash needs to be conducted using chemical cross-linking ECH and acid treated, respectively. The cross-linked chitosan / oil palm ash composite beads prepared by embedding equal weights of chitosan and activated palm ash can be effectively used as an adsorbent for the removal of anionic dye such as Reactive Orange 16 from synthetic wastewater. The amount adsorbed of reactive orange 16 on cross-linked chitosan/palm ash composite beads increased with increasing of initial dye concentration. The experimental data were correlated reasonably well by the Freundlich adsorption isotherm and pseudo-first-order kinetic model.

Acknowledgement

The authors acknowledge the research grant provided by University Sains Malaysia, under short term grant that has resulted in this article.

References

- B. Armagan, M. Turan, M.S. Celik, Equilibrium studies on the adsorption of reactive azo dyes into zeolite, *Desalination* 170 (2004) 33-39.
- C. O'Neill, F.R.Hawkes, S.R.R. Esteves, D.L. Hawkes, S.J.Wileox, Anaerobic and aerobic treatment of a simulated textile effluent, *J.Chem. Technol Biotechnol*, 74 (1999) 993-9.
- C.Namasivayam, R.Radhika, S.Subha, Uptake of dyes by promising locally available agricultural solid waste: coir pith. *Waste Manage.* 38 (2001) 381-7.
- F.C.Wu, R.L.Tseng, R.S.Juang, Comparative adsorption of metal and dye on flake-and bead- types of chitosans prepared from fishery waste, *J. Hazard.Mater.* B73 (2000) 63-75.
- G. McKay, Y.S. Ho, The sorption of lead(II) on peat, *Water Res.*33 (1999) 578-584.
- G. McKay, Y.S.Ho, Pseudo-second order model for sorption processes, *Process Biochem.*34 (1999) 451-465.
- G. Mishra and M. Tripathy, A critical review of the treatment for decolorization of dye wastewater. *Colourage*, 40 (1993) 35-38
- H.Yoshida, S. Fukuda, A.Okamoto, T. Kataoka. Recovery of direct dye and acid dye by adsorption on chitosan fiber-equilibria, *Water Sci. Technol.* 23 (1991) 1667-76.
- I. D. Mall, S.N. Upadhyay, Y.C. Sharma., A review on economical treatment of wastewaters, effluents by adsorption, *Int. J. Environ. Studies* 51 (1996) 77-124.
- I. Uzun, F. Guzel. Kinetics and thermodynamics of the adsorption of some dyestuffs and *p*-nitrophenol by chitosan and MCM-chitosan from aqueous solution, *J.colloid InterfaceSci* 274 (2004) 398-412.
- Kumar MNVR. A review of chitin and chitosan applications. *React. Funct. Polym.* 46 (2000) 1-27.
- K. Fytianos, E. Voudrias, E. Kokkalis, Sorption-desorption behavior of 2,4-dichlorophenol by marine sediments, *Chemosphere* 40 (2000) 3-6.
- M.Ozacar, I.A.Sengil, Adsorption of acid dyes from aqueous solutions by calcined alunite and granular activated carbon. *Adsorption* 8 (2002)301-8.
- M.S. Chiou, H.Y. Li, Equilibrium and kinetic of adsorption of reactive dye on cross-linked chitosan beads, *Journal of Hazardous Materials* B93 (2002) 233-248.
- M.S. Chiou, G.S. Chuang, Competitive adsorption of dye metanil yellow and RB15 in acid solutions on chemically cross-linked chitosan beads, *Chemosphere* 62 (2006) 731-740.
- M.M. Davila-Jimenez, M.P. Elizalde-Gonzalez, A.A. Pelaez-Cid, Adsorption interaction between natural adsorbents and textile dyes in aqueous solution, *Colloid and Surfaces A: Physicochem. Eng. Aspects* 254 (2005) 107-114.
- M.-Y.Chang, R.-S.Juang, Adsorption of tannic acid, humic acid and dyes from water using the composite of chitosan and activated clay, *Journal of Colloid and Interface Science*, 278(2004)18-25.
- N.F. Zainuddin, K.T.Lee, A.H. Kamaruddin, S. Bhatia, A.R. Mohamed, Study of adsorbent prepared from oil palm ash (OPA) for flue gas desulfurization, *Separation and Purification Technology* 45 (2005) 50-60.
- N. Sakkayawong, P. Thiravetyan, W. Nakbanpote, Adsorption mechanism of synthetic reactive dye wastewater by chitosan, *Journal of Colloid and Interface Science* 286 (2005) 36-42.
- N.Kannan, M.M. Sundaram, Kinetics and mechanism of removal of methylene blue by adsorption on various carbons-a comparative study. *Dyes and Pigments* 51 (2001)25-40.
- S.J. Bailey, T.J. Olin, R.M. Bricka, D.D. Adrian., A Review of potentially low cost sorbents for heavy metals. *Water Res.*33 (1999) 2469-2479.
- S.Karcher, A. Kornmuller and M.Jekel, Screening of commercial sorbents for the removal of reactive dyes. *Dyes Pigments*, 51(2001) 111-125.
- V.K.Gupta, I.Ali,Suhas, D.Mohan, Equilibrium uptake and sorption dynamics for the removal of a basic dye (basic red) using low-cost-adsorbent. *J.Colloid Interface Sci.* 265(2003)257-64.

W.J.Weber, J.C.Morris Advances in water pollution research : removal of bio-logically resistant pollutants from waste waters by adsorption, in: *Proc. Int. Conf. on Water Pollution Symposium*, Vol. 2. Pergamon, Oxford, (1962) 231-266

X.F.Zeng, E. Ruckenstein, Cross-linked macroporous chitosan anion-exchange membranes for protein separations, *J. Membr. Sci.* 148 (1998) 195-205.

X.F. Zeng, E.Ruckenstein, Control of pore sizes in macroporous chitosan and chitin membranes. *Ind. Eng. Chem. Res.* 35 (1996) 4169-4175.

Y.S.Ho, G.McKay, Comparative sorption kinetics studies of dyes and aromatic compounds onto fly ash, *J. Environ. Sci.Health A* 34 (1999) 1179-1204

Y.Al-Degs, M.A.M.Khraisshah, S.J.Allend,M.N. Ahmad, Effect of carbon surface chemistry on the removal of reactive dyes from textile effluent, *Water Res.*34 (2000)927.

Z. Eren and F.N. Acar, Adsorption of Reactive Balack 5 from aqueous solution: equilibrium and kinetics studies, *Desalination* 194(2006) 1-10

Z. Aksu and D. Donmez, A comparative study on the biosorption characteristics of some yeast for Remazol Blue reactive dye, *Chemosphere*, 50(2003) 1075-1083.

Table 1. Langmuir and Freundlich isotherm constants for adsorption of Reactive Orange 16 on cross-linked chitosan/palm ash composite beads.

Langmuir isotherm				Freundlich isotherm		
Q_0 (mg/g)	b (1/mg)	R^2	R_L	n	K_F (mg/g)(L/mg) ^{1/n}	R^2
303.03	0.054	0.94	0.036	1.599	21.672	0.99

Table 2. Comparison of pseudo first-order and pseudo second-order adsorption rate constants, calculated q_e and experimental q_t values for different initial dye concentrations.

Initial dye concentration (mg/L)	Pseudo-first order kinetic model				Pseudo-second order kinetic model		
	q_e,exp (mg/g)	q_e,cal (mg/g)	k_1 1/hr	R^2	q_e,cal (mg/g)	k_2 (g/mg.hr)	R^2
50	23.02	18.61	0.1474	0.95	23.58	0.015525	0.88
100	45.33	37.61	0.0993	0.96	38.17	0.011734	0.95
200	90.43	82.24	0.0976	0.97	76.34	0.004038	0.87
300	136.93	126.36	0.0753	0.96	147.06	0.000769	0.34
400	183.78	167.73	0.0624	0.95	128.21	0.002008	0.86
500	227.82	216.32	0.0698	0.99	172.41	0.001228	0.82

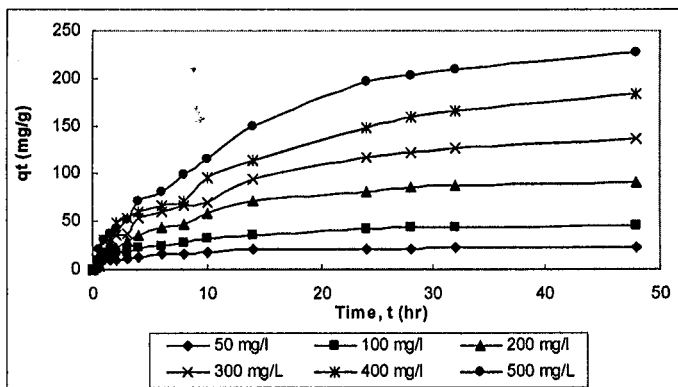


Figure 1. Effect of initial concentrations on the adsorption of Reactive Orange 16 dye at 30°C.

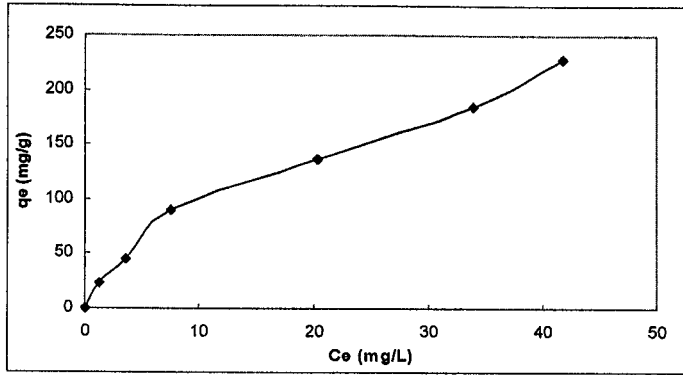


Figure 2. Equilibrium adsorption isotherm of RO16 on cross-linked chitosan/palm ash composite bead at different initial dye concentration.

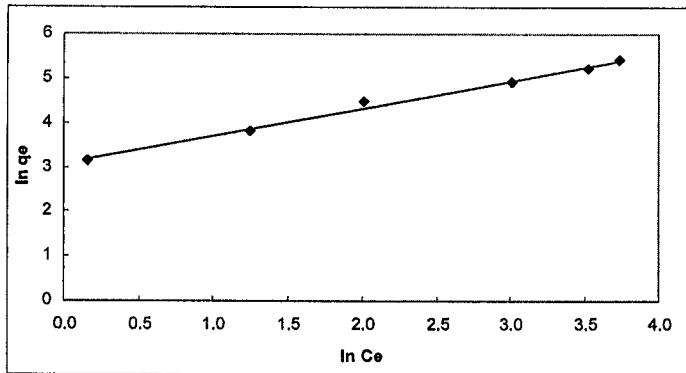


Figure 3. Freundlich isotherm of RO16 at different initial dye concentrations on cross-linked chitosan/palm ash composite bead.

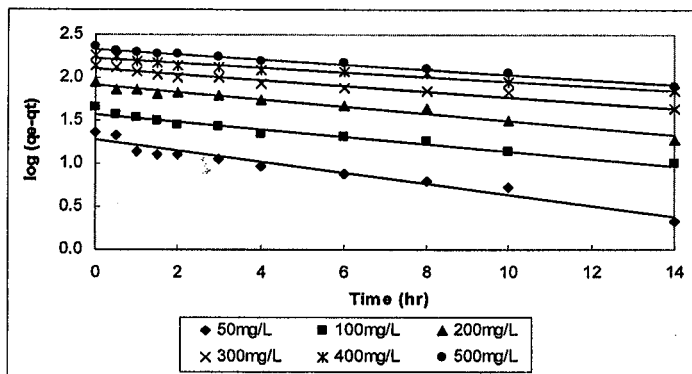


Figure 4. Pseudo-first order kinetic model for adsorption of RO16 at different initial dye concentrations.

1st USM-PENANG INTERNATIONAL POSTGRADUATE CONVENTION

Innovating research through scientific and technological interchanges



Program and abstracts

1st Penang International Conference for Young Chemists.

Blazing A New Frontier In Chemical Sciences.

• 24-27 May 2006

Universiti Sains Malaysia, Penang.



ADSORPTION OF REACTIVE AZO DYE USING CHITOSAN/OIL PALM ASH COMPOSITE ADSORBENT

Masitah Hasan, Bassim H. Hameed* and A. Latiff Ahmad

*School of Chemical Engineering, Engineering Campus, University Science Malaysia,
14300 Nibong Tebal, Penang, Malaysia*

**Corresponding author. Fax: + 604-5941013*

E-mail address: chbassim@eng.usm.my

ABSTRACT

The adsorption of reactive dye (Reactive Blue 19) from aqueous solutions on chitosan/palm ash composite beads was studied in a batch system at initial concentration (50 - 300 mg/L) and 30 °C. The Langmuir and Freundlich adsorption models were applied to describe the experimental isotherms and found that Langmuir isotherm fits well the data. The maximum adsorption capacity of the adsorbent obtained from the Langmuir model was 285.7 mg g⁻¹. In addition, two simplified kinetics models, i.e., pseudo-first order and pseudo-second order were used to describe the kinetic data and found that pseudo-first order kinetic describes the experimental data well.

Keywords : Reactive blue19 dye; Chitosan/palm ash composite; Adsorption isotherm; Kinetic model

INTRODUCTION

The main problem found in the decontamination of wastewater is the removal of colour. Decolourisation are one of the major problem in wastewaters pollutants. Various kinds of synthetic dyestuffs appear in the effluents of wastewater in some industries such as dyestuffs, textiles, leather, paper-making, plastics, food, rubber, and cosmetic (O'Neil *et al.*, 1999). It has been estimated that about 9 % (or 40,000 tons) of the total amount (450, 000 tons) of dyestuffs produced in the world are discharged in textiles wastewaters (O'Neil *et al.*, 1999). Removing color from wastes often more important because the presence of small amounts of dyes (below 1ppm) is clearly visible and influences the water environment considerably (Habibi *et al.*, 2005). These coloured compounds are not only aesthetically displeasing, but also impede light penetration in the treatment plants, thus upsetting the biological treatment processes within the treatment plant.

Most dyes are non-biodegradable in nature, which are stable to light and oxidation. Therefore, the degradation of dyes in wastewater either traditional chemical or biological process have not been very effective (Metivier-Pignon *et al.*, 2003; Orthman *et al.*, 2003; Waranusantigul *et al.*, 2003). Dyes are release into wastewaters from various industrial units, mainly from the dye manufacturing and textiles and other fabric finishing (Janos *et al.*, 2003). About a half of global production of synthetic textile dyes (700,000 tons per year) are classified into azo compounds that have the chromophore of -N=N- unit in their molecular structure and over 15 % of the textiles dyes are lost in wastewater stream during dyeing operation (Habibi *et al.*, 2005). The dyes are, generally mutagenic and carcinogenic and can cause severe damage to humans

beings, such dysfunction of the kidneys, reproductive system, liver, and brain and central nervous system (Kadirvelu *et al.*, 2003).

Reactive dyes are most problematic compounds among others dyes in textile wastewater. Reactive dyes are the largest single group of dyes used in textiles industry. It is highly water-soluble and estimated that 10 -20% of reactive dyes remains in the wastewater during the production process of these dyes (Koprivanac *et al.*, 2000) and nearly 50 % of reactive dyes may lost to the effluent during dyeing processes of cellulose fibers (Netpradit *et al.*, 2004). Reactive dye wastewater have limited biodegradability in an aerobic environment and many azo dyes under anaerobic conditions decompose into potentially carcinogenic aromatic amines (Netpradit *et al.*, 2003; Panswad *et al.*, 2000).

Today, attention has been focused on the low-cost adsorbents as alternative adsorbent materials. Fytianos *et al.*, (2002) investigated the removal of dyes on three low-cost adsorbents, fly ash, bentonite, bleaching earth and also on activated carbon. A large number of low-cost adsorbents have been treated for dyes removal. The successful removal using low cost adsorbents has been carried out by several researchers (Mall *et al.*, 1996 and Bailey *et al.*, 1999). Armagan *et al.*, (2004) have studied the adsorption of reactive azo dyes on zeolite and modified of zeolite. Besides that, waste materials from seafood processing industry such as chitosan (Sakkayawong *et al.*, 2005), cross-linked chitosan (M.S. Chiou *et al.*, 2002) used to adsorb anionic dyes. Natural materials such as rice husk, sawdust and plum kernels also occupy a position in the production of inexpensive adsorbents (Davila-Jimenez *et al.*, 2005).

Recently, chitosan that is used as an adsorbent has drawn attentions due to its high contents of amino and hydroxy functional groups showing high potentials of the adsorption of dyes (Uzun *et al.*, 2004), metal ions (Wu *et al.*, 2000) and proteins (Zeng *et al.*, 1998). Chitosan is the deacetylated form of chitin, which is linear polymer of acetylamino-D-glucose. Other useful features of chitosan include its abundance, non-toxicity, hydro-philicity, biocompatibility, biodegradability and anti-bacterial property (Kumar ., 2000). Moreover, the adsorption of reactive dyes (Reactive Red 189, Reactive Red 222, Reactive Yellow 2 and Reactive Black 5), basic dyes (methylene blue), and acidic dyes (Acid Orange 51, Acid Green 25) in natural solutions using chitosan shows large adsorption capacities (Uzun *et al.*, 2004 and Yoshida *et al.*, 1991). Although chitosan shows better adsorption ability in the bead form than in the flake form due to its higher specific surface area (Wu *et al.*, 2000), the weak mechanical property (highly swollen in water) and low specific gravity of the beads make them inconvenient for practical use in column mode adsorption.

The oil palm ash is chosen because of it is highly abundant in Malaysia. The high oxide contents in palm ash give its structure the creditibility as a good adsorbent (Zainuddin *et al.*, 2005). Hence, the addition of activated palm ash not only enhance the capability of chitosan to agglomerate and round gel beads, but also improve the hardness of the beads. This can facilitate the separation of the adsorbents from the solution, which is especially important for practical applications. The objective of this work was to evaluate the potential of chitosan / oil palm ash composite for the adsorption of reactive blue 19 dye.

MATERIALS AND METHODS

Chitosan and activated palm ash

The dried oil palm ash (OPA) are sieved through a stack of U.S. standard sieves, and the fine particle size of 63 μm are used. Then, OPA are wash with deionized water until neutral. Fifty grams of OPA are activated by refluxing with 250 ml of 1 mol L⁻¹ H₂SO₄ at 80 °C in a round-bottom flask for 4 hours. The slurry is air-cooled and filtered with a glass fiber. The filter cake is repeatedly washed with deionized water until the filtrate are neutral. It is then dried in an oven at 110 °C before use.

The adsorbate selected in this work is Reactive Blue 19 (Sigma-Aldrich Sdn. Bhd). The solution are prepared by dissolving adsorbate in deionized water to the required concentrations without any pH adjustment.

Preparation of composite beads

Chitosan flake (1g) is dissolved in 1 mol L⁻¹ acetic acid (100 ml) and mixed with activated oil palm ash (1g) and are agitated for 1 hour. Then the viscous solution is sprayed dropwise through a syringe, at a constant rate, into neutralization solution containing 15 % NaOH and 95 % ethanol in a volume ratio of 4:1. They are left in the solution for one day. The formed composite beads are washed with deionized water until solution become neutral. Then, the beads are first dried in a freeze dryer for 6 h before used as an adsorbent

Experimental Procedures

Adsorption isotherm are performed in a set of 43 Erlenmeyer flasks (250 ml), where solution of dye (100 ml) with different initial concentrations (50-300 mg l⁻¹) are placed. An equal masses of 0.1 g of particle size (3 mm) composite bead (adsorbent) are added to dye solution, and the mixture are then kept in an isothermal shaker (30 °C \pm 1) for 48 hours to reach equilibrium. A similar procedure is followed for another set of Erlenmeyer flask containing the same dye concentration without adsorbent to be used as a blank.. The flasks are then removed from the shaker, and the final concentrations of dyes in the solution was measured at 592nm, using UV-Visible spectrophotometer (Shimadzu UV/Vis1601 Spectrophotometer, Japan). The amount of adsorption at equilibrium time t , q_e (mg g⁻¹), is calculated by:

$$q_e = \frac{(C_0 - C_e)V}{W} \quad (1)$$

where C_0 and C_t (mg l⁻¹) are the liquid-phase concentrations of dye at initial and any time t , respectively. V is the volume of the solution (l), and W is the mass of dry adsorbent used (g).

The procedures of kinetic experiments are basically identical to those of equilibrium tests. The aqueous samples are taken at present time intervals, and the concentrations of dye are similarly measured.

The amount of adsorption at time t , q_t (mg/g), is calculated by:

$$q_t = \frac{(C_0 - C_t)V}{W} \quad (2)$$

where C_0 and C_t (mg/L) are the liquid-phase concentrations of dye at initial and any time t , respectively. V is the volume of the solution (L), and W is the mass of dry adsorbent used (g).

RESULTS AND DISCUSSION

Effect of initial dye concentration

Figure 1 shows the effect of initial RB 19 concentration on the adsorption kinetics of composite beads at pH 6.0, 30 °C. From figure, the amount of the adsorbed dye onto composite beads increase with time and, at some point in time, reaches a constant value beyond which no more is removed from solution. It is evident that time to reach equilibrium is 24 h for adsorption of RB 19. The time required to attain this state of equilibrium is termed the equilibrium time, and the amount of dye adsorbed at the equilibrium time reflects the maximum adsorption capacity of the adsorbent under those operating condition. Therefore, an increase in the initial dye concentration leads to an increase in the adsorption capacity of the dye on chitosan. This is due to increase in the driving force of the concentration gradient, as an increase in the initial dye concentration.

Equilibrium adsorption

The adsorption isotherm are the most important information for indicates how the adsorbate molecules distribute between the liquid phase and the solid phase when the adsorption process reaches an equilibrium state. The Langmuir and Freundlich equations are in common use for describing adsorption isotherms at a constant temperature for water and wastewater treatment applications (M.Ozacar *et al.*,2002). Figure 2 shows the equilibrium adsorption of RB 19 at pH6.0 , 30 °C, on the composite beads.

Langmuir isotherm

The equilibrium adsorption isotherm is fundamental in describing the interactive behavior between solutes and adsorbent, and is important in design of adsorption system. The linear form of Langmuir isotherm is expressed as:

$$\frac{1}{q_e} = \frac{1}{Q} + \frac{1}{bQ} \frac{1}{C_e} \quad (3)$$

where q_e is amount of dye adsorbed per unit weight of adsorbent (mg/g), C_e is the equilibrium concentration of dye in solution (mg/l). The constant Q signifies the adsorption capacity (mg/g) and b is related with the energy of the adsorption (l/mg). A plot of $1/q_e$ versus $1/C_e$ yields a straight line slope $1/bQ$ and intercept $1/Q$. Table 1 indicates that the computed maximum adsorption capacity Q (285.7 mg/g) of RB 19 on the composite beads.

Freundlich isotherm

The Freundlich isotherm is an empirical equation based on a heterogenous surface. A linear form of the Freundlich expression will yield the constants K_F and n . Hence,

$$\log q_e = \log K_F + \frac{1}{n} \log C_e \quad (4)$$

Therefore , a plot of $\log q_e$ versus $\log C_e$ (plot is not given) enables the constant K_F and exponent n to be determined. K_F can be defined as adsorption of distribution coefficient and represents the quantity of dye adsorbed onto adsorbent for an equilibrium concentration. The slope $1/n$, ranging between 0 and 1, is a measure of adsorption intensity or surface heterogeneity, becoming more heterogenous as its value gets closer to zero. These values together with the correlation coefficient are presented in Table 1 .

Based on the correlation coefficient (R^2) shown in Table 1, the adsorption isotherm with composite beads can better described by Langmuir equation. Also, the Langmuir equation yields a better fit of the experimental data than Freundlich equation (Figure 3). The applicability of the Langmuir isotherm suggest a monolayer of the RB 19 on surfaces of composite beads. It is found that the adsorption capacity of RB 19 on composite beads is 285.7 mg/g.

The essential characteristics of the langmuir isotherm can be expressed by the dimensionless constant called equilibrium parameter, R_L (Y. Al-Degs *et al.*,2000 and C. Namasivayam *et al.*, 2001), which is defined by

$$R_L = \frac{1}{1 + bC_0} \quad (5)$$

where b is the Langmuir constant and C_0 ithe highest initial dye concentration (mg/l). The value R_L indicates the type of the isotherm to be either unfavorable ($R_L > 1$), linear ($R_L = 1$), favorable ($0 < R_L < 1$) or irreversible ($R_L = 0$). From the calculation in this work shows that $R_L = 0.0896$, which the Langmuir isotherm model is favorable.

Adsorption kinetics

In order to investigate the mechanism of adsorption, the pseudo first-order and pseudo second-order equations were used to test the experimental data of initial concentration. The first order rate expression of Lagergren is given as:

$$\log(q_e - q) = \log q_e - \frac{k_1}{2.303} t \quad (6)$$

where q_e and q are the amounts of dye adsorbed on adsorbent at equilibrium and at time t , respectively (g/kg), and k_1 is the rate constant of first order adsorption (per min).

The second-order kinetic model (McKay *et al.*, 1999) expressed as:

$$\frac{t}{q} = \frac{1}{k_2 q_e^2} + \frac{t}{q_e} \quad (7)$$

where k_2 (kg/g per min) is the rate constant of second-order adsorption. If second-order kinetics are applicable, the plot t/qt versus t show a linear relationship. There is no need to know any parameter beforehand and q_e and k_2 can be determined from the slope and intercept of the plot. Also, it is more likely to predict the behavoir over the whole the range of adsorption and is in agreement with chemical sorption being the rate-controlling step (McKay *et al.*,1999) which may involve valency forces through sharing or exchange of electrons between dye anions and adsorbent.

The values of the parameters k_1 and k_2 and also calculated and experimental q_e and correlation coefficients are also presented in Table 2. The correlation coefficient for the first-kinetic model were greater than second-kinetic model. The calculated q_e values agree very well with experimental data in the case of pseudo-first order kinetics. These results suggest that the dye sorption is first-order model, based on the assumption that the rate limiting step may be chemisorption. Similar results were reported in the adsorption of dye RR222 on composite beads using chitosan and activated clay (M.Y.Chang *et al.*, 2004). Besides that, similar phenomenon are also observed in adsorption of dye RY2 and RB5 on chitosan (M. Shen Chiou *et al.*, 2002).

CONCLUSIONS

The chitosan / oil palm ash composite beads prepared by embedding equal weights of chitosan and activated palm ash can be effectively used as an adsorbent for the removal of anionic dye such as Reactive Blue 19 from synthetic wastewater. The amount adsorbed of reactive blue 19 on composite beads increased with increasing of initial dye concentration. The experimental data were correlated reasonably well by the Langmuir adsorption isotherm and pseudo-second order kinetic model.

REFERENCES

- B. Armagan, M. Turan, M.S. Celik, Equilibrium studies on the adsorption of reactive azo dyes into zeolite, *Desalination* 170 (2004) 33-39.
- C.Namasivayam, R.Radhika, S.Suba, Waste Manage.21 (2001) 381.
- F.C.Wu, R.L.Tseng, R.S.Juang, Comparative adsorption of metal and dye on flake-and bead- types of chitosans prepared from fishery waste, *J. Hazard.Mater.* B73 (2000) 63-75.
- G. McKay, Y.S. Ho, The sorption of lead(II) on peat, *Water Res.*33 (1999) 578-584.
- G. McKay, Y.S.Ho, Pseudo-second order model for sorption processes, *Process Biochem.*34 (1999) 451-465.
- H.Metivier-Pignon, C.Faur-Brasquet, P.Le Cloirec, Adsorption of dyes onto activated carbon cloths: approach of adsorption mechanisms and coupling of ACC with ultrafiltration to treat coloured wastewaters, *Sep. Purif. Technol.* 31(1) (2003) 3-11.
- H.Yoshida, S. Fukuda, A.Okamoto, T. Kataoka. Recovery of direct dye and acid dye by adsorption on chitosan fiber-equilibria, *Water Sci. Technol.* 23 (1991) 1667-76.
- I. D. Mall, S.N. Upadhyay, Y.C. Sharma., A review on economical treatment of wastewaters, effluents by adsorption, *Int. J. Environ. Studies* 51 (1996) 77-124.
- I. Uzun, F. Guzel. Kinetics and thermodynamics of the adsorption of some dyestuffs and *p*-nitrophenol by chitosan and MCM-chitosan from aqueous solution, *J.colloid InterfaceSci* 274 (2004) 398-412.
- I.Uzun, Kinetics of the adsorption of reactive dyes by chitosan, *Dyes and Pigments* 70 (2006) 76-83.
- J.Orthman, H.Y.Zhu, G.Q.Lu, Use of anion clay hydrotalcite to remove coloured organics from aqueous solutions, *Sep. Purif. Technol.* 31 (1) (2003) 53-59.
- K.Kadirvelu, M.Kavipriya, C. Kārthika, M. Raehika, N. Vennimalani, S. Pattabhi, Utilization of various agricultural wastes for activated carbon preparation and application for the removal of dyes and metal ions from aqueous solutions, *Bioresour. Technol.* 87(1) (2003) 129.
- Kumar MNVR. A review of chitin and chitosan applications. *React. Funct. Polym.* 46 (2000) 1-27.
- K. Fytianos, E. Voudrias, E. Kokkalis, Sorption-desorption behavior of 2,4-dichlorophenol by marine sediments, *Chemosphere* 40 (2000) 3-6.
- M.Ozacar, I.A.Sengil, Adsorption 8 (2002)301.
- M.S. Chiou, H.Y. Li, Equilibrium and kinetic of adsorption of reactive dye on cross-linked chitosan beads, *Journal of Hazardous Materials* B93 (2002) 233-248.
- M.H. Habibi, A. Hassanzadeh, S. Mahdavi., The effect of operational parameters on the photocatalytic degradation of three textiles azo dyes in aqueous TiO₂ suspensions, *Journal of Photochemistry and Photobiology A: Chemistry* 172 (2005) 89-96.

- M.M. Davila-Jimenez, M.P. Elizalde-Gonzalez, A.A. Pelaez-Cid, Adsorption interaction between natural adsorbents and textile dyes in aqueous solution, *Colloid and Surfaces A: Physicochem. Eng. Aspects* 254 (2005) 107-114.
- N. Kopvanac, A.L. Bozic, S. Papic, Cleaner Production processes in the synthesis of blue anthraquinone reactive dyes, *Dyes Pigments* 44 (2000) 33.
- N.F. Zainuddin, K.T.Lee, A.H. Kamaruddin, S. Bhatia, A.R. Mohamed, Study of adsorbent prepared from oil palm ash (OPA) for flue gas desulfurization, *Separation and Purification Technology* 45 (2005) 50-60.
- N. Sakkayawong, P. Thiravetyan, W. Nakbanpote, Adsorption mechanism of synthetic reactive dye wastewater by chitosan, *Journal of Colloid and Interface Science* 286 (2005) 36-42.
- P. Janos, H. Buchtova, M. Ryznarova. Sorption of dyes from aqueous solutions onto fly ash, *Water Res.* 37 (2003) 4938-4944.
- P. Waranusantigul, P. Pokethitiyook, M.Kruatrachue, E.S.Upatham. Kinetics of basic dye (methylene blue) biosorption by giant duckweed (*Spirodela polyrrhiza*), *Environ. Pollut.* 125(3) (2003) 385.
- S. Netpradita, P. Thiravetyan, S. Towprayoon, Application of 'waste' metal hydroxide sludge for adsorption of azo reactive dyes, *Water Res.* 37 (2003) 763-772.
- S. Netpradit, P. Thiravetyan, S. Towprayoon, Evaluation of metal hydroxide sludge for reactive dye adsorption in a fixed-bed column system, *Water Res.* 38 (2004) 71.
- S.J. Bailey, T.J. Olin, R.M. Bricka, D.D. Adrian,. A Review of potentially low cost sorbents for heavy metals. *Water Res.* 33 (1999) 2469-2479.
- T. Panswad, W. Luangdilok, Decolorization of reactive dyes with different molecular structures under different environmental conditions. *Water Res.* 34 (2000) 4177- 4184
- X.F.Zeng, E. Ruckenstein, Cross-linked macroporous chitosan anion-exchange membranes for protein separations, *J. Membr. Sci.* 148 (1998) 195-205.
- Y.Al-Degs, M.A.M.Khraishah, S.J.Allend,M.N. ahmad, *Water Res.* 34 (2000)927.

Table 1: Langmuir and Freundlich isotherm constants for adsorption of Reactive Blue 19 on composite beads.

Langmuir isotherm				Freundlich isotherm		
Q_0 (mg/g)	b (1/mg)	R_2	R_L	n	K_F (mg/g)(L/mg) ^{1/n}	R^2
285.714	0.034	0.974	0.090	1.853	20.830	0.949

Table 2: Comparison of pseudo first-order, pseudo second-order adsorption, and intraparticle diffusion rate constants, calculated q_e and experimental q_i values for different initial dye concentrations.

Initial dye concentration (mg/L)	Pseudo-first order kinetic model				Pseudo-second order kinetic model		
	$q_{e,exp}$ (mg/g)	$q_{e,cal}$ (mg/g)	k_1 1/min	R^2	$q_{e,cal}$ (mg/g)	k_2 (g/mg.min)	R^2
50	50.71	48.67	0.077	0.874	29.59	0.012	0.591
100	95.38	88.67	0.105	0.944	76.34	0.004	0.778
200	143.07	142.66	0.078	0.971	102.04	0.007	0.884
300	210.31	198.15	0.077	0.974	131.58	0.003	0.821

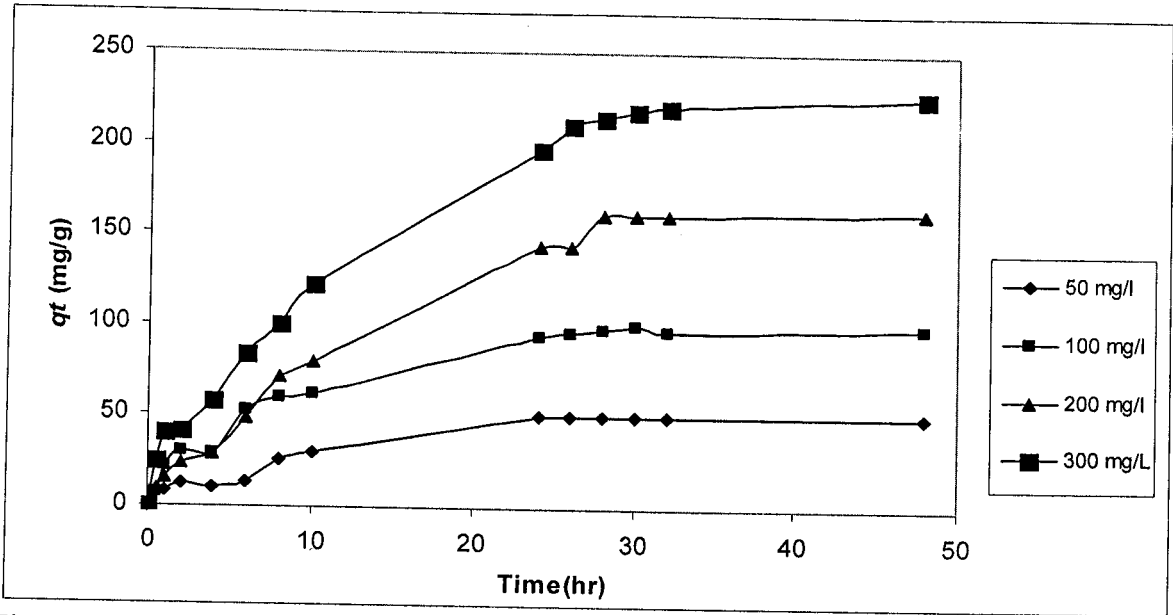


Fig. 1. Time profiles of amounts of RB 19 adsorbed onto various initial dye concentration with dosage 0.1 g at 30°C.

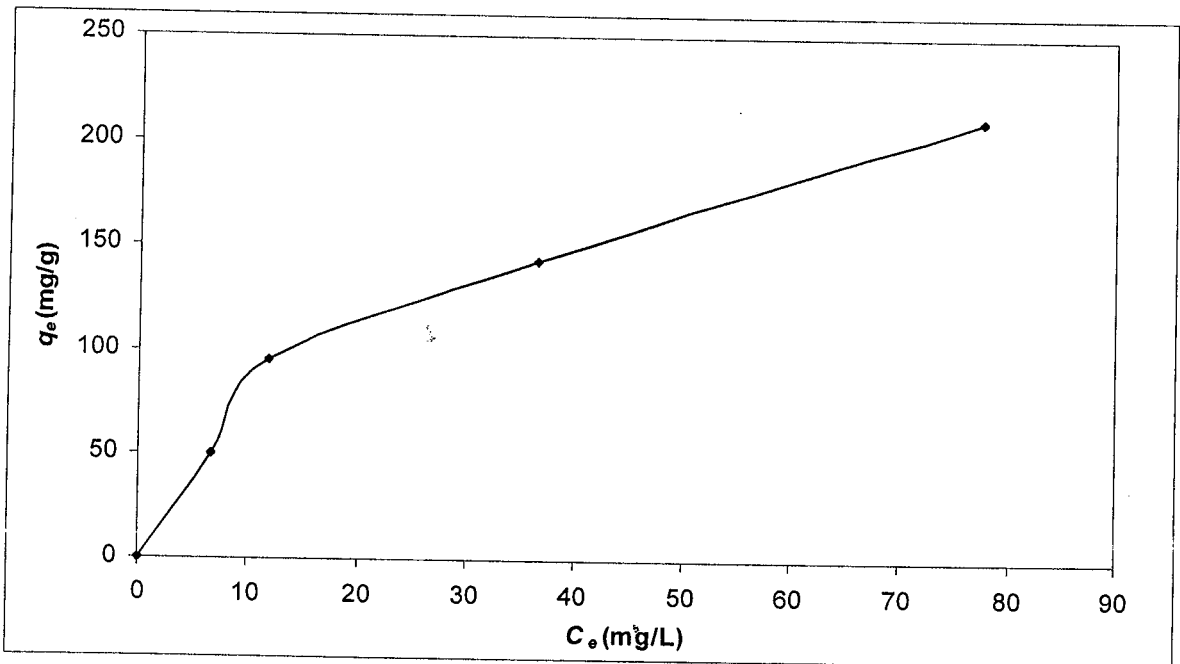


Fig. 2. Equilibrium adsorption isotherm of RB 19 on composite beads at different initial dye concentration.

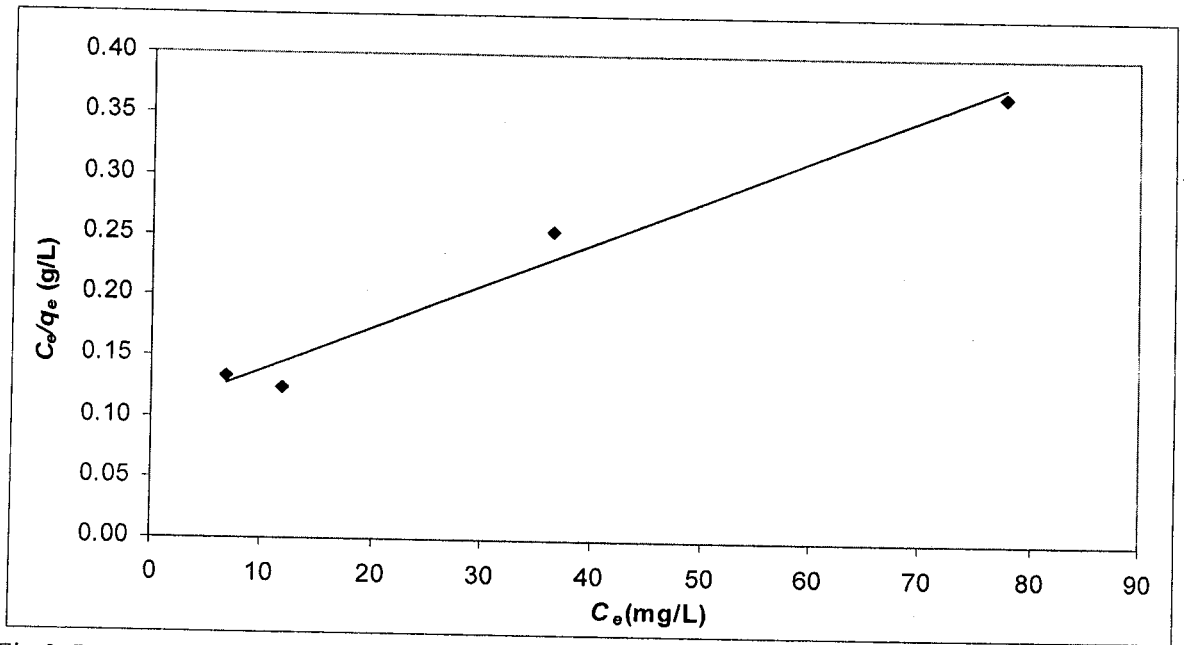


Fig.3. Langmuir isotherm of RB 19 at different initial dye concentrations on composite bead.

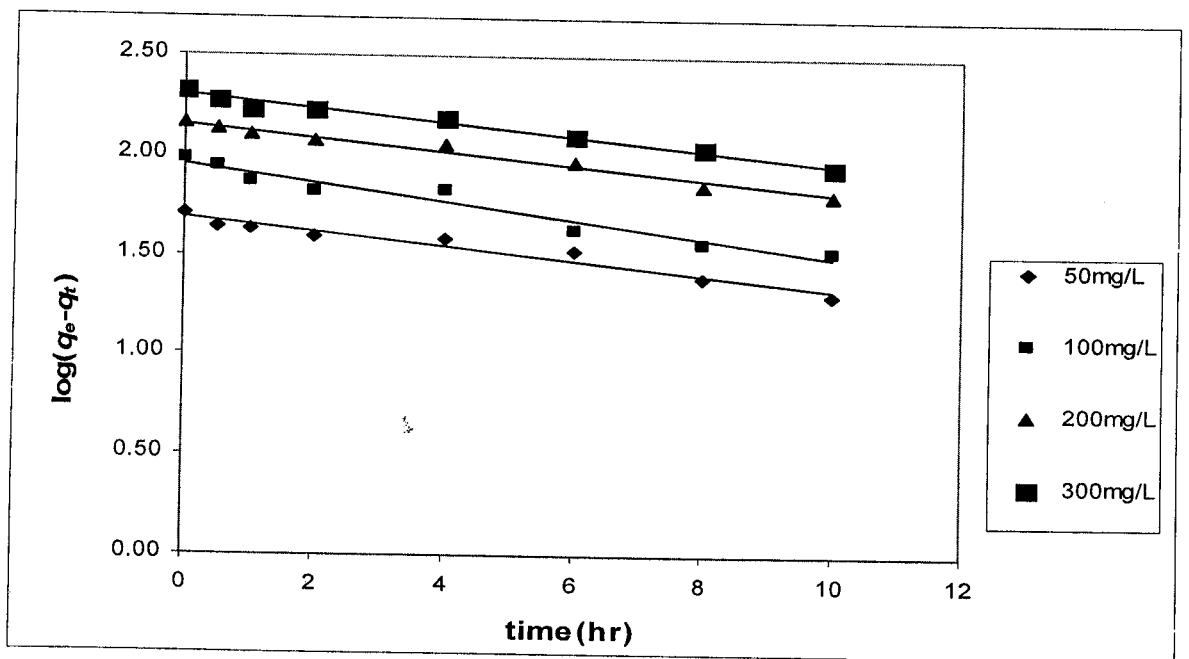


Fig.4. Plot of pseudo-first order kinetic model for adsorption of RB19 onto various initial dye concentrations.

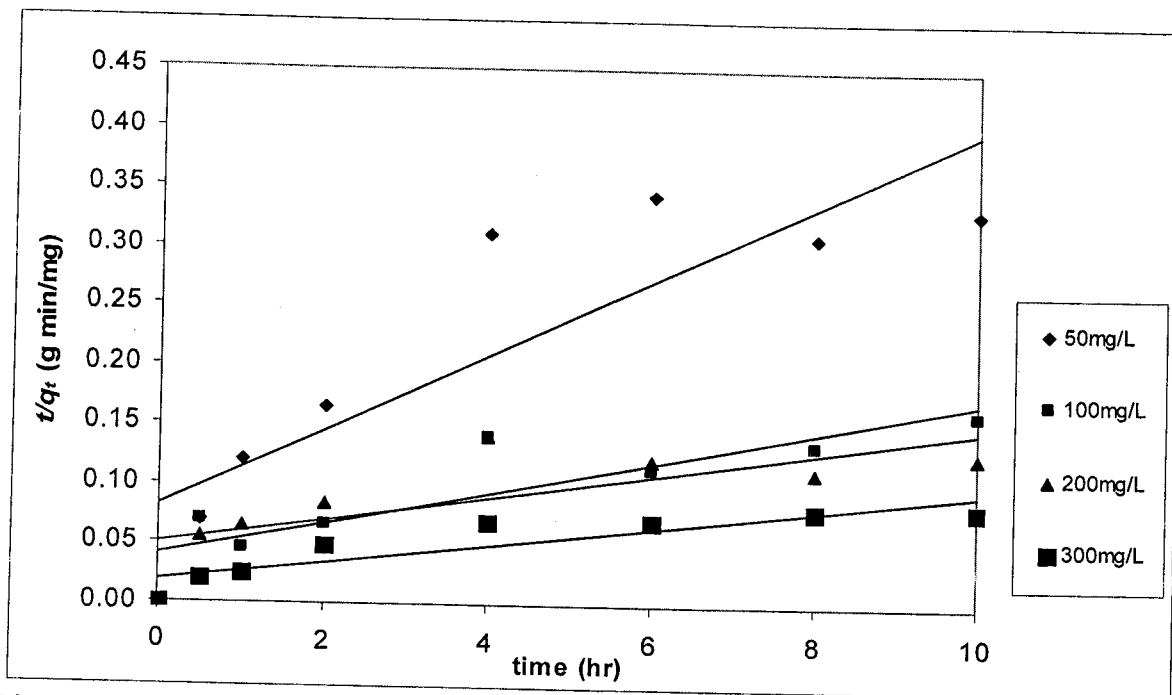


Fig.5. Plot of pseudo-second order kinetic model for adsorption of RB19 onto various initial dye concentrations.

APPENDIX C :

**ADSORPTION OF REACTIVE AZO DYES ON CHITOSAN/OIL-PALM ASH
COMPOSITE ADSORBENT: BATCH AND CONTINUOUS STUDIES**

by

MASITAH BINTI HASAN

**Thesis submitted in fulfillment of the
requirements for the degree of
Master of Science**

JANUARY 2008

ADSORPTION OF REACTIVE AZO DYES ON CHITOSAN / OIL-PALM ASH COMPOSITE ADSORBENT: BATCH AND CONTINUOUS STUDIES

ABSTRACT

The adsorption of reactive blue 19 (RB19), reactive orange 16 (RO16) and reactive black 5 (RB5) on cross-linked chitosan/oil palm ash composite beads was studied in batch and column modes of operation. Batch adsorption studies were carried out for adsorption of reactive dyes onto cross-linked chitosan/ oil palm ash composite beads. Various experimental parameters were studied including initial dye concentration (50 - 500 mg/L), contact time, pH of solution (2 - 13) and temperature (30 - 50 °C). The experimental data were analyzed using Langmuir, Freundlich, Temkin and Dubinin-Raduskevich isotherm model. The adsorption of RB19 and RO16 was found to follow Freundlich model, while RB5, showed a better fit to the Langmuir and Freundlich isotherm model. Pseudo-first-order, pseudo-second-order kinetic model and intraparticle diffusion model were used to analyze the kinetic data. It was found that the data follow the pseudo-first-order kinetic model at lower concentration, while at higher concentrations, it followed pseudo-second-order kinetic model for RB19 for all temperature studied. Contrary, RO16 and RB5 dye followed pseudo-first-order kinetic model for whole initial concentration and temperature studied. However, based on the standard normalized deviation, the pseudo-second-order kinetic model fitted well for whole system of dyes studied. Various thermodynamic parameters, such as Gibbs energy (ΔG^0), enthalpy change (ΔH^0) and entropy change (ΔS^0), were calculated, which indicated that the present system was spontaneous and endothermic process for RB19 and RO16. However, exothermic process of adsorption of RB5 was observed. The cross-linked chitosan/oil palm ash composite beads were characterized by Scanning Electron microscopy (SEM) and Fourier Transform Infrared (FT-IR) Spectroscopy. Evidence from FT-IR spectra showed the participation of amine groups in the adsorption of RB19, RO16 and RB5 dyes and the mechanism was proposed to be electrostatic interaction between the positive charge amine groups and negative

charge dyes. The performance of column are described through the concept of the breakthrough curve for the adsorption of RB19, RO16 and RB5 on adsorbents under different operating conditions including initial dye concentration (100, 200, 300 mg/L), flowrate (5 – 25 mL/min) and height of adsorbent bed (60, 80, 100 mm). It was found that the amount of adsorbate adsorbed, q_{eq} (mg/g) increased with increasing initial dye concentration and height of adsorbent bed; and decreased with increasing flow rate. The $t_{1/2}$ for the adsorption of RB19, RO16 and RB5 dye was found 10, 21 and 22 min, respectively. Boharts and Adam, Thomas and Yoon and Nelson models were applied to the experimental data to simulate the breakthrough curves. It was found that the Thomas model was best fitted to describe the adsorption of RB19, RO16 and RB5 dyes on cross-linked chitosan/oil palm ash composite beads, which analysis on average percentage error, $\epsilon\%$ give less than 3.1%.

PENJERAPAN PENCELUP AZO REAKTIF MENGGUNAKAN BAHAN PENJERAP KOMPOSIT CHITOSAN/ABU KELAPA SAWIT: KAJIAN KELOMPOK DAN BERTERUSAN

ABSTRAK

Penjerapan pencelup reaktif biru 19 (RB19), reaktif oren 16 (RO16) dan reaktif hitam (RB5) menggunakan manik-manik komposit chitosan/abu kelapa sawit terpaut silangan dikaji pada kedua-dua keadaan operasi iaitu kelompok dan terus. Kajian penjerapan kelompok dijalankan untuk penjerapan pencelup reaktif pada manik-manik komposit chitosan/abu kelapa sawit terpaut silangan. Pelbagai parameter eksperimen dikaji termasuklah kepekatan awal pencelup (50-500 mg/L), masa sentuh, pH bagi larutan (2-13) dan suhu (30-50 °C). Data-data eksperimen dianalisa menggunakan model garis sesuhu seperti 'Langmuir', 'Freundlich', 'Temkin' dan 'Dubinin-Raduskevich'. Penjerapan pencelup RB19 dan RO16 didapati menuruti model 'Freundlich', manakala pencelup RB5 lebih menunjukkan kesesuaian dengan model garis sesuhu 'Langmuir' dan 'Freundlich'. Model kinetik pseudo tertib pertama, pseudo tertib kedua dan model resapan intra zarah digunakan untuk menganalisa data kinetik. Didapati daripada keseluruhan suhu kajian yang dijalankan pencelup RB19* menuruti model kinetik pseudo tertib pertama pada kepekatan yang rendah, manakala pada kepekatan yang tinggi pula menuruti model kinetik pseudo tertib kedua. Berbeza pula dengan pencelup RO16 dan RB5 yang menuruti model kinetik pseudo tertib pertama untuk keseluruhan kajian kepekatan awal dan suhu yang dijalankan. Walaubagaimanapun, berdasarkan sisihan ternormal piawai, model kinetik pseudo tertib pertama sangat sesuai untuk keseluruhan sistem yang dikaji. Pelbagai parameter termodinamik seperti tenaga Gibbs (ΔG^0), perubahan entalpi (ΔH^0) dan perubahan entropi (ΔS^0) dikira, dimana ianya menunjukkan sistem tersebut adalah spontan dan merupakan proses serap haba untuk pencelup RB19 dan RO16. Walaubagaimanapun, proses luah haba pula didapati berlaku pada penjerapan pencelup RB5. Manik-manik komposit chitosan/abu kelapa sawit terpaut silangan dicirikan oleh Mikroskop Elektron

Imbasan (SEM) dan Spektrosopi Infra-merah Jelmaan Fourier (FT-IR). Spektrum FT-IR yang terhasil menunjukkan penglibatan kumpulan-kumpulan amine dalam penjerapan pencelup RB19, RO16 dan RB5 dan mekanisme yang terlibat adalah interaksi elektrostatik di antara cas positif kumpulan-kumpulan amine dan cas negatif pencelup. Prestasi sesuatu turus adalah berdasarkan konsep lengkung bulus 'breakthrough' untuk penjerapan pencelup RB19, RO16 dan RB5 pada bahan penjerap dalam pelbagai kepekatan awal pencelup (100, 200, 300 mg/L), kadar aliran (5-25 mL/min) dan ketinggian turus bahan penjerap (60, 80, 100 mm). Didapati jumlah bahan pencelup terjerap q_{eq} (mg/g) meningkat dengan peningkatan kepekatan awal pencelup dan ketinggian turus bahan penjerap dan berkurangan dengan peningkatan kadar aliran. Masa separuh hayat, $t_{1/2}$ untuk penjerapan pencelup RB19, RO16 dan RB5 adalah 10, 21 dan 22 minit masing-masing. Model-model seperti Boharts dan Adam, Thomas dan Yoon dan Nelson diaplikasikan pada data-data eksperimen untuk simulasi lengkung bulus. Didapati model Thomas adalah yang terbaik untuk memperihalkan penjerapan pencelup RB19, RO16 dan RB5 pada manik-manik komposit chitosan/abu kelapa sawit terpaat silangan dimana analisa purata ralat peratusan, $\epsilon\%$, adalah kurang daripada 3.1%.

JABATAN BENDAHARI
 UNIT KUMPULAN WANG AMANAH
 UNIVERSITI SAINS MALAYSIA
 KAMPUS KEJURUTERAAN
 SERI AMPANGAN

PENYATA KUMPULAN WANG

TEMPOH BERAKHIR 30/04/2008

Tempoh Projek: 01/04/2006 - 31/03/2008

DR BASSIM H.HAMEED

304.PJKIMIA.6035173

JUMLAH GERAN :- 18,078.90

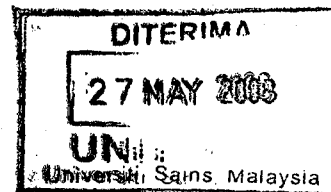
NO PROJEK :-

PANEL : JPENDEK

DEV. OF CHITOSAN BASED ADSORBENT FOR REMOVAL OF REACTIVE AZO DYES

PENAJA :- JANGKA PENDEK

<u>Vot</u>	<u>Peruntukan</u>	<u>Perbelanjaan sehingga 31/12/2007</u>	<u>Tanggungjawab semasa 2008</u>	<u>Perbelanjaan Semasa 2008</u>	<u>Jumlah Perbelanjaan 2008</u>	<u>Jumlah Perbelanjaan Tertumpuk (b+c+d)</u>	<u>Baki Peruntukan Semasa 2008 (a-(b+c+d))</u>
	(a)	(b)	(c)	(d)	(c + d)	(b+c+d)	(a-(b+c+d))
11000 GAJI KAKITANGAN AWAM	3,136.30	1,007.45	0.00	0.00	0.00	1,007.45	2,128.85
21000 PERBELANJAAN PERJALANAN DAN SARAH	975.00	0.00	0.00	0.00	0.00	0.00	975.00
23000 PERHUBUNGAN DAN UTILITI	200.00	11.00	0.00	9.30	9.30	20.30	179.70
26000 BAHAN MENTAH & BAHAN UNTUK PENYEL	0.00	0.00	0.00	0.00	0.00	0.00	0.00
27000 BEKALAN DAN ALAT PAKAI HABIS	7,357.70	1,422.00	12,588.00	677.60	13,265.60	14,687.60	(7,329.90)
29000 PERKHIDMATAN IKTISAS & HOSPITALITI	6,410.00	1,882.00	0.00	19.70	19.70	1,901.70	4,508.30
	<u>18,079.00</u>	<u>4,322.45</u>	<u>12,588.00</u>	<u>706.60</u>	<u>13,294.60</u>	<u>17,617.05</u>	<u>461.95</u>
Jumlah Besar	<u>18,079.00</u>	<u>4,322.45</u>	<u>12,588.00</u>	<u>706.60</u>	<u>13,294.60</u>	<u>17,617.05</u>	<u>461.95</u>



PAGE 02/02

J_BENDAHARI_USM_KKJ

045941003 07:28 22/05/2008